Titre: Title:	Prediction of the Performance of Aged Powder Activated Carbon (PAC) for the Adsorption of Natural Organic Matter (NOM)
Auteur: Author:	Vahid Salehi
Date:	2022
Type:	Mémoire ou thèse / Dissertation or Thesis
Référence: Citation:	Salehi, V. (2022). Prediction of the Performance of Aged Powder Activated Carbon (PAC) for the Adsorption of Natural Organic Matter (NOM) [Mémoire de maîtrise, Polytechnique Montréal]. PolyPublie. https://publications.polymtl.ca/10775/

URL de PolyPublie: PolyPublie URL:	https://publications.polymtl.ca/10775/
Directeurs de recherche: Advisors:	Benoit Barbeau
Programme: Program:	Génie civil

POLYTECHNIQUE MONTRÉAL

Affiliée à l'Université de Montréal

Prediction of the performance of aged powder activated carbon (PAC) for the adsorption of natural organic matter (NOM)

VAHID SALEHI

Département des génies civil, géologique et mines

Mémoire présenté en vue de l'obtention du diplôme de Maîtrise ès sciences appliquées

Génies civil

Décembre 2022

POLYTECHNIQUE MONTRÉAL

Affiliée à l'Université de Montréal

Ce mémoire intitulé:

Prediction of the performance of aged powder activated carbon (PAC) for the adsorption of natural organic matter (NOM)

Présenté par : Vahid SALEHI

en vue de l'obtention du diplôme de : *Maîtrise ès Sciences Appliquées*

a été dûment accepté par le jury d'examen constitué de :

Dominique CLAVEAU-MALLET, présidente

Benoit BARBEAU, membre et directeur de recherche

Kim Marren LOMPE, membre

DEDICATION

تقدیم به مهسا امینی، که نامش رمز پیروزی ما است.

Roughly translated to:

Dedicated to Mahsa Amini, whose name is a symbol of Iran's freedom

ACKNOWLEDGMENTS

First and foremost, I would like to thank my research supervisor, Mr. Benoît Barbeau, who gave me a chance to participate in such an exciting project under his supervision at the Chair of drinking water at Polytechnique. His expertise, knowledge, open mind to new ideas, and professionalism have taught me so much.

Special thanks to Yves Fontaine, Tetiana, Elyart, Julie, Philibert, and Jacinthe Mailly, who have always been available to help me and answer my question about my experimental studies in the lab. I consider myself lucky to work in such a welcoming and professional team.

I want to thank my beloved wife, Faezeh Absalan, for encouraging me to study in this field and always accompanying and guiding me with her knowledge and skills in every moment of this project. I would never have been able to achieve my master's degree without her help. The experience of being a colleague in a group with her was undoubtedly unique. It was the best moment of my professional life.

I am sure that without the support of my parents, I would never have been able to take a step. I am always grateful to them, whose presence encourages me.

Ultimately, I would like to thank my classmates and friends, Luan Nguyen and Hadia Terro; without their presence, these two years of studying at the university (most of which were spent during the pandemic) would have been impossible. I am glad that this project led to finding such friends.

RÉSUMÉ

La matière organique naturelle (MON) est un mélange complexe de composés organiques naturels provenant de la végétation en décomposition de l'environnement qui se trouvent dans toutes les sources d'eau douce utilisées dans les usines de traitement de l'eau potable. L'adsorption au charbon actif est l'un des procédés les plus efficaces pour éliminer la MON. La société Veolia a commercialisé un réacteur charbon actif en poudre (CAP) recirculé sous le nom d'Actiflo® Carb. L'objectif final de ce projet est de développer un système simple et rapide pour prédire les performances des CAP recirculés aux côtés des CAP vierges dans le procédé Actiflo® Carb.

Après une revue de la littérature sur les caractéristiques de la MON, le procédé d'adsorption et le réacteur Actiflo® Carb, deux approches distinctes sont définies pour atteindre l'objectif final. La première approche consiste à prédire le procédé Actiflo® Carb en modélisant le réacteur à procédé à membrane hybride (PMH) à écoulement continu l'échelle du laboratoire. La deuxième approche est l'étude de l'effet du vieillissement des CAP et du mélange des mélanges de CAP d'âge varié sur les paramètres de sorption. Ensuite, en déterminant les paramètres de sorption d'une suspension des mélanges de CAP d'âge varié, le réacteur Actiflo® Carb serait modélisé par le modèle de diffusion sur surface homogène (HSDM).

Des expériences sur un réacteur PMH à écoulement à l'échelle du laboratoire ont montré que : 1- L'accumulation de CAP sur la surface de la membrane dans le réacteur est inévitable. 2- Les conditions physiques du réacteur influencent significativement les performances du CAP. 3- Bien que plusieurs modèles empiriques puissent ajuster avec précision les performances d'un réacteur, aucun de ces modèles n'est en mesure de prédire les performances du réacteur s'il est rempli de CAP recirculé. Par conséquent, l'hypothèse d'utiliser un réacteur HPM à écoulement à l'échelle du laboratoire pour prédire le procédé Actiflo® Carb est réfutée.

Dans la deuxième approche, l'influence du vieillissement des CAP et des mélanges de CAP d'âge varié sur les paramètres de sorption a été étudiée. Des expériences isothermes sur du CAP à un seul âge ont montré que la capacité des CAP recyclés ne diminue pas au cours du vieillissement; ceci montre que l'adsorption de MON ne bloque pas les pores du CAP. Par conséquent, les conditions d'équilibre pourraient être prédites avec l'équation de Freundlich. Des tests cinétiques sur du CAP

à un seul âge ont montré que le vieillissement des PAC n'affecte pas Ds. Ainsi, la cinétique des CAP vieillis dans un réacteur discontinu pourrait être bien décrite par le HSDM.

Des expériences cinétiques/isothermes sur du mélange des mélanges de CAP d'âge varié ont démontré qu'en utilisant la charge moyenne pondérée en masse de carbone organique dissous (COD) pour tous les CAPs âgés dans une suspension, le modèle HSDM pouvait prédire la concentration de COD à l'effluent du réacteur.

L'étape finale de ce projet consistait à prédire l'adsorption de MON sur du CAP dans le procédé Actiflo® Carb et à vérifier la prédiction par des échantillons issus d'un procédé Actiflo® Carb à l'échelle industrielle. Ce processus a été modélisé en combinant le HSDM et le jar test. Il a été prédit que ce procédé spécifique Actiflo® Carb élimine 64% de la concentration en COD, alors qu'en réalité, la performance de ce procédé Actiflo® Carb est de 58%.

Au total, les résultats de cette recherche montrent que la réalisation de tests cinétiques/isothermes sur des CAP vierges est une approche fiable et rapide pour prédire le procédé Actiflo® Carb.

Mots-clés : charbon actif en poudre vieilli ; matière organique naturelle; carbone organique dissous; adsorption; courbe de percée; ajustement du modèle; HSDM ; Actiflo® Carb.

ABSTRACT:

Natural organic matter (NOM) is a complex mixture of natural organic compounds from the environment's decaying vegetation found in all freshwater sources used in drinking water treatment plants. Adsorption with activated carbon (AC) is one of the most effective processes to remove NOM. The Veolia company commercialized a recirculated Powder AC (PAC) reactor under the name Actiflo® Carb. The final objective of this project is to develop a simple and rapid system to predict the performance of recirculated PAC alongside virgin PAC in the Actiflo® Carb process.

After a literature review on NOM characteristics, the adsorption process, and the Actiflo® Carb reactor, two separate approaches are defined to reach the final goal. The first approach is predicting the Actiflo® Carb process by modeling the bench-scale flow-through hybrid membrane process (HMP) reactor. The second approach is the investigation of the effect of PAC aging and mixing different aged PACs on sorption parameters. Then, by determining sorption parameters for a suspension with different aged PACs, the Actiflo® Carb reactor would be modeled by the homogeneous surface diffusion model (HSDM).

Experiments on bench-scale flow-through HMP reactor showed that: 1- PAC accumulation on the membrane surface in the reactor is unavoidable. 2- The physical conditions of the reactor influence the PAC performance significantly. 3- Although several empirical models can accurately fit the performance of a reactor, none of these models are able to predict the performance of the reactor if it is filled by recirculated PAC. Therefore, the hypothesis of using a bench-scale flow-through HPM reactor to predict the Actiflo® Carb process is refuted.

In the second approach, the influence of PAC aging and mixing different aged PACs on sorption parameters were studied. Isotherm experiments on single-aged PAC showed that the capacity of the recycled PAC does not decrease over aging; this shows that the NOM adsorption does not block the pores of the PAC. Therefore, the equilibrium conditions could be predicted with the Freundlich equation. Kinetic tests on single-aged PAC showed that PAC aging does not affect Ds, so the aged PAC kinetics in a batch reactor could be well described by the HSDM. Kinetic/isotherm experiments on a mixture of different aged PACs demonstrated that by using the mass-weighted average of the dissolved organic carbon (DOC) loading for all aged PACs in a suspension, the HSDM model could predict DOC concentration at the effluent of the reactor.

The final stage of this project was modeling the NOM adsorption on PAC in the Actiflo® Carb process and verifying the model by samples from an industrial-scale Actiflo® Carb process. This process was modeled by combining the HSDM and jar test. It was predicted that this specific Actiflo® Carb process removes 64% of DOC concentration, while in reality, the performance of this Actiflo® Carb process is 58%.

All in all, the results of this research show that performing kinetic/isotherm tests on virgin PAC is a reliable rapid approach to predict the Actiflo® Carb process.

Keywords: aged powdered activated carbon; natural organic matter; dissolved organic carbon; adsorption; breakthrough curve; model fitting; HSDM; Actiflo® Carb.

TABLE OF CONTENTS

LIST OF FIGURES

LIST OF TABLES

LIST OF SYMBOLS AND ABBREVIATIONS

1/n	Freundlich constant describes the affinity between the adsorbent and the pollutant
α	Desorption constant at the Elovich model
β	Initial adsorption rate at the Elovich model
τ	Residence time of the reactor
AC	Activated carbon
Ceq	Adsorbate concentration at the equilibrium point
C_{eff}	Adsorbate concertation in the effluent stream (in the reactor)
C_{inf}	Initial adsorbate concentration (influent stream)
Cs	Adsorbate concentration in the liquid
CSTR	Continuously stirred tank reactor
CUR	Carbon usage rate
DBPs	Disinfection by-products
DOC	Dissolved organic carbon
Ds	Surface diffusion coefficient
GAC	Granular activated carbon
HAA	Haloacetic acid
HMP	Hybrid membrane process
HRT	Hydraulic retention time
HSDM	Homogeneous surface diffusion model
KF	Freundlich constant describes adsorption capacity
kp1	Kinetic constant of the pseudo-first-order model
kp2	Kinetic constant of the pseudo-second-order model
MAE	Mean absolute error
NOM	Natural organic matter

PAC	Powdered activated carbon
q	Adsorbent load (mass of adsorbed adsorbate per mass of adsorbent)
q_0	initial load
q_{eq}	Adsorbent load at the equilibrium point
qs	Adsorbate concentration in the external layer of the adsorbent
R	Radius of the adsorbent particle
SDM	Surface diffusion model
SRS	Stirrer's rotation speed
SUVA	Specific UV absorption
TC	Total carbon
TIC	Total inorganic carbon
TOC	Total organic carbon
UV254	UV light absorption at 254 nm
TSS	Total suspended solids

CHAPTER 1 INTRODUCTION

In 1854, a cholera epidemic on Broad Street in London killed hundreds of people. John Snow, a British doctor, discovered that a contaminated water pump caused the cholera epidemic. He prevented the outbreak by stopping the flow of polluted water. Although Snow did not understand the mechanism of water-borne diseases, his research marked the beginning of our understanding of the concept of the impact of microorganisms on public health (Hempel, 2007).

Since the late nineteenth century, we have known that some aquatic microorganisms are pathogenic and can have catastrophic effects on human and public health (Botes et al., 2013). From the beginning of the twentieth century until today, the disinfection of water by chlorine and its compounds has been the most common method of removing microorganisms from water (Pendashteh, 2015). While water disinfection is critical, the residual reaction of disinfectants and microorganisms can lead to the production of disinfection by-products (DBPs) (such as trihalomethanes, haloacetic acids, nitrosamines, etc.) in the water distribution system (Duan et al., 2020). Therefore, avoiding the formation of DBPs became another critical public health issue. One of the effective ways to reduce the production of DBPs is to remove natural organic matter (NOM) from raw water before the disinfection stage. Many methods and processes have been introduced for this purpose. One of the most economical, simple, and efficient of these processes is the adsorption process. (Delgado et al., 2012; Hu et al., 2014; Karanfil & Kilduff, 1999; Loganathan et al., 2022). Activated carbon (AC) is the oldest and most common adsorbent in the drinking water and wastewater treatment industry (Bhatnagar et al., 2013).

AC is used in two different ways, in fixed bed reactors using granular AC (GAC) (particle size 0.5 to 4 mm), and in slurry reactors, powdered AC (PAC) (particle size <40 μm)(Worch, 2012). Each way has advantages and disadvantages. One of the disadvantages of using PAC in the slurry reactor is the short hydraulic retention time (HRT) of slurry reactors compared to the time that PAC needs to reach the saturation state. Therefore, in this type of reactor, the total capacity of carbon is not used (Worch, 2012). Hybrid membrane processes (HMPs) were introduced in the last years of the 20th century to solve this problem. In the HMPs process, "*one or more membrane processes is coupled with another unit process such as adsorption, ion exchange, coagulation, bioconversion, catalysis, etc.*"(Crozes et al., 1993). In the HMPs in which membrane filtration is combined with

PAC, the membrane allows PAC to remain in the reactor for longer than a slurry reactor and reduces the consumption of virgin PAC.

The Actiflo® Carb process is an HMP that is commercialized by Veolia company. In the resume, the Actiflo® Carb process recirculates a portion of the used PAC. Therefore, the HRT of PAC increases dramatically (Veolia, 2022).

The operating costs of each system are a crucial factor in the success or failure of that system compared to similar systems. Optimizing a plan is a critical issue in its development. This project aims to develop a simple and fast tool to predict the performance of recirculated PAC alongside virgin PAC in the Actiflo® Carb process. In this way, the consumption of virgin PAC will be minimized, and it is possible to use the maximum adsorption capacity of PAC.

This thesis, at first, provides an overview of the literature on NOM, the adsorption process, and the Actiflo® Carb process. In the following, the specific objectives and hypothesis of the research are presented, and the methodology of the laboratory experiments, as well as the model used to describe the dataset, are described in the methodology part. The results of the laboratory experiments and modeling are described and discussed, and finally, the examination of each specific objective, in conclusion, is made.

CHAPTER 2 LITERATURE REVIEW

The literature review section first describes natural organic matter's characteristics and removal techniques. Then, the mechanism of adsorption on activated carbon is explained in detail. Finally, the patented commercial using PAC processes for drinking water treatment is studied.

2.1 Providing background on the natural organic matter (NOM)

2.1.1 Characterization of NOM

NOM is a multiplex mixture of organic compounds from the environment's decaying vegetation found in all freshwater sources used in drinking water treatment plants (Sleighter & Hatcher, 2007). NOM generally consists of all organic compounds except synthetic organic compounds (such as insecticides) (Levchuk et al., 2018). It includes a wide variety of chemical compositions, even the composition of NOM from one water source to another is sometimes quite different. (Matilainen et al., 2011; Peydayesh et al., 2021). At the molecular level, the number of NOM compounds is over thousands, and most of its constituent molecules are still unknown (York & Bell, 2020). In recent decades, many papers have reported a significant increase in NOM in surface waters of Europe, North America, and other parts of the world (Eikebrokk et al., 2004; Rakovic et al., 2018; Sillanpää et al., 2018). And according to the climate changes, it is expected that the increase in temperature and, therefore, the increase in the biological decomposition of soil organic matter will lead to a rise in the amount of NOM (Lipczynska-Kochany, 2018; O'Driscoll et al., 2018). This shows how important it is to understand NOM better.

To describe NOM, NOM is typically divided into two groups, dissolved NOM and particulate NOM. Dissolved NOM is defined by compounds whose size is less than 0.45 μm, while particulate NOM is defined as those greater than 0.45 μm (Leenheer & Croué, 2003). particulate NOM contains a minor fraction (below 10%) of NOM (Thurman, 2012). The other method to describe NOM is dividing NOM into hydrophobic/ hydrophilic based on polarity or by acid/neutral/base (Hua & Reckhow, 2007; Matilainen et al., 2011).

The main components of the hydrophobic fractions of NOM are humic and fulvic acids, and the hydrophobic fraction is rich in aromatic carbon, phenolic structures, and conjugated double bonds. The hydrophilic fraction usually contains low-molecular-weight carbohydrates, aliphatic carbon, proteins, and amino acids (Hua & Reckhow, 2007; Krasner et al., 1996).

Indeed, no single method exists to characterize each NOM compound, but a better understanding of NOM composition is necessary to interact with NOM-derived pollutants more effectively. They can be identified as groups of compounds. In general, NOM is usually characterized by measuring one or more of the following characteristics: total organic carbon (TOC), dissolved organic carbon (DOC), UV light absorption (UV254), specific UV absorption (SUVA), fluorescence, yellow-brown color in the water, and chemical oxygen demand (Kornegay et al., 2000; Sillanpää et al., 2015).

Total organic carbon (TOC)/dissolved organic carbon (DOC)

The total carbon (TC) in a solution includes two parts, TOC and total inorganic carbon (TIC) (St-Jean, 2003). TIC consists of all carbon in an aqueous sample of inorganic origin, which can be in the form of dissolved carbonate/bicarbonate and CO_2, as well as inorganic suspended particles (Le Clercq et al., 1998). TOC includes all the carbon in an aqueous sample of organic origin. TOC contains particulate organic carbon and DOC. (Kalev & Toor, 2020).

TOC/DOC measurement is the most common measurement method used to quantify the presence of NOM. The advantage of this method is that TOC/DOC measurement equipment is inexpensive and can be used online in treatment plants where there is a possibility of rapid NOM change (Leenheer & Croué, 2003; Sillanpää et al., 2015).

Spectrophotometry measurements

As mentioned earlier, DOC/TOC measurements only measure NOM quantity. Spectrophotometric measurements, such as ultraviolet and visible (UV–Vis) absorption spectroscopy and fluorescence measurements, along with DOC measurements, lead to a better view of the NOM profile (Leenheer & Croué, 2003). The concentration of an analyte in an aqueous solution can be calculated by measuring the absorbance at a specific wavelength by applying the Beer-Lambert law (Kocsis et al., 2006). Wavelengths from 220 to 280 nm can be used to measure NOM in a solution, although it should be noted that each wavelength tends to represent a range of NOM. For example, absorption at 254 nm is mainly related to aromatic compounds with varying degrees of activation, while absorption at 220 nm is related to carboxylic and aromatic chromophores compounds (Matilainen et al., 2011). Many studies have proven a good correlation between TOC and UV_{254}, and UV_{254} is considered the most established method of measuring TOC (Albrektienė et al., 2012;

Shi et al., 2022). This simple and fast technical method for NOM determination does not require expensive measuring equipment, chemical reagents, or pretreatment but can also be installed online at water treatment sites (Shi et al., 2022).

The SUVA term is defined as the UV absorbance of a given sample at 254 nm divided by the concentration of DOC in an aqueous solution as follows (Montreuil, 2011):

$$SUVA = 100\ X\ ((UV_{254}\ (cm^{-1})) / DOC\ (mg/L) \qquad \text{Equation 2-1}$$

This ratio describes the nature of NOM in water in terms of hydrophobicity. (Health-Canada, 2019).

The term SUVA is widely used for NOM characterization because, on the one hand, it is easy to determine and does not require the installation of new equipment. On the other hand, it is a good indicator of water source quality changes. (Westerhoff et al., 2004).

Table 2-1 Relation between SUVA and NOM Characteristics

$SUVA_{254}$ (L/mg·m)	**Hydrophobicity**	**UV_{254} absorbance**
<2	Mostly hydrophilic	Low
2-4	A mixture of hydrophobic and hydrophilic components	Medium
>4	Hydrophobic with aromatic compounds	High

More classifications are also mentioned in other articles and books for NOM. Since, in this project, only the three methods described above are used for the efficiency of NOM removal by PAC, the explanation of other techniques is excluded. The reader is invited to consult (Health-Canada, 2019; Krasner et al., 1996; Matilainen et al., 2011; Sillanpää et al., 2015) for more information regarding NOM characterization.

2.1.2 Treatment of NOM

The presence of NOM in water can have several harmful and adverse effects on water purification and distribution processes and water quality, including 1- Creating aesthetic problems such as unpleasant colors, odors, and tastes. 2- Microbial growth in the distribution network. 3- Increasing the demand for coagulant and disinfectant materials in treatment plants. 4- causing fouling of membranes 5- decreasing the efficiency of adsorbents such as AC (Matilainen et al., 2011; Thurman, 2012). 6- NOM reacts with chlorine and ozone used in drinking water treatment and forms approximately 600 to 700 DBPs (Krasner et al., 2006), such as trihalomethane and haloacetic acid.

Depending on exactly what components the NOM is made of, various DBPs can be produced. The hydrophobic fraction of NOM generally constitutes the main precursors of DBPs. However, hydrophilic NOM can also significantly form DBPs, especially in waters with low humic components (Bolto et al., 2004; Krasner et al., 2006; Matilainen et al., 2011). On average, NOM in river water consists of 40% fulvic acids, 10% humic acids, 30% hydrophilic acids, 10% carbohydrates, 6% carboxylic acids, and 4% amino acids (Afghan & Chau, 1989).

Therefore, the removal of NOM is one of the main goals of raw drinking water treatment. In the last decades, various technologies have been invented to remove NOM. The most common and cost-effective NOM treatment process is coagulation and flocculation, followed by sedimentation/flotation and filtration (Okoro et al., 2021). The sub-micron size and negative surface charges of NOM particles lead to their stability in aqueous solutions and prevent flocculation and sedimentation. In the coagulation/ flocculation process, coagulants such as aluminum and iron salts are used to destabilize NOM solutions and form flocs; this process is usually accompanied by gravity settling (Sillanpää et al., 2018). The hydrophilic and low molecular weight fractions of NOM appear less prone to removal by coagulation/ flocculation than the hydrophobic and high molecular weight compounds. However, coagulation/ flocculation can sometimes be insufficient to achieve the desired treatment objectives. (Mirnasab et al., 2021).

Other treatment options for NOM removal include the anion exchange resin technique (Liu et al., 2021), membrane filtration techniques (Alresheedi et al., 2019), and advanced oxidation processes (Amiri et al., 2021), AC adsorption (Lompe et al., 2017). While NOM removal is often done before the disinfection stage, in recent years, it has been determined that if granular activated carbon

(GAC) is used during the water chlorination process, the amount of DBPs production will be lower than when the NOM removal step by GAC precedes the chlorination step (Jiang et al., 2017).

Considering that the focus of this thesis is on the adsorption of NOM on AC, in the following, this topic will be discussed in detail, and the explanation of other methods will be ignored.

2.2 An overview of adsorption processes

2.2.1 Adsorption mechanisms

Adsorbents and adsorption processes as an effective, efficient, and economical approach were widely studied and applied in drinking water (Jiuhui, 2008) and wastewater treatment (Siyal et al., 2020), as well as air (Luengas et al., 2015) and soil (Calvet, 1989) treatment. Adsorption processes are used in drinking water treatment to remove natural and synthetic organic chemicals (such as DBPs precursors) and inorganic compounds (such as some heavy metals) (Crittenden et al., 2012). Adsorption is a mass transfer operation that occurs due to the contact of a solid phase with a fluid phase. The solid phase is known as adsorbent, and the species in the liquid phase (solvent) that will be adsorbed is known as adsorbate. Adsorbate materials are transferred from the solvent into the porous solid adsorbent and are adsorbed on the surface (internal and external) of the adsorbent (Crittenden et al., 2012; Worch, 2012). This process continues until the equilibrium between the adsorbate concentration in the solution and on the adsorbent surface (Bonilla-Petriciolet et al., 2017). In some cases, such as changes in the properties of the fluid phase (temperature, pH, and concentration of adsorbate/ adsorbent) (Worch, 2012) or the presence or absence of a competing adsorbate (Pan et al., 2022), the transfer of the adsorbate from the solid phase to the solvent can also occur. This transfer of adsorbate from adsorbent to solvent is known as the desorption process. Figure *2-1* shows the general scheme of the adsorption/ desorption process.

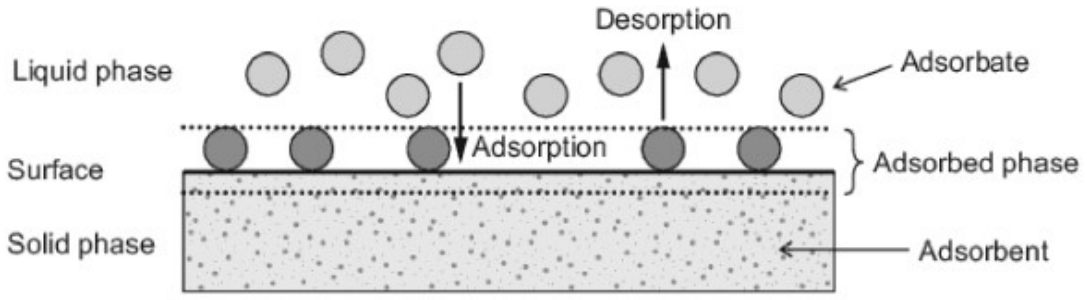

Figure 2-1 The general scheme of the adsorption/desorption process (Worch, 2012).

The process of adsorption of the adsorbate material on the surface of the adsorbent occurs for two reasons: chemical reaction (Chemisorption) (such as adsorption of carbon monoxide on palladium single crystal surfaces (Bradshaw & Hoffmann, 1978)) or physical attraction (Physical adsorption) (such as adsorption of HAAs on GAC at early stages) (Crittenden et al., 2012; Kim & Kang, 2008). Physical adsorption is usually a rapid process, reversible, with low adsorption capacity, and caused by Van der Waals interaction or electrostatic interaction between the adsorbent and adsorbate (Xia et al., 2019). Chemisorption is more selective, usually leading to irreversible adsorption. But on the other hand, it needs high activation energy and often accompanies by-products which can be considered secondary pollutions (Aljamali et al., 2021; Xia et al., 2019). Table 2-2 compares physical adsorption and chemisorption

Table 2-2 Comparison between physical adsorption and chemisorption(Crittenden et al., 2012).

Parameter	**Physical Adsorption**	**Chemisorption**
Use in water treatment	Common	Not common
Adsorption speed	Usually low and limited by mass transfer	Variable
Reaction	Reversible, exothermic, caused by Van der Waals interaction or electrostatic interaction	irreversible, exothermic, needs high activation energy

The adsorption process is a non-linear, multi-parameters function affected by the nature and concentration of the adsorbate and adsorbent and the properties of the solvent matrix (Ali & Gupta, 2006; Lompe, 2018). Also, multiple mechanisms act simultaneously in adsorption, including covalent and electrostatic interactions, surface precipitation, and chemical reactions (Tan et al., 2015).

Since chemisorption is not common in water treatment(Crittenden et al., 2012), only physical adsorption is considered in the following discussions.

2.2.2 Parameters that influence the adsorption process

Nature of the adsorbate

The nature of an adsorbent is the first and most crucial factor in the adsorption process. To better understand this process, it is necessary to know the nature of the adsorbent. Adsorbents used in the water treatment industry are divided into natural and engineered (Worch, 2012). Natural adsorbents such as chitin, natural zeolite, clay, peat moss, wood, and coal were successfully used to remove heavy metal ions, dyes, and NOM from water and wastewater (Singh et al., 2018). Engineered adsorbents are classified into the following types: carbonaceous, zeolite molecular sieves, metal-organic frameworks, mesoporous silica, and graphene oxides (Fernández-Reyes et al., 2020). Since the adsorption process takes place on the surface of the adsorbent, the surface area and porous structure of an adsorbent significantly affect its performance. The porous structure of an adsorbent allows it to have a much larger internal surface area than its external surface area. Porous-engineered adsorbents have a higher adsorption capacity than natural adsorbents due to their enormous surface area (from 500 to 2000 $m^2\ g^{-1}$ for ACs) and high pore volumes (Gupta et al., 2016; Worch, 2012). Therefore, the adsorption capacity in porous engineered adsorbents can reach up to 0.2 grams of adsorbate per gram of adsorbent (Crittenden et al., 2012). Figure 2-2 shows the pore structure and the inner surface of AC.

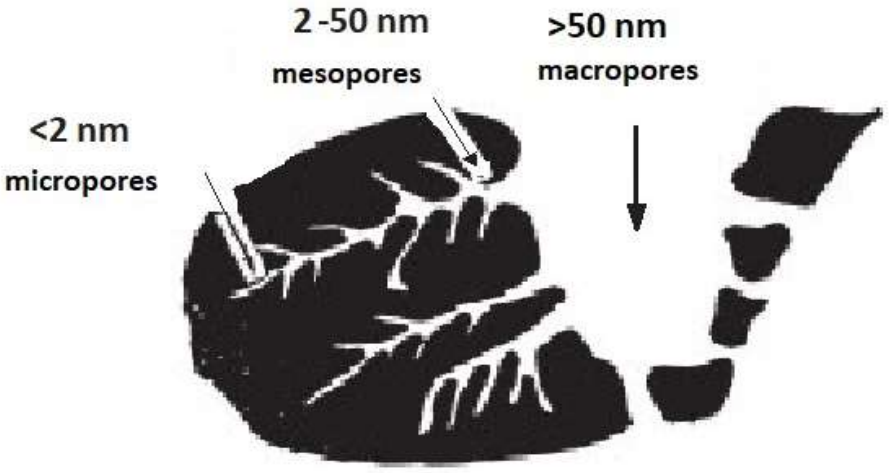

Figure 2-2 Pore structure and the inner surface of AC (Manocha, 2003).

Particle size (Pan et al., 2017), pore size (Sethia & Sayari, 2016), and surface functional groups (El-Shafey et al., 2022) of the adsorbent are other parameters that affect the kinetics and adsorption capacity.

Nature of the adsorbate

The adsorption process also is affected by the nature of the adsorbent, such as shape, size, radius, polarity, molecular weight, functional groups, hydrophobicity, aromaticity, and solubility (Aljamali et al., 2021; del Hombre Bueno et al., 2019; Lompe, 2018). Adsorbates larger than the size of the adsorbent pores cannot contact the internal surfaces of the adsorbent— considering that a significant part of the adsorption process occurs on the adsorbent's inner surface; therefore, the adsorption rate increases with the reduction of adsorbate size (Aljamali et al., 2021; Crittenden et al., 2012). For non-polar adsorbates, the affinity between an adsorbate and a polar solvent (like water) is generally weaker than the affinity between an adsorbent and a hydrophobic adsorbent (such as AC). Therefore, hydrophobic adsorbents are most effective when used to remove less polar, more hydrophobic, and uncharged adsorbates (Lompe, 2018).

The properties of the solvent matrix

The change in properties of the solvent matrix (such as temperature, pH value, ionic force, and presence of competing adsorbates) affects the adsorbent surface chemistry and the properties of the adsorbate, thereby affecting the capacity and kinetic of adsorption (Worch, 2012).

The pH value of the solution changes the surface charge of the adsorbate molecules, thus changing the affinity with water. In general, the optimal pH for adsorption neutralizes organic molecules, (Dauphin, 2017).

Temperature affects the adsorption process in several ways, sometimes oppositely. A change in temperature affects the polarity and ionization of solvent, adsorbate solubility, and affinity between adsorbent and adsorbent. Therefore, for each adsorption system, the effect of temperature should be measured according to the system conditions (Bonilla-Petriciolet et al., 2017). For example, for NOM adsorption on AC, it is generally accepted that adsorption is *slightly* more efficient at lower temperatures (Dauphin, 2017). In contrast, the rate of adsorption kinetics of phenoxy pesticides on AC increases with increasing temperature (Marczewski et al., 2016). In the water treatment

process, the effect of temperature change is relatively small and neglected in most cases (Worch, 2012).

In solutions that contain more than one adsorbate component, the number of parameters required to describe the process increases. The competition between adsorbates for access to the adsorbent surface will change the attraction between adsorbent and adsorbate. Therefore, the adsorption kinetics and equilibrium concentration of each adsorbent is a function of the concentration of other pollutant components (Noroozi & Sorial, 2013). For instance, NOM reduces the removal efficiency of organic target molecules (such as 2-methylisoborneol) by PAC (Matsui et al., 2012). In general, two main processes were identified in the competition of adsorbates, 1- direct competition between adsorbates for adsorption sites, 2- blocking of the pores by larger adsorbates, which prevents smaller adsorbates from reaching the internal surfaces of the adsorbent (Çeçen & Aktas, 2011).

2.2.3 The general principles of adsorption equilibrium and kinetic

In the next section, adsorption models and theories are discussed. Due to the multitude of models and theories, only the basic principles of adsorption models and the models used in this thesis will be discussed.

Single-solute adsorption

As mentioned above, the presence of more than one adsorbate in the solution may affect the adsorption performance. Therefore, the adsorption models are usually based on single-solute adsorption and then address the effect of the presence of multiple adsorbates on the adsorption process of each of them.

multi-solute solutions adsorption

In practice in the water treatment industry, removing only one adsorbate on an adsorbent is an infrequent phenomenon. The purpose of adsorption in most real systems is to remove several pollutants simultaneously (Crittenden et al., 2012). Several models and theories were developed to describe and predict multi-solute adsorption isotherm. The extended Langmuir isotherm (Butler & Ockrent, 1930; Jain & Snoeyink, 1973) is the earliest method for multi-solute adsorption. In solutions that behave ideally in both liquid and adsorbent phases, ideal adsorbed solution theory (Myers & Prausnitz, 1965) (IAST) can be used to predict the adsorption equilibrium of multiple

solutes based on the single solute isotherms. The other theory is the vacancy solution theory (Suwanayuen & Danner, 1980a, 1980b) which is suitable for describing multi-solute adsorption in dilute solutions (Noroozi & Sorial, 2013). The fact that NOM contains an unknown complex mixture of natural organic compounds makes none of the above original theories able to correctly predict and describe the adsorption of NOM. Therefore, only the collective parameter DOC is commonly used in isotherm equations rather than individual NOM components (Worch, 2012). However, NOM is considered a *pseudo-single solute* by accepting the model's errors.

Isotherm Equilibrium

The adsorption capacity of an adsorbent is a fundamental parameter for an adsorption process that is usually measured in batch experiments at constant temperature and pH. Adsorption equilibrium is achieved when the concentration of the adsorbate in the liquid phase and on the surface of the adsorbent does not change with time; at the equilibrium point in irreversible adsorption (mainly chemisorption), the rate of transfer of the adsorbate from the liquid phase to the solid phase is equal to the rate desorption from the solid phase. And in reversible adsorption processes (mainly physical adsorptions), the transfer of the adsorbate from the liquid phase to the solid phase will be stopped (Bonilla-Petriciolet et al., 2017). The adsorbent loading (q_{eq}) (M/M) on a specific adsorbent in equilibrium is a function of the adsorbate concentration (C_{eq}) (M/L^3) and the temperature.

$Q_{eq} = f\,(C_{eq}, T)$ *Equation 2-2*

In practice, the temperature is kept constant in the adsorption equations, and the equilibrium relation is rewritten as below: (Worch, 2012)

$q_{eq} = f\,(C_{eq},), \quad T=constant$ *Equation 2-3*

The adsorbent load is obtained from the difference between the initial concentrations (C_0) (M/L^3) and final concentrations (C_{eq}) (M/L^3) of the adsorbate, solute volume, and the mass of the adsorbent: (Worch, 2012)

$$q_{eq} = \frac{V_L}{m_A}\left(C_0 - C_{eq}\right) \quad \textit{Equation 2-4}$$

Where V_L is the solute volume(L^3), and m_A is the mass of the adsorbent (M).

There are many models for equilibrium isotherms, among which Langmuir and Freundlich are the most used for adsorption in aqueous solutions. Langmuir's model is based on theoretical considerations, and Freundlich's model is based on experimental data (Crittenden et al., 2012).

The Langmuir isotherm is based on the following assumptions:

- There are several adsorption sites on the surface of the adsorbent.
- Each of these sites can adsorb a single molecule.
- Each of these sites has the same affinity for adsorbate.
- Activity of the site does not affect other sites (Desjardins, 1997).

$$q_{eq=} = \frac{q_m\, bC_{eq}}{1+bC_{eq}} \quad \textit{Equation 2-5}$$

Where q_m (with the same unit of q) and b (reciprocal unit of the adsorbate concentration) repesent coefficients of Langmuir's equation.

The Freundlich isotherm is an empirical equation widely used in the water treatment industry, which fits well in the adsorption of pollutants on PAC. However, it does not always obey Henry's law, and omits the thermodynamics of the reaction (Worch, 2012).

$$q_{eq} = q_0 + \int dq = K_F\, C_{eq}^{\frac{1}{n}} \quad \textit{Equation 2-6}$$

Or

$$\textit{Log } q_{eq} = \textit{log } K_F + \textit{1/n log } C_{eq} \quad \textit{Equation 2-7}$$

Where adsorption coefficient K_F represents the adsorption capacity (unit depends on units of q_{eq} C_{eq} and 1/n) and adsorption coefficient 1/n (unitless) describes the affinity between the adsorbent and the adsorbate (Worch, 2012).

Adsorption kinetics models

In water purification processes, the contact time between PAC and the raw water (solvent + pollutants) is usually much shorter than the time the adsorbent needs to reach equilibrium. Therefore, the kinetic and thermodynamic aspects of adsorption must be involved to characterize the function and mechanisms of adsorption before the total capacity is reached. In such cases, the

determination of the residence time of adsorbate in the reactor is one of the most critical factors in designing an adsorption process (Worch, 2012).

Two categories of adsorption kinetic models are presented. The first category includes adsorption reaction models (empirical models), which are based on the entire process of adsorption. In these methods do not consider the adsorption mechanism steps. The second category includes adsorption diffusion models, which are based on three steps: 1- external diffusion in the boundary film around the adsorbent, 2- internal diffusion in the pores of adsorbents, and 3- adsorption and desorption between the adsorbate and adsorption sites. (Qiu et al., 2009). The pseudo-first-order, the pseudo-second-order, and the Elovich equations are among the most widely used adsorption reaction models (Bonilla-Petriciolet et al., 2017). Diffusion models include one or both the surface diffusion coefficients (D_s) and the pore volume diffusion coefficients (d_p) in their assumptions and equations. The most widely used models are pore volume diffusion model (PVDM), surface diffusion model (SDM), pore volume and surface diffusion model (PVSDM), and homogeneous surface diffusion model (HSDM) (Lima et al., 2020; Queiroz et al., 2022). Figure 2-3 shows the adsorption process's primary mass transfer and diffusion mechanisms (Bonilla-Petriciolet et al., 2017).

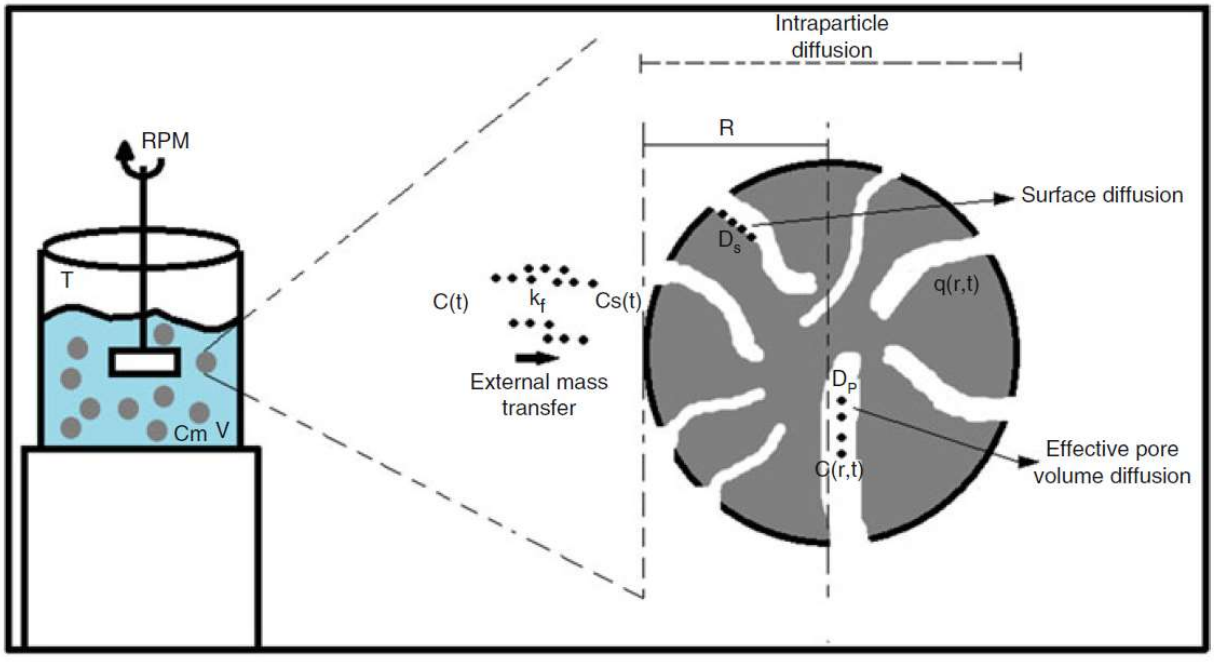

Figure 2-3 The primary mass transfer and diffusion mechanisms in the adsorption process

- Pseudo-first-order model

The pseudo-first-order equation was first demonstrated by Lagergren in 1898. Assuming that adsorption follows a first-order rate law, the kinetics of adsorption can be written as follows (Qiu et al., 2009):

$$\frac{dq(t)}{dt} = k_{p1}(q_{eq} - q(t)) \quad \textit{Equation 2-8}$$

Where k_{p1} (T^{-1}) represents the first-order rate constant, q_{eq} the adsorption capacity at equilibrium (M adsorbate / M adsorbent), and q(t) the adsorption capacity at a given time. Integration with the condition q(t)=0 at t=0 gives:

$$ln\left(\frac{q_{eq}}{q_{eq}-q(t)}\right) = k_{p1}t \quad \textit{Equation 2-9}$$

- Pseudo-second-order model

The pseudo-second-order rate law is another reaction kinetic approach, which is successfully applied to the adsorption of metal ions, dyes, and organic compounds from aqueous solutions (Bonilla-Petriciolet et al., 2017). For instance, Dauphin showed that NOM adsorption on the surface of PAC in bench-scale hybrid reactors could be modeled with a pseudo-second-order model (Dauphin, 2017). The pseudo-second-order model is expressed as follows (Ho & McKay, 1998):

$$\frac{dq_t}{dt} = k_{p2}\left(q_{eq} - q_{(t)}\right)^2 \quad \textit{Equation 2-10}$$

Where k_{p2} (T^{-1}) represents the first-order rate constant. Integration with the condition q(t)=0 at t=0, and q(t)=q(t) at t=t gives:

$$\frac{t}{q(t)} = \frac{1}{K_{p2}q_{eq}^2} + \frac{1}{q_{eq}}t \quad \textit{Equation 2-11}$$

- The Elovich equation

The kinetic equation of Elovich was originated by Zeldowitsch (1934) and used to describe the adsorption rate of carbon monoxide on manganese dioxide in a gaseous environment; in this process, the adsorption rate decreases exponentially with the increase of adsorbed gas. The following differential equation expresses the Elovich equation (Qiu et al., 2009):

$$\frac{dq_t}{dt} = \alpha e^{-\beta q(t)} \quad \textit{Equation 2-12}$$

Where α represents the desorption constant, and β represents the initial adsorption rate. Integration with the condition q(t)=0 at t=0, and q(t)=q(t) at t=t gives:

$$q(t) = \beta\, ln(\alpha\beta) + \beta\, ln\, t$$ *Equation 2-13*

This equation was later used to describe the adsorption process of different adsorbates from an aqueous environment. For instance: the adsorption of lead by activated carbon (Largitte & Pasquier, 2016), adsorption of chromium (VI) by bioadsorbents (Villabona-Ortíz et al., 2020).

However, in recent years, many articles have been published describing adsorption kinetics with simple models based on chemical reaction kinetics. It should be kept in mind that because these models are not based on adsorption chemistry, the constants of each equation are limited to their test conditions (Worch, 2012). For example, if the concentration of the adsorbent or adsorbate changes, the constant coefficient of the pseudo-first-order equation will change, and the coefficient must be obtained separately for the new conditions.

- HSDM model

Adsorption on a solid adsorbent in a liquid medium includes film diffusion, intraparticle diffusion, and mass action. In general, in physical adsorptions, mass action is a fast process that can be negligible (Qiu et al., 2009). Suppose the adsorption medium is stirred homogeneously with high shaking velocities. In that case, the external diffusion of the adsorbate towards the adsorbent surface is not limited, and the mass transfer can be determined by pore or surface diffusion models (Lompe, 2018). As an intraparticle diffusion model, the HSDM is the most frequently used model. which can describe the surface loading rate change over time at any distance from an amorphous and homogeneous sphere adsorbent particle center. In the HSDM model, it is assumed that the instantaneous equilibrium of the adsorbate concentration in the liquid (Cs) and the adsorbate concentration in the external layer of the adsorbent (q_s). The following differential equation expresses the HSDM equation:(Worch, 2012)

$$\frac{\partial q}{\partial t} = D_s \left(\frac{\partial^2 q}{\partial r^2} + \frac{2}{r}\frac{\partial q}{\partial r}\right)$$ *Equation 2-14*

Where D_s (L2/T) represents the rate of diffusion of the adsorbate along the surface of the adsorbent and r is the distance from the center of the adsorbent, in general form, the adsorbent have a preloaded concentration at t=0,

at $t= 0, \quad 0 \leq r \leq R \quad q=q_0(r)$ *Equation 2-15*

if the virgin adsorbent use;

$q_0(r) = 0$ *Equation 2-16*

with two boundary conditions:

at $r=0, \quad t \geq 0 \quad \frac{\partial q}{\partial q}=0$ *Equation 2-17*

at $r=R \quad q_s=K_F C_s^{1/n}$ *Equation 2-18*

Where K_F and n represent the Freundlich equilibrium constants, R is the radius of the adsorbent particle (L), and C_{eq} (M/L^3) is the adsorbate concentration at the equilibrium point. In a batch reactor (or plug flow reactor), Najm used the equation's numerical integration to describe adsorption of organic compounds onto virgin PAC (Najm, 1996):

For batch or plug-flow reactors:

$$0 = C_{inf} - C_{eff} - 3C_{PAC}K_F C_{eff}^{1/n}\left\{0.33334 - 0.04903e^{\left(-142.634\frac{tD_s}{R^2}\right)} - 0.05399e^{\left(-3\ .996\frac{tD_s}{R^2}\right)} - 0.20240e^{\left(-9.8686\frac{tD_s}{R^2}\right)}\right\}$$ *Equation 2-19*

Considering the initial condition:

at $t = 0 \quad C_{eff} = C_{inf}$ *Equation 2-20*

Where C_{eff} represents the concertation of organic matter (adsorbate), C_{inf} is the initial concentration of organic matter, and C_{PAC} is the PAC concentration.

For continuously stirred tank reactor (CSTR):

$$0 = C_{inf} - C_{eff} - C_{PAC}K_F C_{eff}^{1/n}\left\{1 - \frac{6}{\pi^2}\sum_{i=1}^{\infty}\left(\frac{1}{i^2\left(1+\left(\frac{\pi^2 i^2 D_S \tau}{R^2}\right)\right)}\right)\right\}$$ *Equation 2-21*

Where, τ (T) is residence time of the reactor.

Table 2-3 – Kinetic models of adsorption.

Process Control	Kinetic law	Nonlinear form	Linear form
Adsorption	Pseudo-first-order	$\frac{dq(t)}{dt} = k_{p1}(q_{eq} - q(t))$	$ln\left(\frac{q_{eq}}{q_{eq} - q(t)}\right) = k_{p1}t$
	Pseudo-second-order	$\frac{dq_t}{dt} = k_{p2}\left(q_{eq} - q_{(t)}\right)^2$	$\frac{t}{q(t)} = \frac{1}{K_{p2}q_{eq}^2} + \frac{1}{q_{eq}}t$
	Elovich	$\frac{dq_t}{dt} = \alpha e^{-\beta q(t)}$	$q(t) = \beta\, ln(\alpha\beta) + \beta\, ln\, t$
Internal diffusion	HSDM	$\frac{\partial q}{\partial q} = D_s\left(\frac{\partial^2 q}{\partial r^2} + \frac{2}{r}\frac{\partial q}{\partial r}\right)$	$0 = C_{inf} - C_{eff} - 3C_{PAC}K_F C_{eff}^{1/n}\left\{0.33334 - 0.04903e^{\left(-142.634\frac{tD_s}{R^2}\right)} - 0.05399e^{\left(-39.996\frac{tD_s}{R^2}\right)} - 0.20240e^{\left(-9.8686\frac{tD_s}{R^2}\right)}\right\}$
			$0 = C_{inf} - C_{eff} - C_{PAC}K_F C_{eff}^{1/n}\left\{1 - \frac{6}{\pi^2}\sum_{i=1}^{\infty}\left(\frac{1}{i^2\left(1 + \left(\frac{\pi^2 i^2 D_s \tau}{R^2}\right)\right)}\right)\right\}$

2.3 Activated carbon for NOM control

2.3.1 Advantages and disadvantages of using PAC vs GAC

NOM adsorption onto AC is an effective process in water treatment, which can be used as PAC or GAC. PAC is typically used seasonally, during coagulant dosing before the coagulation/flocculation step or during settling before sand filtration. For example, in the case of a sudden increase in NOM or cyanobacterial toxins, PAC is added to the system and removed as a waste product in the sedimentation step (Figure 2-4). In contrast, GAC is usually used as a continuous application, as the last treatment step before water disinfection and distribution (Figure 2-5). Unlike PAC, GAC can be regenerated and reused by heat or steam (Pivokonsky et al., 2021; Worch, 2012).

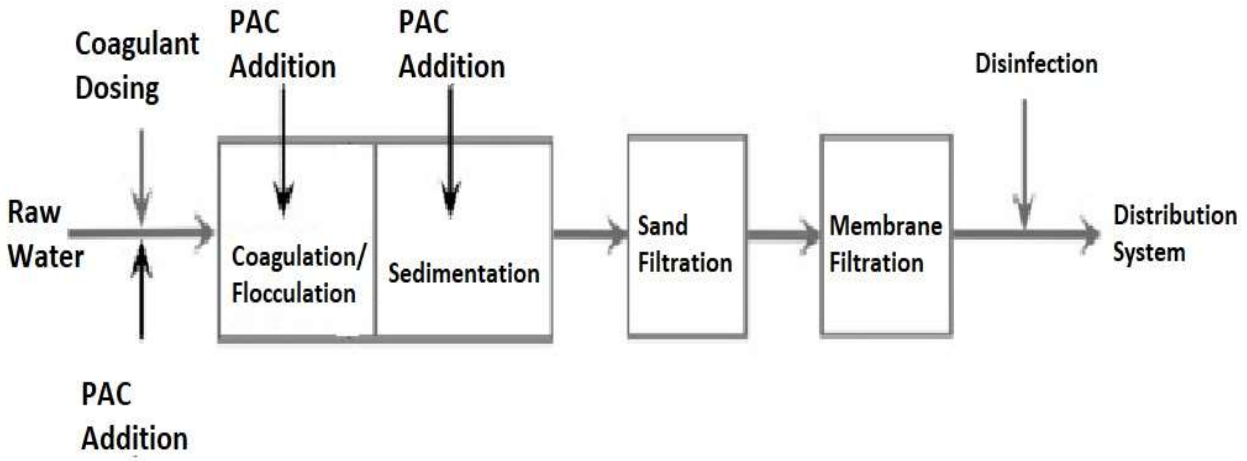

Figure 2-4 An example of a common PAC application in a water treatment plant.

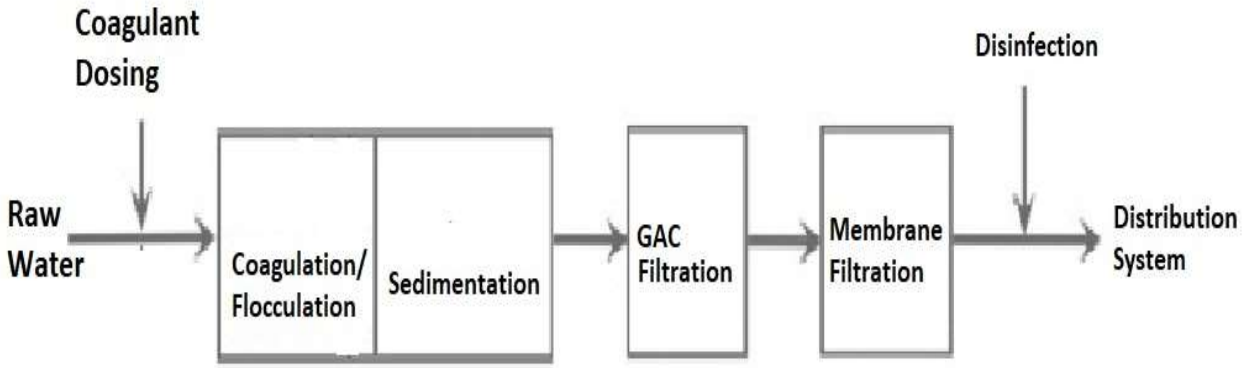

Figure 2-5 An example of a common GAC application in a water treatment plant (Pivokonsky et al., 2021).

Table *2-4* shows the characteristic of GAC and PAC, also compares advantages and disadvantages of using of them.

Table 2-4 Comparison of GAC with PAC

	GAC	PAC
Particle Size	0.6 - 2.0 mm	10 - 40 μm
Reactor type	Fixed bed	Slurry
Advantages	- The entire absorption capacity of the GAC is used - Can be regenerated (reactivated)	- Easy application - Suitable for uncertain level of contaminants such as seasonal contaminants - Inexpensive infrastructure
Disadvantages	- Expensive filters are needed to keep GAC inside the reactor	- Only a small fraction of the adsorption capacity is used, due to the short hydraulic retention time (HRT) of PAC in slurry reactors
Consumption rate	Low	High

2.3.2 Hybrid Membrane Processes (HMPs)

Low-pressure membrane filtration processes are one of the conventional treatment processes in both drinking water and wastewater treatment units. However, the broader implementation of Low-pressure membrane is limited due to membrane fouling and incomplete removal of dissolved organic constituents (Li et al., 2019). In the HMPs, in which membrane filtration is combined with PAC, dissolved organic compounds can be removed by adsorption on PAC and then membrane separation (Campos et al., 2000). This combination increases the HRT of PAC in the system with more than one slurry reactor. On the other hand, by adsorption of a certain fraction of NOM, the flocculation on the surface of the membrane filter will be decreased, increasing the filtration cycle period (Löwenberg et al., 2014). Since the adsorption process is time-dependent, the efficiency of PAC in an HMPs system is increased compared to slurry reactors. Typically, three procedures are

used to dose virgin PAC into a membrane reactor and remove aged PAC from the reactor. These procedures determine the residence time of PAC particles and whether the process is carried out under steady-state or transient conditions (Campos et al., 2000). Virgin PAC can be added to the HMP continuously at a constant rate, whereby the PAC concentration in the reactor constantly increases during the filtration period (step input). Also, virgin PAC can be added to the HMP at the beginning of the filtration cycle (pulse input). In non-steady state systems, adsorbate concentration is not constant during the filtration cycle. In the step input HMPs, the adsorbate concentration in the permeate stream increases continuously. In the pulse input HMPs, it may decrease or increase depending on the PAC injection rate. In steady state systems, the PAC concentration is kept constant by continuous injection on the one hand and purging, on the other hand, considering that the PAC concentration and adsorbate in these systems are constant during the filtration cycle, they can be modeled as continuous-flow-stirred-tank-reactor (CSTR) (Campos et al., 2000; Stoquart et al., 2012). Figure 2-6 shows a Schematic of the HMP with integrated PAC treatment.

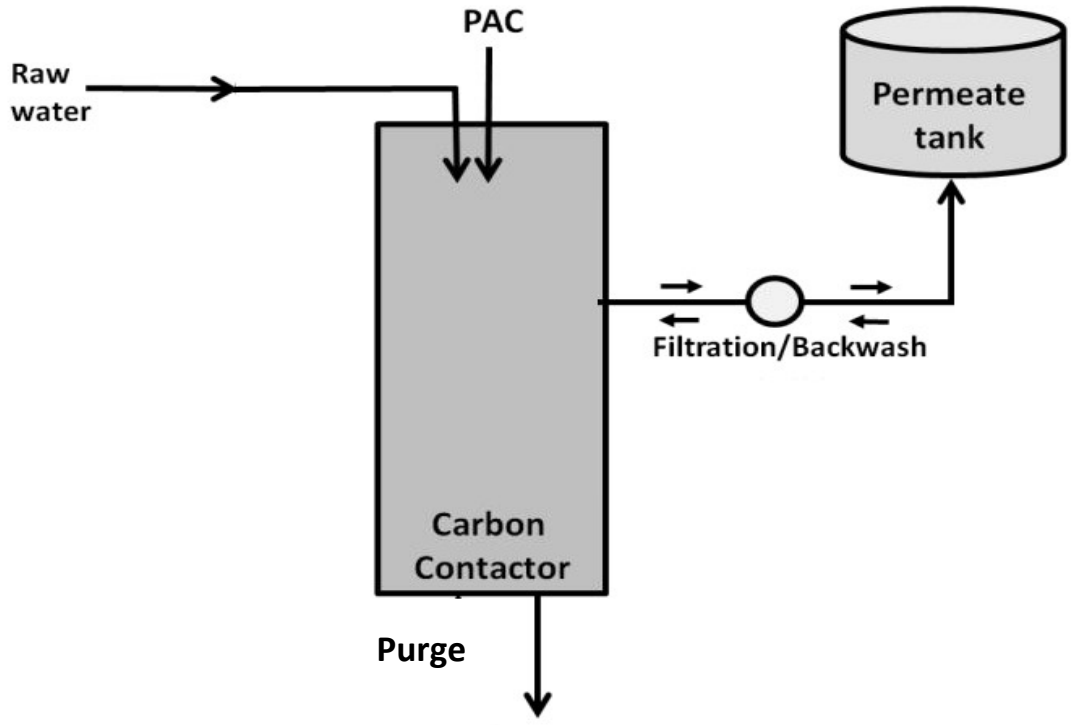

Figure 2-6 Schematic of the HMP with integrated PAC treatment.

2.4 Actiflo® Carb/ OpalineTM

2.4.1 Actiflo® Carb/ OpalineTM process

The OpalineTM process, is an HMP which developed by Veolia company, to remove NOM from raw water. In this process, membrane reactors is coupled with integrated AC treatment. Veolia provides two configurations for the OpalineTM process; the first is a fixed bed filter with GAC. And in the second approach, the carbon contactor uses suspension PAC, which usually is the Actiflo® Carb process.

In the Actiflo® Carb process, two methods of coagulation/ flocculation, and adsorption on PAC, are used to remove NOM. As mentioned earlier, the process of coagulation/ flocculation can remove a significant part of NOM. Combining this process with PAC maximizes the removal of coagulable and non-coagulable NOM and produces high-quality water. The Actiflo® Carb process includes the following steps:

- PAC Tank: In this stage, PAC (including virgin PAC and reticulated PAC) is added to raw water inside a mixer. The hydraulic retention time in this reactor is usually 5 to 10 minutes. A significant part of the adsorption process takes place in this reactor.
- Coagulation Tank: In the second tank, a coagulant is added to the water; the coagulation operation completes the NOM removal process and causes PAC coagulation.
- Flocculation Tank: In this tank, micro sand and polymer are injected into the water to flocculate and complete the coagulation process.
- Sedimentation Tank with mixers and scraper: At this stage, dense clots are separated from the purified water. Clean water comes from the upper part and flows towards the membrane filters. And the sludge (aged PAC, micro-sand, and coagulant sludge) is transferred to hydrocyclone.
- Hydrocyclone: In the hydrocyclone, the micro-sand is separated from the sludge and returned to the flocculation tank.
- Sludge Purge: Normally, 5 to 10% of the sludge (which contains aged PAC) is removed from the system to maintain the PAC concentration constant, and the rest of the sludge is injected into the first tank along with the virgin PAC.

Figure 2-7 shows a diagram of the Actiflo® Carb process.

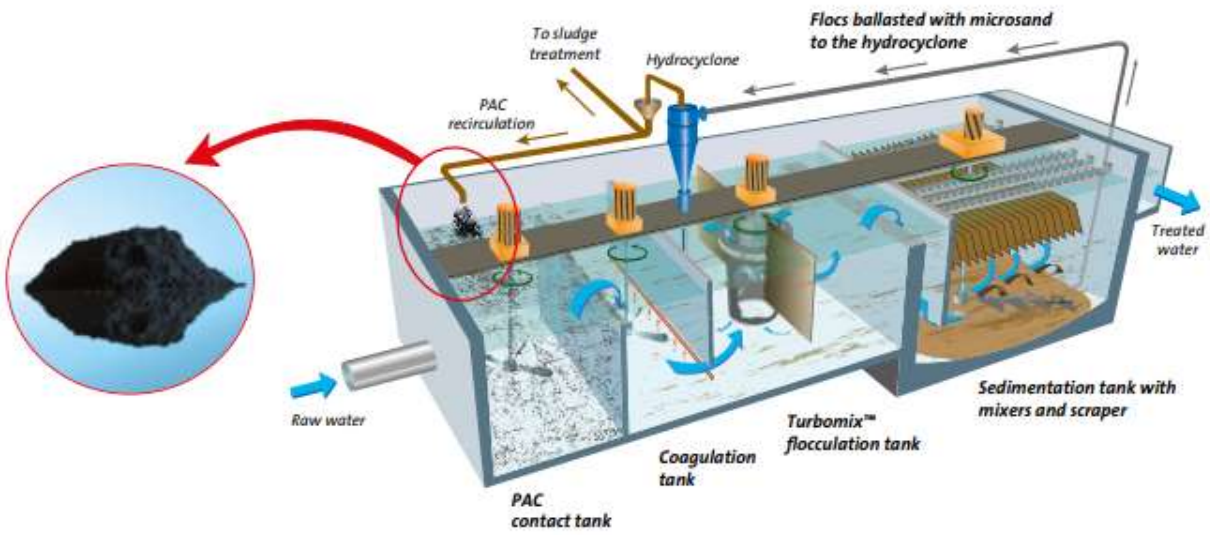

Figure 2-7 Diagram of the Actiflo® Carb process (Veolia, 2022)

2.4.2 Prediction of Actiflo® Carb process

Actiflo® Carb process uses recirculated PAC and virgin PAC in the same reactor simultaneously. Therefore, the performance of adsorption in this process is difficult to predict without the development of a rapid laboratory method.

In previous studies, it is shown that HSDM could be applied for CSRT reactors and batch reactors where they are fed by virgin PAC. (Najm, 1996). On the other hand, HSDM could also be applied for HMP reactors where raw water is fed continuously and virgin PAC is fed continuously or once (step input or pulse input, respectively) (Campos et al., 2000). But a model applicable to the configuration of the Actiflo® Carb does not currently exist.

It is suggested that modeling the bench-scale flow-through HMP reactor (Amicon cell) filled with pulse input of virgin PAC is useful to predict the Actiflo® Carb. In this figuration, virgin PAC gets exhausted (aged) over time. On the other hand, as the virgin PAC is fed once, the load of all PACs is the same. Therefore, the performance of the reactor at any given moment represents the performance of the aged PAC corresponding to that time. So, by modeling the Amicon cell, the performance of aged PAC would be predictable.

In the end, by considering the age distribution in the Actiflo® Carb process and using Amicon cell models, the Actiflo® Carb will be modeled (Dauphin, 2017). However, this hypothesis has not been tested with an industrial-scale Actiflo® Carb process. Figure 2-8 shows the schematic of the Amicon cell.

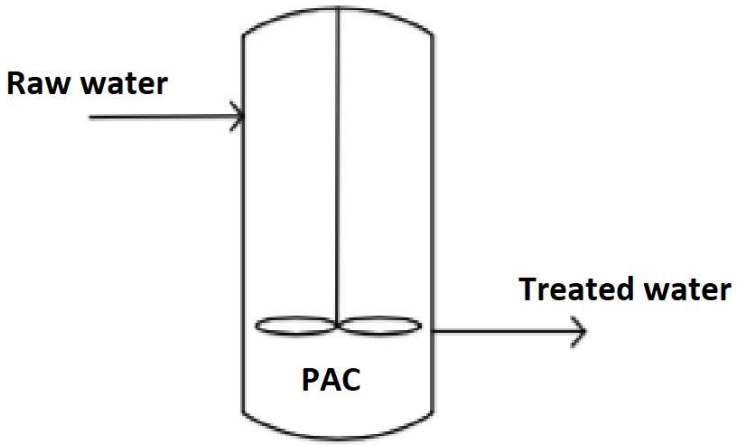

Figure 2-8 the schematic of the Amicon cell.

2.5 Desorption process from the aged PAC

As mentioned above, the physical adsorption process is a reversible reaction. In systems that use AC as adsorbate, desorption is an undesirable consequence that results from: a) reduction in the concentration of a pollutant in water b) change in the composition of the influent stream c) longer retention of adsorbent than adsorbates in a system with several adsorbates. So systems work with GAC filters or recirculated PAC stages could be affected by potential desorption (Aschermann, Schröder, et al., 2019) (Aschermann, Neubert, et al., 2019). In the case of water treatment, the desorption of pollutants during treatment is undesirable not only because it reverses the process, but also because it leads to an increase in the AC doses, in the result increasing the total treatment process cost (Sang et al., 2022). there are two mechanisms that can lead to desorption (a) a displacement of adsorbate with a competitive adsorbate from an adsorption site (b) a reversion of the reaction pathway due to high adsorbate loading on the surface of the adsorbent and low adsorbate concentration in the liquid phase (Aschermann et al., 2018).

CHAPTER 3 RESEARCH OBJECTIVES AND HYPOTHESIS

3.1 Main objective

The main objective of this project is to develop a simple and rapid laboratory assay to predict the performance of aged PAC alongside virgin PAC in the Actiflo® Carb process for removing NOM from raw water. To reach this goal, two ***separate approaches*** are defined. First approach is using the bench-scale flow-through HMP reactor (Amicon cell) as Dauphin suggested previously.

The second approach is using the batch reactor and investigating the effect of PAC aging and mixing different aged PACs on sorption parameters. Then, by determining sorption parameters for a suspension with different aged PACs, the Actiflo® Carb reactor would be modeled by HDSM.

Sub-objectives 1 and 2 are related to the first and second approaches, respectively.

3.2 Sub-objective 1: To assess the suitability of the bench-scale flow-through HMP reactor (Amicon cell) for modeling the Actiflo® Carb process

Previously, it was shown that the adsorption of NOM on PAC in an Amicon cell reactor would be modeled with pseudo-first-order and pseudo-second-order kinetic models (Dauphin, 2017). In Dauphin's studies, the effect of PAC concentration and HRT on the Amicon Cell breakthrough curve have been studied. But only two different PAC concentrations and two HRTs were studied. Also, the phenomenon of PAC accumulation on the surface of the membrane in the Amicon cell was not studied in detail. Therefore, this sub-objective was divided into three following parts.

PAC accumulation on the surface of the membrane

During the pretests, it was observed that a layer of PAC accumulated on the surface of the membrane, which is an undesirable phenomenon. Therefore, in the first part of this sub-objective, the reason for this accumulation (sedimentation or advection) will be studied. Also, the effect of the PAC concentration, HRT, flow direction, and the stirrer's rotation speed (SRS) on PAC accumulation rate on the surface of the membrane in the Amicon cell will be studied, which helps to select an Amicon cell condition with the less PAC accumulation rate.

The of effect physical conditions of the reactor on the PAC performance

In the second part, the effect of the physical conditions of the reactor (the volume of reactor, membrane diameter, PAC concentration, SRS, and HRT) on the PAC performance in the Amicon cell will be investigated

Modeling the Amicon cell

In the third part, the Amicon cell will be modeled with three empirical models (pseudo-first-order and pseudo-second-order, and Elovich models). And the ability of this model to predict the performance of a reactor filled with aged PAC will be studied.

If the influence of the physical conditions of the reactor on the PAC performance is insignificant, and the above models (at least one of them) have acceptable accuracy in predicting of aged PAC performance, the modeling of the Amicon cell reactor will be considered an inexpensive and rapid tool to predict the more complex reactors such as the Actiflo® Carb. Otherwise, other solutions should be used to achieve this purpose.

3.3 Sub-objective 2: Investigation of the effect of PAC aging and mixing different aged PACs on sorption parameters

This section aims to determine sorption parameters (such as isotherm parameters and surface diffusion coefficient) for the aged PAC and the mixture of different aged PACs. Previous studies used the HSDM model for virgin PAC (Campos et al., 2000; Najm, 1996). In this study, first, the possibility of applying the HSDM model on a reactor filled with single-aged PAC will be studied. And the effect of PAC aging on sorption parameters will be investigated (compared to virgin PAC). Then, the effect of mixing different aged PACs on PAC performance will be studied.

By determining the sorption parameters for aged PAC and the mixture of different aged PACs, it would be possible to use HSDM to model a reactor with a PAC recirculating system.

3.4 Sub-objective 3: Prediction of adsorption in the Actiflo® Carb process

In this step, with the knowledge gained from the previous stages, the NOM adsorption on the PAC in the Actiflo® Carb reactor will be modeled and validated by samples and data taken from a full-scale reactor (installed in a water treatment plant in California (USA)).

Table 3-1shows the assumptions associated with the sub-objectives and the methods to verify the assumptions as well as to refute them

Table 3-1 Hypothesis and objectives of project

Hypothesis and justification	**Objectives**
- The PAC concentration, and HRT do not affect the PAC accumulation rate on the surface of membrane - This hypothesis can be verified by measuring PAC accumulation rate. - This hypothesis will be refuted if PAC accumulation rate for different PAC concentrations and HRT are statistically different.	To assess the ability of the bench-scale flow-through HMP reactor (Amicon cell) for modeling the Actiflo® Carb process
- The physical conditions of the reactor (the volume of reactor, membrane diameter, PAC concentration, SRS, and HRT does not affect the Amicon cell breakthrough curve when the performance of the reactor is normalized by Carbon usage rate (CUR) (L water/g PAC) - This hypothesis can be verified by making breakthrough curves with different physical conditions of the reactor. - This hypothesis will be refuted if the Amicon cell breakthrough curves for different physical conditions of the reactor are statistically different.	To assess the ability of the bench-scale flow-through HMP reactor (Amicon cell) for modeling the Actiflo® Carb process
- The Amicon cell models can predict the performance of a second Amicon cell filled with aged PAC - This hypothesis can be verified by making breakthrough curves with different aged PAC. - This hypothesis will be refuted if the breakthrough curves for different ages of PACs are statistically different.	To assess the ability of the bench-scale flow-through HMP reactor (Amicon cell) for modeling the Actiflo® Carb process

Table 3-1 Hypothesis and objectives of project (continue)

- Initial PAC load does not affect isotherm equilibrium - This hypothesis can be verified by doing isotherm tests with different initial ages of PACs - This hypothesis will be refuted if the isotherm parameters (such as K_F and 1/n) differ for different initial PAC load.	Investigation of the effect of PAC aging and mixing different aged PACs on sorption parameters
- Initial PAC load does not affect the surface diffusion coefficient - This hypothesis can be verified by doing isotherm/kinetic tests with different initial ages of PACs - This hypothesis will be refuted if the surface diffusion coefficient differs for different initial PAC load.	Investigation of the effect of PAC aging and mixing different aged PACs on sorption parameters
- A mixture of different ages of PAC performs as a solution with mass-weighted average loading of all PACs. - This hypothesis can be verified by doing isotherm/kinetic tests with mixed-aged PACs - This hypothesis will be refuted if predicted concentration DOC at the effluent (C_{eff}) differs from measured C_{eff}.	Investigation of the effect of PAC aging and mixing different aged PACs on sorption parameters
- The HSDM can predict the Actiflo® carb process - This hypothesis can be verified by performing isotherm/kinetic tests with samples from a real-scale reactor and modeling the Actiflo® Carb process. - If the HSDM result differs from the Actiflo® Carb process data, the assumption will be rejected.	Prediction of adsorption in the Actiflo® Carb process

3.5 The originality of the research

The originality of the research subject is justified since there is currently no method to simulate the Actiflo® Carb process at laboratory-scale for NOM removal. Several factors (such as the nature of raw water and adsorbent characteristic) affect the adsorption process. Laboratory tests can determine these effects at a low cost. This study provides the possibility of predicting the effectiveness of the NOM treatment for the potential customer of the process, minimizing the time and cost of setting up/piloting or optimizing the performance of existing infrastructures.

CHAPTER 4 METHODOLOGY

In this chapter, the methods used to achieve the goals of the project are presented.

4.1 To assess the suitability of the bench-scale flow-through HMP reactor (Amicon cell) for modeling the Actiflo® Carb process

4.1.1 Bench-scale HPM reactor assembly

The experimental setup is developed as a bench-scale set up, the same as used in Dauphin's study (as shown in Figure 4-1). The reactor used in this test is a flow-through Amicon cell filled by pulse input of virgin PAC and continuous flow of water.

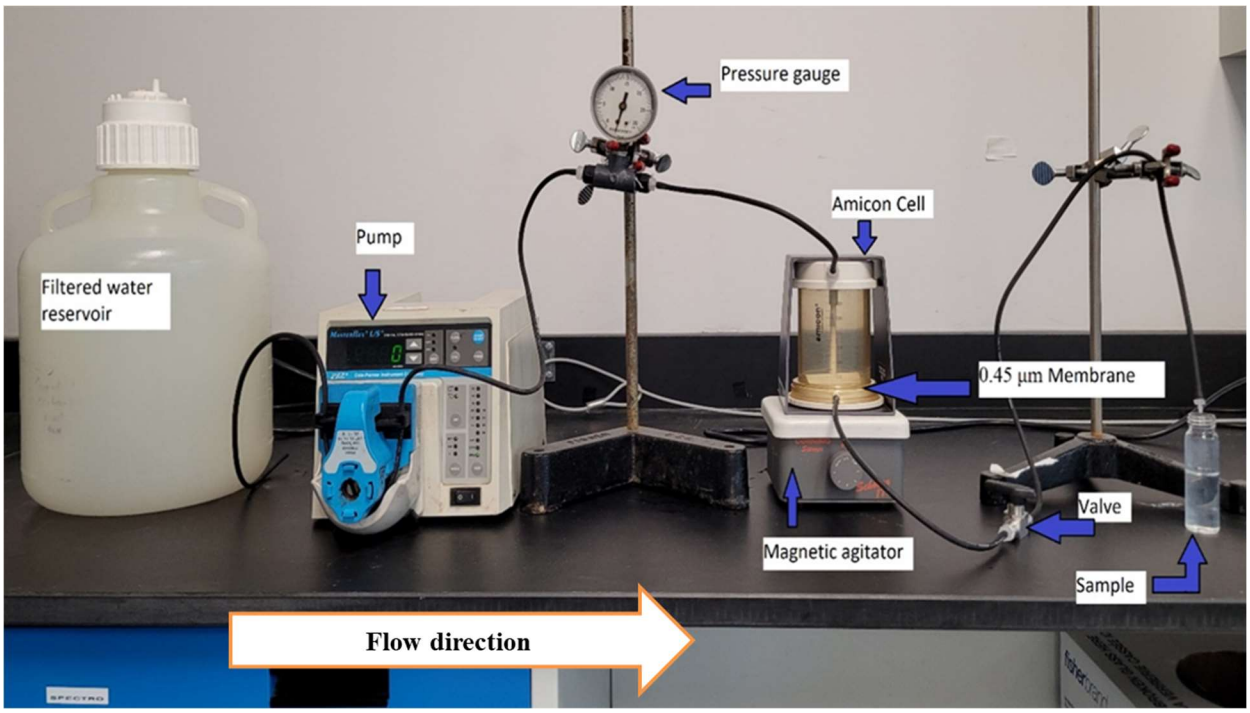

Figure 4-1 Bench-scale HPM reactor (Amicon cell) assembly

Before the experiments, PACs were dried in an oven (at 105℃) to remove moisture. Then, a highly concentrated aqueous solution of PAC/Milli-Q water (10000-12000 mg/L) was prepared with the dried PAC. This suspension was placed on the horizontal shaker for at least one day for PAC deaeration and then, the required PAC was taken from this solution. The amount of the required PAC is calculated using the following equation:

$C_1 V_1 = C_2 V_2$ Equation 4-1

In this equation, C_1 and C_2 represent PAC concentrations (mg/L) in the Amicon cell and the highly concentrated aqueous solution of PAC/Milli-Q water respectively. Also, V_1 and V_2 (L) are the volumes of the Amicon cell and the required PAC respectively. This virgin PAC is injected into the Amicon cell as a pulse input (once) at the beginning of the experiment. Therefore, the PAC concentration will be constant during the experiment. To run the Amicon cell, the following steps were taken:

1- Injecting the virgin PAC into the Amicon cell

2- Pre-filtering the raw water with a 0.45µm membrane and storing in a tank. Prefiltration removes particles, which allows running long sorption tests without excessive head loss.

3- Pumping the pre-filtered water into the Amicon cell at a fixed rate using a peristaltic pump. The Amicon cell includes a 0.45 µm membrane and magnetic stirrer that retains PAC suspended inside the reactor.

4- When the reactor is filled with water (this time is equal to HRT), the effluent valve is opened, and the treated water is discharged continuously

5- The reactor effluent is sampled to read the DOC and the UV_{254} absorbance

The main equipment and materials required for the experimental setup are shown in Table 4-1

Table 4-1 List of main equipment and materials in HMP set up

Equipment	**Description**
Raw Water Tank	50 L
Peristaltic pump	Masterflex L/S
Pump head	Masterflex 77800-60
Pump tubing	Masterflex, 13 to 25
Pressure sensor	Burke (0-30psi)
Amicon cell	Amicon 8400 (400mL)
Filters:	Supplier: Pall, Supor 450, 60173 and 60206 Porosity: 0.45µm Diameter: depending on the reactor (75 mm and 45mm)
PAC	1- AquaSorb MP 23 (JACOBI) of PAC-F 2- Calgon Carbon WPH-w900

Figure 4-2 shows the flow direction in the Amicon cell. The inlet of the Amicon cell reactor is installed on top of the reactor, while the membrane filter (reactor outlet) is in the lower part of the reactor. The Amicon cell has a magnetic stirrer inside the reactor on the top of the membrane (it does not touch the membrane surface). This stirrer is turned by an external magnetic agitator.

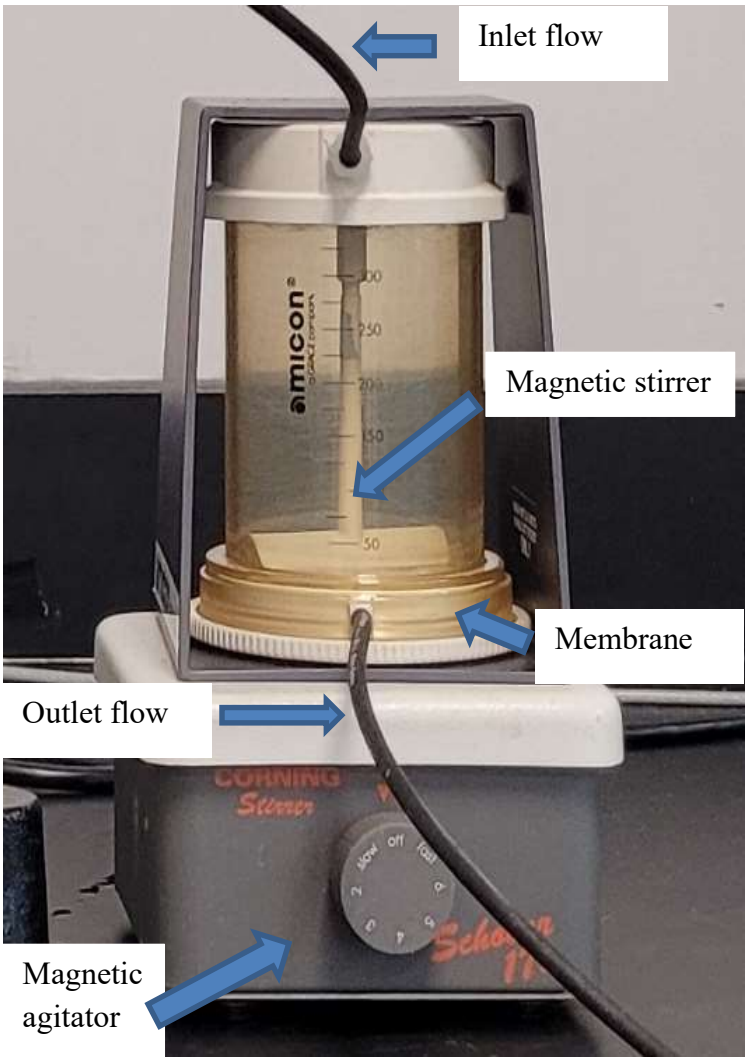

Figure 4-2 Amicon cell flow direction

4.1.2 PAC accumulation on the filter of the HMP reactor

Since the Actiflo® Carb reactor is a slurry reactor, not a fixed bed reactor, the bench-scale reactor conditions must be designed to keep the PAC in suspension and not accumulated on the filter. During the pre-tests, it was found that a layer of PAC accumulated on the filter, as shown in Figure

4-3 (even though the reactor was fully mixed). Therefore, to minimize the accumulation, it was necessary to determine the reason for accumulation which could be sedimentation or advection.

PAC accumulation is measured by weighing the membrane filter before and after the experiment. Before each experiment, the membrane filter is dried and weighted. Then, at the end of the experiment, the reactor (including suspended PAC) is emptied from above, and the filter (with accumulated PAC) is dried again in an oven at 105°C. The PAC accumulation percentage is obtained using the following analytical balance.

$$PAC\ accumulation\ percentage = (W_2 - W_1) / W_{pac} \qquad Equation\ 4\text{-}2$$

Where W_1 (g) is the weight of the dried filter (at 105 °C), W_2 (g) is the weight of the filter plus accumulated PAC after the test (dried at 105 °C), and W_{pac} () is the weight of total PAC used in the reactor.

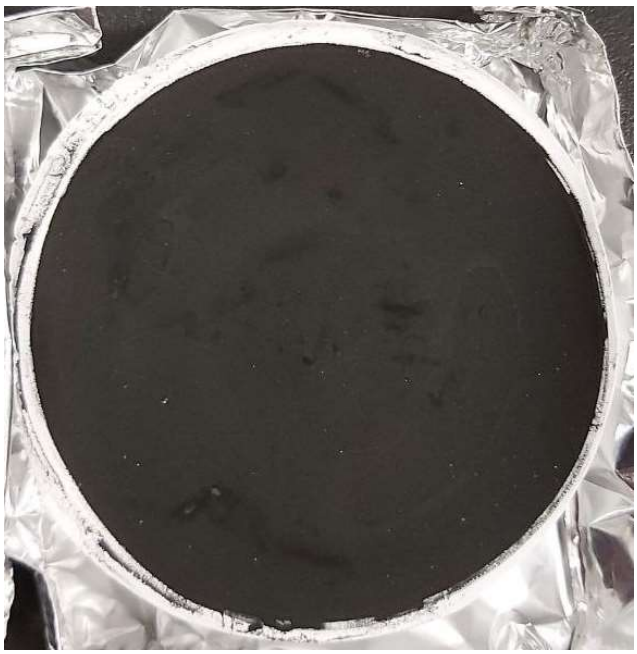

Figure 4-3 PAC accumulation on the filter surface after drying

The effect of PAC concentration, HRT, flow direction, CUR, and the stirrer's rotation speed (SRS) on PAC accumulation are studied.

In this work, the range of PAC concentration was chosen to be close to the operating range of the Actiflo® Carb process. Therefore, research on very high concentrations (such as 3000 mg/L) or low concentrations (such as 50 mg/L) was avoided. A total of 17 tests were performed (Table 4-2).

All tests are done with raw water from St. Lawrence River and CB1-MW-F PAC AquaSorb ® from Jacobi.

Table 4-2 List of the various tests performed to parameter adjusting

Test number	PAC concentration (mg/L)	CUR (L_{water} / g_{PAC})	HRT (min)	SRS (rpm)	Flow direction
1	***100***	50	15	300	Up to down
2	***250***	50	15	300	Up to down
3	***500***	50	15	300	Up to down
4	***1000***	50	15	300	Up to down
5	500	50	***7.5***	300	Up to down
6	500	50	***15***	300	Up to down
7	500	50	***30***	300	Up to down
8	500	50	15	***0***	Up to down
9	500	50	15	***165***	Up to down
10	500	50	15	***300***	Up to down
11	500	50	15	***400***	Up to down
12	500	***25***	15	300	Up to down
13	500	***50***	15	300	Up to down
14	500	***100***	15	300	Up to down
15	500	***125***	15	300	Up to down
16	500	50	15	300	***Down to Up***
17*	500	50	15	300	**Up to down**

*In test #17, only the membrane diameter is reduced, and the rest of the parameters are the same as in test #3.

In Test#16, the effect flow direction was studied. The normal flow direction was previously shown in Figure 4-2 (for all tests excluding test#16). In this way, the flow direction is aligned with the direction of the gravitational force on the PAC particles. Therefore, both phenomenon of advection and sedimentation impress PAC accumulation on the filter surface. In test #16, the flow direction is reversed to distinguish between these two phenomenon. In this way, the inlet of the reactor is placed in the lower part, and the filter is moved to the upper part of the reactor (Figure 4-4). This test shows how two phenomenon of advection and sedimentation affect PAC accumulation. If the

PAC accumulates on the membrane surface, it shows that advection is more important than sedimentation. If the PAC accumulated in the bottom of the Amicon cell, it shows that sedimentation is more important than advection.

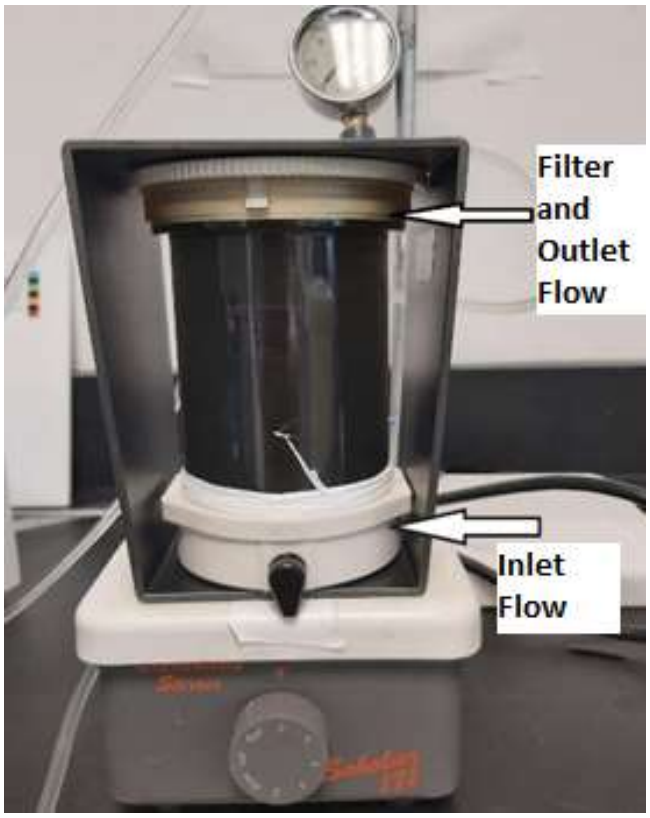

Figure 4-4 Amicon cell reactor with the reverse flow direction

In test #16, the stirrer's location is near the reactor's inlet. In the other tests, the stirrer is near the outlet. To eliminate the effect of changing the position of the stirrer, test #17 is designed to confirm the result. In test #17, all conditions and parameters were identical with test #3. The only difference between test #17 and test #3 is the size of the membrane. In test #3 (and other tests), the membrane covers all the lower surface of the reactor, but in test #17, a portion of the filter is covered with wax paper.

4.1.3 The effect of physical conditions of the reactor on the PAC performance

After adjusting the reactor to keep the PAC in suspension, the effect of PAC concentration, Membrane diameter, HRT, and SRS on the Amicon cell breakthrough curve (q over CUR) is studied using two PAC types.

Monitoring the breakthrough curve

The breakthrough curves normally show the adsorbate concentration at effluent over time. But here, to be able to compare breakthrough curves of different PAC concentrations, and HRTs, breakthrough curves are normalized by q (instead of DOC concentration at the effluent) and CUR (instead of time). As a result, the breakthrough curve shows the average performance of each PAC particle. Figure 4-5 shows a hypothetical breakthrough curve normalized by q and CUR

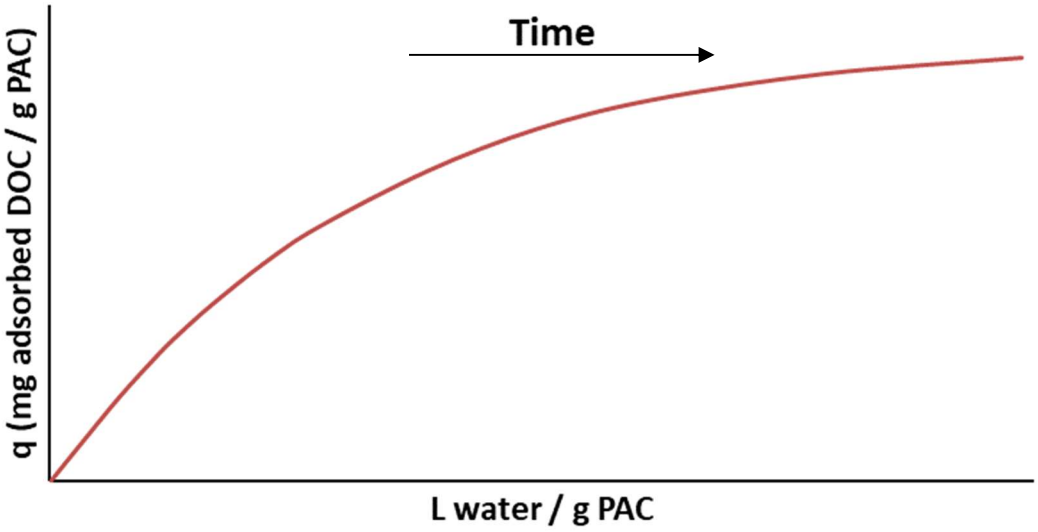

Figure 4-5 A sample of normalized breakthrough curve by q and CUR

- Calculation of CUR

CUR is calculated as follows:

$$CUR = \frac{\frac{V_{reactor}}{HRT} x\ Time}{PAC\ weight} \qquad \textit{Equation 4-3}$$

Where PAC weight (g) is the total weight of the PAC inside the reactor. $V_{reactor}$ (L) is the volume of the reactor. HRT (min) is the average time each unit volume of water held inside the reactor.

And it is also equal to the initial filling time of the reactor. Time (min) is calculated from the moment of pumping.

The above equation can be rewritten in terms of the influent flow as follows:

$$CRU = \frac{Influent\ flow\ rate\ x\ Time}{PAC\ weigh} \qquad \textit{Equation 4-4}$$

The influent flow rate (L/min) equals the pump flow rate.

- Calculation of q(t)

As described in Chapter 2, q(t) is the adsorption rate of the adsorbate (DOC) on the adsorbent (PAC) at a given time. In the Amicon cell reactor, q(t) is calculated as follows:

$$q(t) = \frac{Adsorbed\ DOC\ (mg)}{PAC\ mass\ (g)} = \int_{t=H}^{t} \frac{Q\ (C_{inf} - C_{eff})}{PAC\ mass}\ dt + q(t = HRT) \quad \textit{Equation 4-5}$$

And,

$$q(t = HRT) = \frac{C_{inf} - C_{eff}}{PAC\ mass} \times V_{reactor} \quad \textit{Equation 4-6}$$

Where C_{inf} is the concentration of DOC at the influent, and C_{eff} is the concentration of DOC in the effluent at time=HRT. When DOC is measured intermittently, and the time between t(i) and t(i-1) is small (time between two DOC readings), Equation 4-6 will be rewritten as Equation 4-7.

$$q(i) \approx q(i-1) + \frac{\frac{Volume}{HRT} \times \left(\frac{C_i - C_{i-1}}{2}\right) \times (t_i - t_{i-1})}{PAC\ mass} \qquad \textit{Equation 4-7}$$

Where (i) corresponds to the numbering of a value according to the operation time it is calculated. Then, (i-1) corresponds to the value for an operation time preceded by a time step.

Table 4-3 describes the various tests carried out during this step of the project. These tests are done on different samples of raw water from the St. Lawrence River. Tests #18 to test#22 are done with the first batch. Tests #23 to test #24 are done second batch. Tests #25 to test#27 are done with third batch, and test #28 is done with the same batch of water as tests #1 to #17.

Table 4-3 List of the various tests carried out to evaluate the effect of PAC concentration on the Amicon cell breakthrough curve

Test number	PAC concentration (mg/L)	PAC Type	Reactor Volume (ml)	Membrane	HRT (min)	SRS (rpm)
18	100	AquaSorb MP 23-F	400	Fit to the reactor	15	300
19	250	AquaSorb MP 23-F	400	Fit to the reactor	15	300
20	500	AquaSorb MP 23-F	400	Fit to the reactor	15	300
21	100	CalgonCarbon WPH-w900	400	Fit to the reactor	15	300
22	250	CalgonCarbon WPH-w900	400	Fit to the reactor	15	300
23	500	AquaSorb MP 23-F	400	Fit to the reactor	11	300
24	1000	AquaSorb MP 23-F	400	Fit to the reactor	11	300
25	250	AquaSorb MP 23-F	400	Fit to the reactor	15	300
26	250	AquaSorb MP 23-F	400	Reduced diameter	15	300
27	250	AquaSorb MP 23-F	50	Fit to the reactor	15	300
28	500	AquaSorb MP 23-F	400	Fit to the reactor	15	400

In tests #18 to #24, the effect of PAC concentration on the Amicon cell breakthrough curve will be studied.

By comparing test #25 with test #26, the effect of membrane diameter on the Amicon cell breakthrough curve will be studied. For test #26, the membrane diameter is reduced from 75 mm to 45 mm. By comparing test #25 with test #27, the effect of reactor volume on the Amicon cell breakthrough curve will be studied. By comparing test #28 with test #8, test #10, and test #11, the effect of HRT and SRS on the Amicon cell breakthrough curve will be studied.

4.1.4 Modeling the Amicon cell reactor

Previously, Dauphin showed that the adsorption of NOM on PAC in an Amicon cell reactor would be modeled with pseudo-first-order and pseudo-second-order kinetic. So, the results obtained from test #18 to test #24 are modeled with these models and the Elovich model.

Kinetic empirical models for flow-through reactor

The linear equations of these models found in are used to represent the experimental values of test #18 to test #24.

As mentioned in chapter 2, the pseudo-first-order model includes the q_{eq}. During the tests in the Amicon cell, the balance is never achieved (the balance is achieved when 100% of PAC is accumulated on the membrane surface). Therefore, to fit the pseudo-first-order model, the parameter of q_{eq} is first estimated with the pseudo-second-order model for each test.

Verifying models

The performance of an Amicon cell filled with an aged PAC is predicted by these models and verified by the experimental data. Each aged PAC has a specific q_0, and each q_0 respects a specific time (t_0) in the Amicon cell. These times are varied from one model to another model. Therefore, to predict the performance of the reactor filled with aged PAC by a model, it is necessary to calculate the proportional t_0 first.

Table 4-4 describes the tests performed in this step. All tests are done with the same batch of raw water from the St. Lawrence River, the same type of PAC (AquaSorb CB1-MW PAC from Jacobi ®), and the HRT is 15 min. The performance of the Amicon cell in test#29 is modeled with empirical models. Then these models are used to predict the performance of test#30 to test #32.

Table 4-4 List of the different tests performed to verify the models

Test number	PAC concentration (mg/L)	Reactor Volume (ml)	Membrane	Virgin/ aged PAC
29	250	400	Fit to reactor	Virgin PAC
30	250	400	Fit to reactor	Aged PAC
31	250	400	Fit to reactor	Aged PAC
32	250	400	Fit to reactor	Aged PAC

The condition of test#19 is the same as test #19. The conditions of test #30 to test #32 are the same as test #29; the only difference between them is that for tests #30 to #32, the Amicon test is filled with aged PAC. While in test #29 it is filled with virgin PAC.

Providing aged PAC

Three aged PACs are produced for this part of the project. An Amicon cell reactor with a high PAC concentration (about 2500 mg/L) is used to produce an aged PAC. When the load of PAC reaches the desired amount, raw water pumping is stopped. The volume of the suspension inside the Amicon cell is reduced until the PAC concentration reached more than 7000 mg/L. This highly concentrated suspension is given one day to reach the equilibrium point. This suspension is used for the tests that required the use of aged PAC. Also, the PAC concentration is determined by measuring the total suspended solid (TSS test) as follows:

$$TSS\ \left(\frac{mg}{L}\right) = C_{PAC}\left(\frac{mg}{L}\right) + q\left(\frac{mg\ of\ adsrobded\ NOM}{g\ of\ PAC}\right) * C_{PAC}\left(\frac{g}{L}\right)$$ *Equation 4-8*

As the raw water is prefiltered, the TSS equals PAC concentration plus adsorbed NOM on the PAC surface.

For Amicon cells filled by aged PAC, q(t) is calculated as follows:

$$q(t) = q_0 + \int_{t_0}^{t} dq$$ *Equation 4-9*

Where q_0 (mg C/g PAC) is the PAC initial load, dq is the adsorption amount in the Amicon cell during the test, and t_0 is the equivalent time to reach q_0 (mg C/g PAC). To check the accuracy of prediction of each model, the graph of experimental q versus predicted q was plotted. Then, the linear equation was fitted to the data:

$$Y = mX$$ *Equation 4-10*

The prediction is more accurate as much m is closer to 1. Another term that is used to verify the goodness of prediction is the mean absolute error (MAE).

PAC age:

In order to compare the load of an aged PAC to the virgin PAC adsorption capacity, the term "PAC age" is defined. PAC age is calculated by the following equation:

$$PAC\ age\ (\%) = \frac{aged\ PAC\ q\ \left(\frac{mg}{g}\right)}{Virgin\ PAC\ adsorption\ capacity\ \left(\frac{mg}{g}\right)}$$ *Equation 4-11*

An isotherm test in batch reactor is performed (this kind of test will be described in detail in section 4.2) to determine the virgin PAC adsorption capacity. The maximum load that a PAC particle can theoretically have occurs when the PAC suspension, with a close to zero concentration, reaches the

equilibrium point in a batch reactor. This term is named virgin PAC adsorption capacity or 100% aged PAC. Therefore, the age of other aged PACs is expressed as a percentage of this amount. Since it is impossible to have a suspension with zero concentration, the virgin PAC adsorption capacity is determined by using the Freundlich equilibrium (Equation 2-7). In such a way, in the Freundlich isotherm curve, the point where DOC of effluent is equal to raw water DOC is considered as the virgin PAC adsorption capacity. Virgin PAC adsorption capacity is uncommon concept and is defined for better understanding of the result of this project. It is depended on the nature of the solvent, adsorbent, and adsorbate. Therefore, it should be calculated for each matrix of adsorption separately.

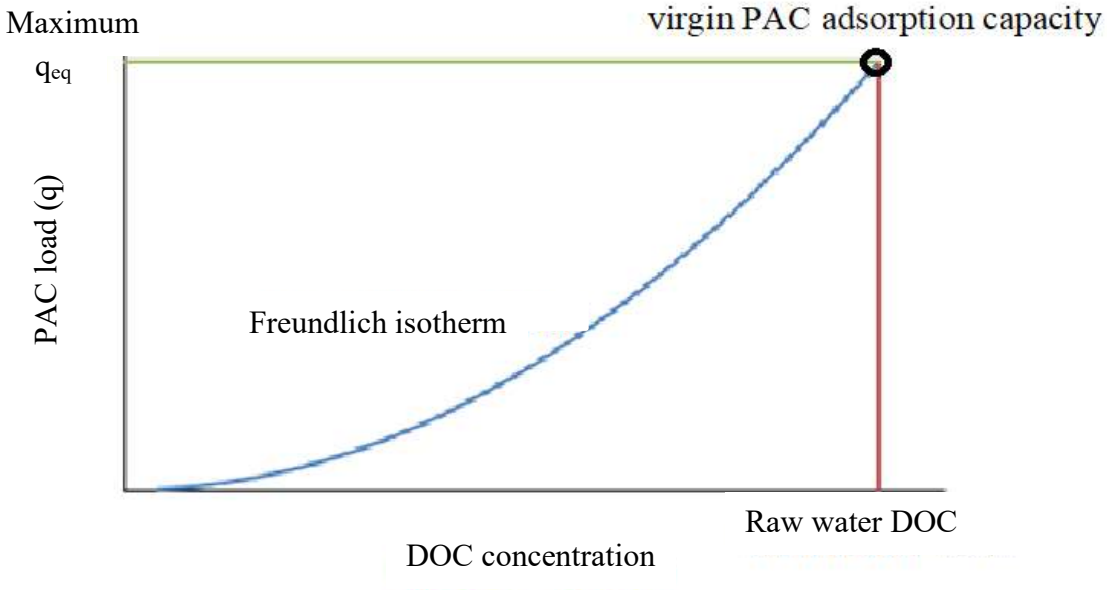

Figure 4-6 the virgin PAC adsorption capacity calculation method through Freundlich isotherm diagram under favorable conditions

4.2 Investigation of the effect of PAC aging and mixing different aged PACs on sorption parameters

As mentioned in Chapter 3, the second approach to predict the performance of the Actiflo® Carb process is using batch reactors and investigating the effect of PAC aging and mixing the aged PAC and virgin PAC on adsorption parameters.

In systems that use recirculated PAC (like the Actiflo® Carb process), virgin PAC and aged PAC are used for NOM adsorption simultaneously. Therefore, it is necessary to be able to model the performance of the mix-aged PAC. To achieve this goal, this approach is divided into two steps:

1. Parameters adjusting of isotherm models and the HSDM for a batch reactor filled with one aged PAC (investigating PAC aging influence on sorption parameters)
2. Parameters adjusting of isotherm models and the HSDM for a batch reactor filled with more than one aged PAC

4.2.1 Modeling of the batch reactor filled with aged PAC

Kinetic/isotherm test

One kinetic/isotherm test is performed for each aged PAC and virgin PAC. To perform each kinetic/isotherm test, following steps are taken:

1- A highly concentrated PAC (7000-11000 mg/L) suspension is prepared (in equilibrium condition), as described earlier in sections 4.1.1 and 4.1.4 for virgin PAC and aged PAC, respectively.
2- At least five suspensions with different PAC concentrations are prepared in different beakers.
3- Each suspension is distributed in 7 carbon-free vials (batch reactor).
4- Vials are located on the horizontal shaker at 300 rpm
5- At time = t, the suspension inside the vial is passed through a 0.45µm membrane and transferred to another carbon-free vial to measure DOC.

For each suspension (specific q_0 and concentration), the amount of adsorption is calculated at the following time steps: 1 min, 5 min, 10 min, 30 min (two vials), 4 hours, and one day. For each reactor (vial), the adsorption load will be calculated based on the Equation 4-12:

$$q(t) = q_0 + \frac{C_{eff}(t) - C_{inf}}{C_{PAC}} * 1000 \quad \textit{Equation 4-12}$$

Where q(t) (mg C/g PAC) is the load of PAC at time t, C_{inf} (mg/L) is the DOC concentration in raw water, and C_{eff}(t) (mg/L) is the DOC concentration of suspension at time t. Figure 4-7 shows batch reactors placed on the horizontal shaker.

Figure 4-7 Batch reactors placed on the horizontal shaker

Isotherm equations

It is considered that the adsorbent and adsorbate reach an equilibrium point in one day. The Langmuir and Freundlich isotherm equilibriums (Equation 2-5 to 2-7) are used to determine the parameters of isotherm equilibriums and the adsorption capacity of the aged and virgin PAC.

Kinetic model / Surface diffusion coefficient (Ds)

HSDM (Najm's equation for batch reactors, Equation 2-19) is applied to kinetic results to determine the Ds of virgin PAC. For each PAC age, there are 35 to 42 points where the C_{eff} is measured in the laboratory. On the other hand, at each point, C_{eff} can also be theoretically calculated with an initial assumption for Ds via Equation 2-19. Since Ds is a fixed number for all these points, adjusting Ds will reach the number that has the lowest MAE value. MAE is calculated as follows:

$$MAE\ (\frac{mg}{L}) = \frac{\sum_{i=1}^{i}|C_{eff}(HSDM) - C_{eff}(mesured)|}{i} \quad \textit{Equation 4-13}$$

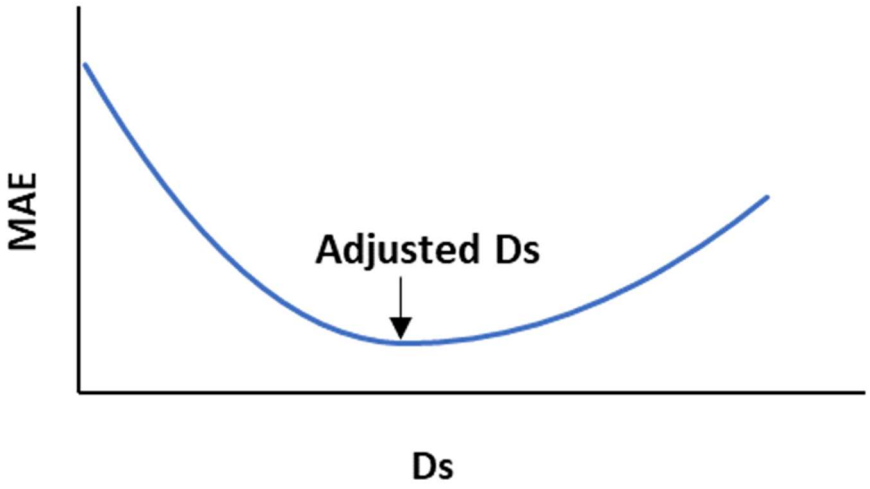

Figure 4-8 Adjusting Ds by minimizing MAE

Modifying Najm's equation for aged PAC

Since Najm solved the HSDM for virgin PAC, Najm's equation does not consider q_0; it is necessary to solve the HSDM (Equation 2-14) for a reactor where q_0 is aged PACs.

Najm's equation (Equation 2-19) is rewritten as Equation 4-14 (for virgin PAC):

$$0 = C_{inf} - C_{eff} - 3C_{PAC}K_F C_{eff}^{1/n}\left\{0.33334 - 0.04903e^{\left(-142.634\frac{tD_S}{R^2}\right)} - 0.05399e^{\left(-39.996\frac{tD_S}{R^2}\right)} - 0.20240e^{\left(-9.8686\frac{tD_S}{R^2}\right)}\right\}$$ *Equation 2-19*

$$\frac{q(t)}{q_\infty} = 3\left\{0.33334 - 0.04903e^{\left(-142.634\frac{tD_S}{R^2}\right)} - 0.05399e^{\left(-39.996\frac{tD_S}{R^2}\right)} - 0.20240e^{\left(-9.8686\frac{tD_S}{R^2}\right)}\right\}$$
Equation 4-14

Where q(t) is the increase in PAC load in the reactor and q_∞ is the maximum possible increase of PAC load at C_{eff} inside the reactor (without considering the initial load). When the reactor is filled by an aged PAC, q_∞ is calculated as follows (by subtracting the initial loading):

$$q_\infty = K_F C_{eff}^{1/n} - q_0$$ *Equation 4-15*

Therefore, the HSDM model for a batch reactor filled by an aged PAC is modified as follows

$$0 = C_{inf} - C_{eff} - 3C_{PAC}\left(K_F C_{eff}^{1/n} - q_0\right)\left\{0.33334 - 0.04903e^{\left(-142.634\frac{tD_S}{R^2}\right)} - 0.05399e^{\left(-39.996\frac{tD_S}{R^2}\right)} - 0.20240e^{\left(-9.8686\frac{tD_S}{R^2}\right)}\right\}$$ Equation 4-16

Initial loads of aged PACs

Three different aged PACs are prepared with the Amicon cell for this step. Table 4-5 shows the load of each aged PAC and the concentration of suspensions used in isotherm tests. The PAC aged is expressed as a % of the virgin PAC adsorption capacity.

Table 4-5 Initial PACs loadings (the virgin PAC adsorption capacity =53.7 mg/g)

Aged PAC	q_0 (mg/g)	PAC age (%)	PAC dosage (mg/L)					
Virgin PAC	0	0	15	50	100	250	500	
1St aged PAC	9.8	17	14.5	24	68.1	163.3	340.6	681.3
2nd aged PAC	15.8	27	15.2	54.4	107.3	272.1	507.9	
3rd aged PAC	23.5	41	18.9	68.1	136.3	333.1	704.0	

4.2.2 Modeling of the batch reactor filled with mix-age PAC

In the reactor that uses a combination of virgin PAC and recirculated PAC (mixed aged PACs), it is impossible to measure each PAC particle adsorption amount in a suspension separately. Therefore, it is necessary to simplify the problem with one or more assumptions. Then, with these assumptions, the performance of the reactor will be predicted by the HSDM and compared with measured data from isotherm/kinetic tests. If the prediction is accurate, the assumption will be accepted. Otherwise, it will be rejected, and it is necessary to solve the problem with a new assumption. Here, it is assumed that a mixture of different ages of PAC performs as a suspension with mass-weighted average loadings of all PACs. The potential advantage of this approach would be to greatly simplify the modeling of reactor performance. The average loading is calculated as follows:

$$\overline{q_0} = \frac{\sum_{i=1}^{n} q_o(i) * C_{PAC}(i)}{\sum_{i=1}^{n} C_{PAC}(i)} \quad \textit{Equation 4-17}$$

Therefore, Equation 4-16 would be written for this situation as follows:

$$0 = C_{inf} - C_{eff} - 3C_{PAC}\left(K_F C_{eff}^{1/n} - \overline{q_0}\right)\left\{0.33334 - 0.04903e^{\left(-142.634\frac{tD_s}{R^2}\right)} - 0.05399e^{\left(-39.996\frac{tD_s}{R^2}\right)} - 0.20240e^{\left(-9.8686\frac{tD_s}{R^2}\right)}\right\}$$

Equation 4-18

To validate this hypothesis, four isotherm/kinetic tests are performed with raw water from the Saint Lawrence River and mix-loadings PAC (AquaSorb MP 23). All preloaded PACs are prepared with the Amicon cell. Table 4-6 shows the assembly of each mix-loads PAC used in isotherm/kinetic tests.

Table 4-6 Matrices of Mix-aged PACs used in isotherm/kinetic tests

Mix-loaded PAC matrix	$\overline{q_0}$ **(mg/g)**	**Initial q_0 (mg/g) of each PAC (% of each fraction)**					
1St Mix-loaded PAC	12.8	0 (52%)	24.5 (48%)	-	-	-	-
2nd Mix-loaded PAC	16.6	0 (53%)	35.0 (47%)	-	-	-	-
3rd Mix-loaded PAC	7.9	0 (15%)	5.1 (60%)	19.7 (25%)	-	-	-
4th Mix-loaded PAC	25.7	0 (5%)	6.3 (5%)	11.2 (9%)	17.5 (10%)	25 (10%)	31.8 (63%)

Each mix-loaded PAC is tested with at least 2 different concentrations. Table 4-7 shows the concentrations of isotherm/kinetic tests for each mix-loaded PAC.

Table 4-7 Mix-loaded PAC concentration in isotherm/kinetic tests

Mix-loaded PAC	**PAC Concentration (mg/L)**				
1St Mix-loaded PAC ($\overline{q_0}$ =12.8)	15	51	103	257	-
2nd Mix-loaded PAC ($\overline{q_0}$ =16.6)	15	48	95	238	475
3rd Mix-loaded PAC ($\overline{q_0}$ =7.9)	45	84	-		
4th Mix-loaded PAC ($\overline{q_0}$ =25.7)	58	193	578	-	

4.3 Prediction of adsorption in the Actiflo® Carb process

Actiflo® Carb is a complex process that combines the adsorption process with the coagulant/flocculation process. The first step in analyzing any complex system is to divide it into simple subsystems. Here, the process is divided in two section “PAC adsorption” in the PAC tank (the first tank from the left in Figure 4-9) and “coagulant/flocculation” in the following tanks. It is

assumed that these phenomena are independent from each other. Here, the main goal is to study the PAC adsorption in the PAC tank.

When the Actiflo® Carb reactor operates at a steady state, each tank acts as a CSTR. Therefore, their performance is described by CSTR reactions and equations. PAC tank works with three influent streams (recirculated PAC, Virgin PAC, and raw water) and one effluent stream.

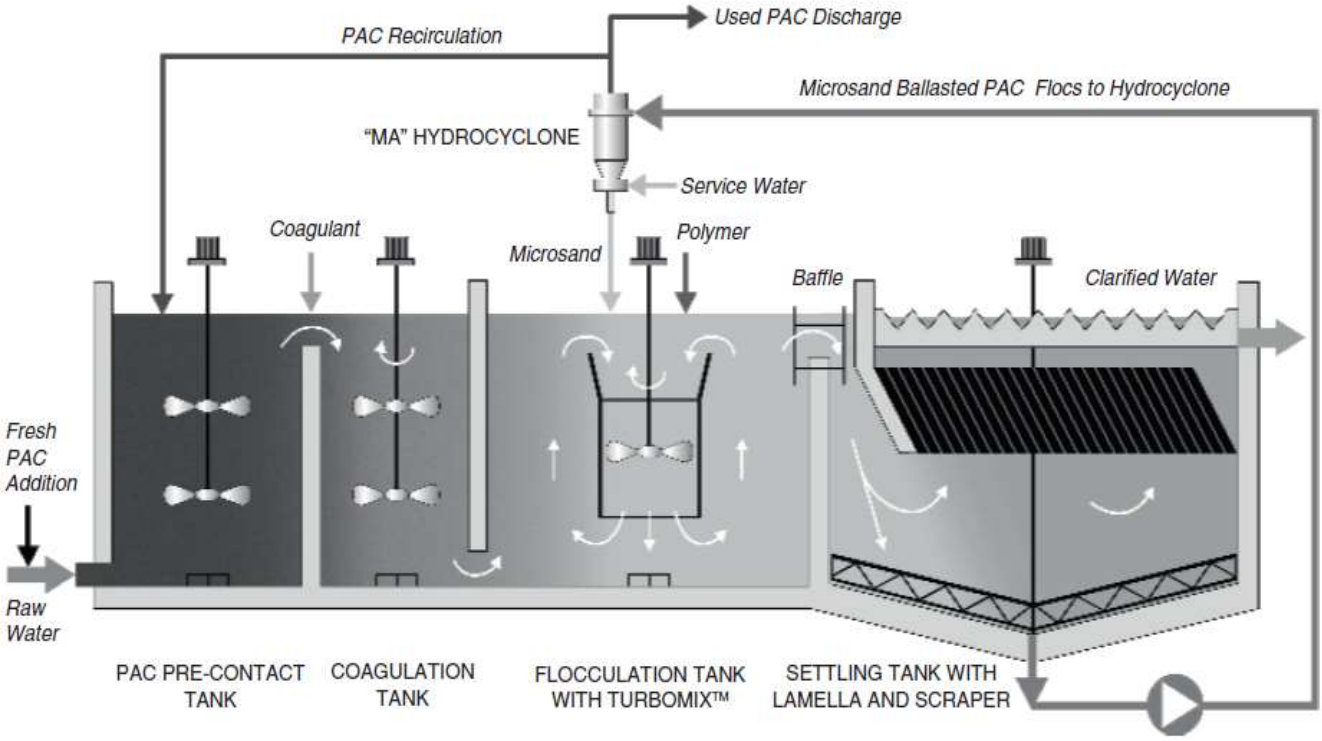

Figure 4-9 Actiflo® Carb process flowsheet (Aliverti et al., 2011)

To predict the PAC tank, besides the previous assumptions about the performance of mix-aged PACs, the following assumptions are made:

- The bulk of NOM removal (by adsorption) achieved through sorption is obtained in the first reactor. Because in the second tank (coagulation tank) by adding fresh coagulant NOM level drops rapidly, therefore the PAC particles will be over saturated compared to NOM level in the second tank. So, adsorption after adding fresh coagulant is negligible.
- Coagulation/flocculation (including recirculated coagulant) does not affect sorption parameters (does not lead to pore plugging)
- PAC particle size is constant during recirculation

- There is no upstream treatment process

As previously, the HSDM equation was solved for the batch reactor considering q_0; for the CSTR, q_0 must also be included in the HSDM. Najm's equation (Equation 2-21) for CSRT is written as follows:

$$0 = C_{inf} - C_{eff} - C_{PAC}K_F C_{eff}^{1/n}\left\{1 - \frac{6}{\pi^2}\sum_{i=1}^{\infty}\left(\frac{1}{i^2\left(1+\left(\frac{\pi^2 i^2 D_s \tau}{R^2}\right)\right)}\right)\right\} \quad \textit{Equation 2-21}$$

$$\frac{q_\tau}{q_\infty} = 1 - \frac{6}{\pi^2}\sum_{i=1}^{\infty}\left(\frac{1}{i^2\left(1+\left(\frac{\pi^2 i^2 D_s \tau}{R^2}\right)\right)}\right) \quad \textit{Equation 4-19}$$

Where q_τ is the amount of adsorption in the CSTR and q_∞ is the maximum possible increase of PAC load at C_{eff}. When an aged PAC fills the CSTR, q_∞ is calculated by Equation 4-13. Therefore, the HSDM for a CSTR filled by an aged PAC is as follows:

$$0 = C_{inf} - C_{eff} - C_{PAC}(K_F C_{eff}^{1/n} - q_0)\left\{1 - \frac{6}{\pi^2}\sum_{i=1}^{\infty}\left(\frac{1}{i^2\left(1+\left(\frac{\pi^2 i^2 D_s \tau}{R^2}\right)\right)}\right)\right\} \quad \textit{Equation 4-20}$$

As discussed earlier, a reactor filled with different PAC ages operates like a reactor filled with a PAC with a mass-weighted average loading. So, the average initial load of PAC in the PAC tank of the Actiflo® Carb will be calculated as follows:

$$\overline{q_0} = \frac{q_{(Virgin\ PAC)} * C_{(virgin\ PAC)} + q_{(Recirculated\ PAC)} * C_{(Recirculated\ PAC)}}{C_c} \quad \textit{Equation 4-21}$$

Where, $\overline{q_0}$ (mg C /g PAC) is the average of the loading of recirculated PAC and virgin PAC, $q_{(virgin\ PAC)}$ (mg C /g PAC) is the preload of virgin PAC that usually equals zero, and $q_{(recirculated\ PAC)}$ (mg C /g PAC) is the average loading in the recirculated PAC . And Cc (mg/L) is the total PAC concentration in the reactor which is calculated as follows:

$$C_c = C_{(Virgin\ PAC)} + C_{(recirculated\ PAC)} \quad \textit{Equation 4-22}$$

When the Actiflo® Carb reactor works in a steady state, the amount of adsorption in each fraction equals the difference between the recirculated PAC load and $\overline{q_0}$.

$$q_\tau = \frac{C_{inf} - C_{eff}}{C_c} = q_{(recirculated\ PAC)} - \overline{q_0} \quad \textit{Equation 4-23}$$

Where q_τ is the amount of adsorption in each circle of the Actiflo® Carb process.

4.3.1 Adsorption prediction in a full-scale Actiflo® Carb process (CA, USA)

To verify the prediction of the Actiflo® Carb process, samples were collected from a full-scale process located in California, USA. Table 4-8 shows the characterization of the water sample. This treatment plant uses groundwater as its raw water.

Table 4-8 Raw water and Virgin PAC characterization

Parameters	Values
TOC of raw water (on-site online measurement) (mg C/L)	3.43
DOC of raw water (laboratory measurement) (mg C/L)	3.56
PAC Type	AquaSorb MP 23-F
PAC size (d_{50}) (measured in the lab with a Mastersizer3000) (µm)	12.5
PAC size range (d50) (from producer's site) (µm)	8-15

Table 4-7 shows the specification of the Actiflo® Carb reactor at the time of sampling. For this specific plant, the HRT in the PAC tank is 30 minutes, while the HRT is reported to be normally between 4 to 10 minutes in other Actiflo® Carb reactors (Aliverti et al., 2011; Veolia, 2022).

Table 4-9 Specifications and operating conditions of the treatment unit

Treatment flow (GPM)	1727	**Coagulant Type**	Ferric chloride
Effluent flow (GPM)	1177	**Coagulant dosage (mg/L)**	32
Volume of the PAC Tank (Cf)	6885	**HRT in pre-coagulation tank (min)**	5
HRT in the PAC tank (min)	30	**HRT in coagulation tank (min)**	5
TSS (On-site online measurement) in the PAC tank (mg/L)	730- 765	**Sodium permanganate dosage (mg/L)**	0.8
Virgin PAC dosage (mg/L)	25	**Polymer (mg/L)**	0.72
TSS at the PAC return tank (On-site online measurement) (mg/L)	7123	**Chlorine (Pre-disinfection) (mg/L)**	0.97
TSS at the PAC return tank (Laboratory measurement) (mg/L)	17500	**Chlorine (Secondary disinfection) (mg/L)**	2.35
PAC ratio in sludge (Percentage)	30	**Residual chlorine (mg/L)**	2.03

Figure 4-10 shows the Actiflo® Carb process flowsheet for the USA treatment plant. Compared to a more normal Actiflo® Carb reactor (Figure 4-9) this treatment facility has one more tank (pre-coagulation tank).

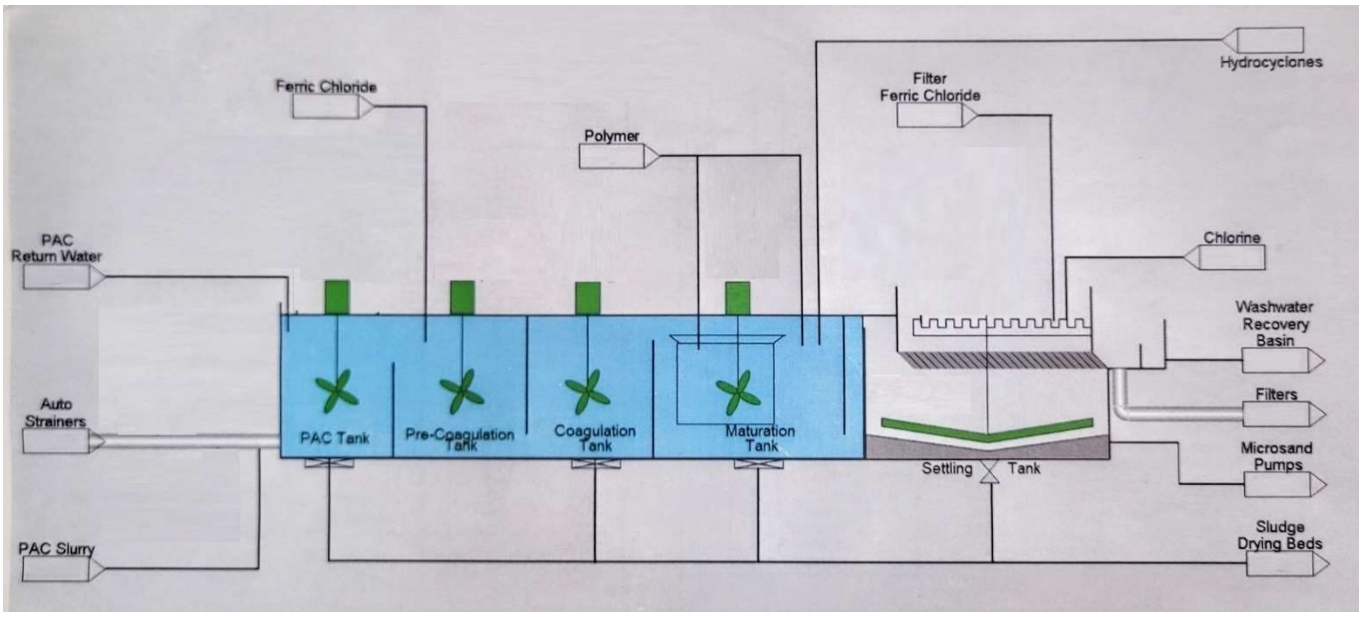

Figure 4-10 Specific Actiflo® Carb process flowsheet for the USA treatment plant

PAC tank modeling

To model the PAC tank the following steps were taken:

1- Performing an isotherm/kinetic test with 0.45 μm filtered raw water and virgin PAC (with six different PAC concentrations, from 5 mg/L to 750 mg/L)
2- Calculating sorption parameters (K_F,1/n, and D_s) by solving Equations 2-6 and 2-19
3- Modeling PAC tank with sorption parameters and solving Equations 4-20 to 4-23
4- Calculating DOC concentration at PAC tank and load of recirculated PAC by PAC tank modeling.

Since samples and data were not collected from the PAC tank of the industrial plant, also, the effluent of the Actiflo® Carb process is influenced by both adsorption and coagulation/flocculation methods. It's not possible to verify the modeling by only comparing the DOC concentration at the effluent of the Actiflo® Carb and PAC tank modeling. Therefore, the two following methods were taken to complete the modeling.

1- Preforming the jar test to estimate the Actiflo® Carb effluent
2- Estimating the $q_{(\text{recirculated PAC})}$ by performing the kinetic/ isotherm test on the sample of sludge (including recirculated PAC) received from the plant. And comparing it to the result of PAC tank modeling

Jar test

At first, a sample of raw water is treated by PAC until the DOC level decreases to the predicted result of the PAC tank by the modeling. Then a jar test is performed on this sample by adding ferric chloride coagulant with the same dosage as in the treatment plant. With this method, it could be possible to compare the DOC level at the Actiflo® Carb process effluent and the modeling results.

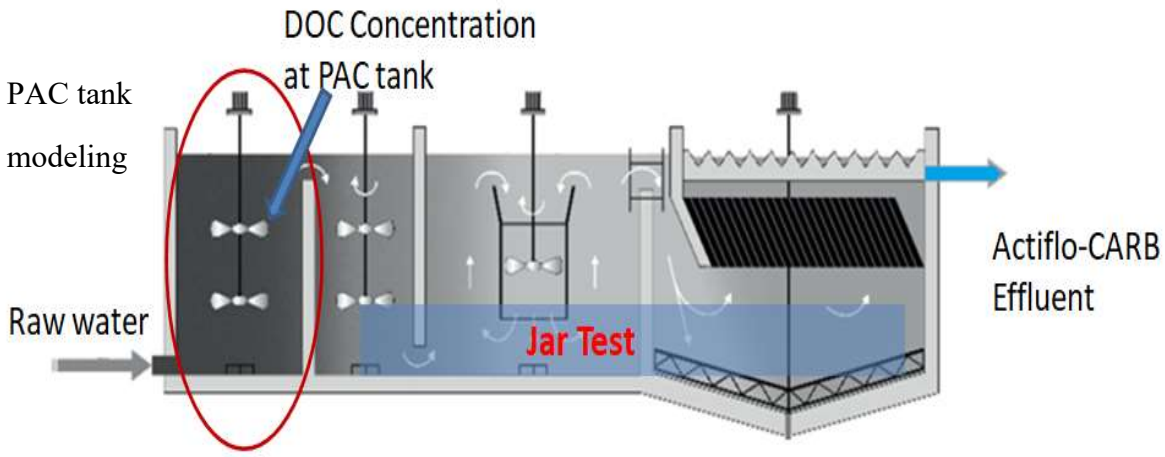

Figure 4-11 Configuration of PAC tank modeling and jar test on the Actiflo® Carb process

To perform the jar test following steps are taken:

1- Filling 1 L of the sample (reduced DOC) in the jar
2- Adding 32 mg Fe/L of ferric coagulant to the jar and mixing at 180 rpm for 2min
3- Mixing suspension at 50 rpm for 10 min
4- Adding 0.2 mg/L of polymer to the suspension to facilitate flocculation and mixing at 25 rpm
5- 30 minutes without mixing for settling
6- Sampling of the suspension and measuring DOC concentration

Kinetic/ Isotherm test on the sludge

In the second method to verify the modeling of the PAC tank, an isotherm/kinetic test is performed with raw water and sludge (including recirculated PAC) to determine the $q_{(recirculated\ PAC)}$. First, PAC concentration in sludge is determined (Equation 4-22 to Equation 4-26) to 5833 mg/L. Then six suspensions with different PAC concentrations are made to perform the isotherm/kinetic test. Table 4-10 shows the PAC concentration in each suspension of the kinetic/ isotherm test.

Table 4-10 PAC concentration in kinetic/ isotherm test on the sludge

Suspension	**1**	**2**	**3**	**4**	**5**	**6**
PAC Concentration (mg /L)	6	11	11	29	88	272

By solving the HSDM (Equation 4-16 to Equation 4-19), and considering that the sorption parameters are constant for virgin PAC and aged PAC, the $q_{(recirculated\ PAC)}$ is calculated.

PAC percentage in sludge

Sludge samples contain recirculated PAC, recirculated coagulant, polymer, and adsorbed NOM. Recirculated PAC and adsorbed NOM are volatile parts. And the non-volatile part includes coagulant and polymer and non-volatile part of PAC. By measuring volatile suspended solids (VSS) in both virgin PAC and sludge, PAC percentage is determined as follows:

$$VSS\ \% = \frac{Mass\ of\ volatile\ suspended\ solid}{Mass\ of\ total\ solid}\ x\ 100 \quad \textit{Equation 4-24}$$

Mass of volatile suspended solid in sludge = Mass of adsorbed NOM on PAC+ Mass of volatile suspended solid in PAC + Mass of absorbed NOM on coagulant *Equation 4-25*

Adsorbed NOM is negligible compared to PAC. Therefore:

Mass of volatile suspended solid in sludge $\cong$ *Mass of volatile suspended solid in PAC* *Equation 4-26*

$$PAC\ percentage\ in\ sludge = 100 \times \frac{VSS_{(Sludge)}}{VSS_{(PAC)}} \quad \textit{Equation 4-27}$$

PAC concentration in sludge is determined by as follows:

$$PAC\ concentration = TSS_{(sludge)} \times PAC\ percentage\ in\ sludge \quad \textit{Equation 4-28}$$

PAC usage reduction rate or efficiency of using Actiflo® Carb process instead of slurry reactor

In order to show the benefit of installation of the Actiflo® Carb system compared to a slurry reactor without PAC recirculation, the term "PAC usage reduction rate" is defined.

This term shows how much the installation of the Actiflo® Carb system reduces virgin PAC dosage compared to a reactor without PAC recirculation (with the same size) to reach a desired DOC concentration. And will be calculated as follows:

$$PAC\ usage\ reduction\ rate\ (\%) = 100 - \frac{PAC\ dosage\ in\ the\ Actiflo®\ Carb\ (\frac{mg}{L})}{PAC\ dosage\ in\ the\ slurry\ reactor\ (\frac{mg}{L})} \times 100 \quad \textit{Equation 4-29}$$

Installing the Actiflo® Carb reactor system is more feasible when the PAC usage reduction rate is higher.

4.3.2 Effect of PAC characteristics and the reactor on the performance of the Actiflo® Carb process

After modeling the full-scale Actiflo® Carb process and verifying the model with data and samples received from the plant. the effect of the following effect on the performance of the Actiflo® Carb process is simulated.

- Increasing and decreasing the virgin PAC dosage
- Increasing and decreasing the total PAC concentration in the PAC tank
- Increasing treatment water flow rate (decreasing HRT in PAC tank)
- Increasing PAC particle size (using PAC-S instead of PAC-F, PAC-S is the same characteristic as PAC-F but with larger particle diameter, d_{50} = 15-35 µm compared to d_{50}= 8-15 µm for PAC-F, both PACs are made by AquaSorb)

4.4 Methods and instruments to measure experimental data

Table 4-11 shows the list of the main equipment used to analyze water quality.

Table 4-11 List of the main equipment to analyze water quality

Equipment	Description
Spectrophotometer	Cary 100 Scan a, Varian
Spectrophotometer cell for UV reading	1 cm
TOC analyzer	Sievers M5310 C, SUEZ
Vial	40- 50 ml
Septum	Supelco® Teflon
Horizontal shaker	Innova 2300 platform shaker

DOC measurements and UV/DOC correlation

The raw water is used throughout this project is prefiltered. Therefore, the organic carbon measured by the TOC analyzer is DOC, not TOC. All sampling for DOC measurement is done in carbon-free vials. For this purpose, the vials are placed in a 550℃ oven for more than four hours. Also, for the decarbonization of the septum, all septum were washed with a 5% potassium persulfate solution and Milli-Q water.

To work with Amicon cell, it is difficult to measure DOC continuously. If a correlation exists between the UV absorbance and the DOC concentration in the effluent of the Amicon cell. It would measure the UV absorbance continuously, instead of DOC concentration. Otherwise, DOC concentration should be measured directly.

For kinetic/isotherm tests, it is not necessary to measure DOC concentration continuously. Therefore, measuring only DOC concentration is sufficient, however, measuring UV absorption is useful to have a better knowledge about the characteristics of NOM in the effluent.

To show that there is a correlation between the UV absorbance and the DOC concentration, 18 samples are taken from the effluent of an Amicon cell. And both the UV absorbance and the DOC concentration are measured.

PAC particle size measurement

The HSDM model depends on the particle radius, so measuring the PAC particle size is necessary. A Malvern Mastersizer 3000 device was used for this purpose. First, a suspension of 100 mg/L PAC in Milli-Q water was prepared. This suspension is used in the instrument to measure the particle size. The size distribution of PAC particles was in the form of a bell diagram (Gaussian distribution). d50 equals a particle size when the cumulative percentage reaches 50 percent. It means that 50% of the particles are larger than d50 and 50% of the particles are smaller than d50. Therefore, d50 is selected as PAC particle diameter and is considered constant during adsorption.

4.5 Raw water quality characteristics

The raw water for Sub-objective 1 and 2 was sampled from the Saint Lawrence River. The sampling of raw water from the Saint Lawrence River was done several times during the project (9 times from April 2021 to March 2022). Since the physical and chemical parameters of river water are not similar on all days. Therefore, before comparing the PAC performance in two different tests, first the DOC concentration in raw water was measured. If the initial DOC concentration in raw water for two tests were different, these series of tests would be repeated. Table 4-12 shows the DOC concentration for each test.

Table 4-12 DOC concentration in Saint Lawrence River samples for each test

Sub- Objective	Test	DOC (mg/L)	Sampling date	Source
Sub- Objective 1	#1 to #17 and #28	2.7	April 2021- May 2021	St. Lawrence River
	#18 to #20, #23, and #24	2.9	May 2021	
	#21 and #22	2.7	May 2021	
	#25 to #27	2.9	November 2021- December 2021	
	#29 to # 32	2.7	January 2022	
Sub- Objective 2	Kinetic/Isotherm tests	2.7	February 2022- March 2022	
Sub- Objective 3	Kinetic/Isotherm tests	3.6	June 2022	Underground water (CA, USA)

CHAPTER 5 RESULTS AND DISCUSSIONS

In this chapter, the results of the laboratory tests and modeling are analyzed and discussed. This chapter is also divided into three parts related to each sub-objective.

5.1 To assess the suitability of the bench-scale flow-through HMP reactor (Amicon cell) for modeling the Actiflo® Carb process

5.1.1 PAC accumulation on the filter of the HMP reactor

PAC concentration

It has already been shown in the experiments conducted in this laboratory that if the test duration be constant, decreasing PAC concentration leads to an increase in the percentage of PAC accumulation on the membrane (Dauphin, 2017). This observation suggests that the deposition is reduced at higher concentrations. Figure 5-1 shows the impact of PAC concentration on the accumulation % on the filter.

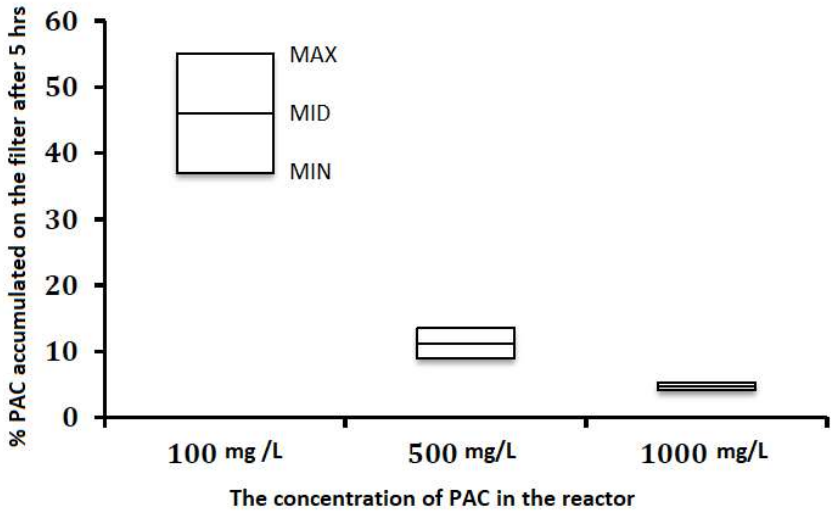

Figure 5-1 Percentage of PAC accumulated on the reactor filter after 5 hours of running the HMP reactor (Dauphin, 2017)

In Dauphin's experiments time for all experiments was constant, therefore, CUR for the reactor with 100 mg/L of PAC was 5 and 10 times more than reactors with 500 mg/L and 1000 mg/L of PAC respectively. Therefore, two factors effected on PAC accumulation simultaneously.

In order to consider the effect of PAC concentration independent of CUR effect, the above experiment was repeated with four different PAC concentrations at a fixed CUR of 50 L $_{water}$/g $_{PAC}$ (equivalent to 20 mg PAC/ L water). As shown in Figure *5-2*, the PAC accumulation % (weight of the accumulated PAC to the total PAC weight) on the filter did not significantly change over PAC concentration.

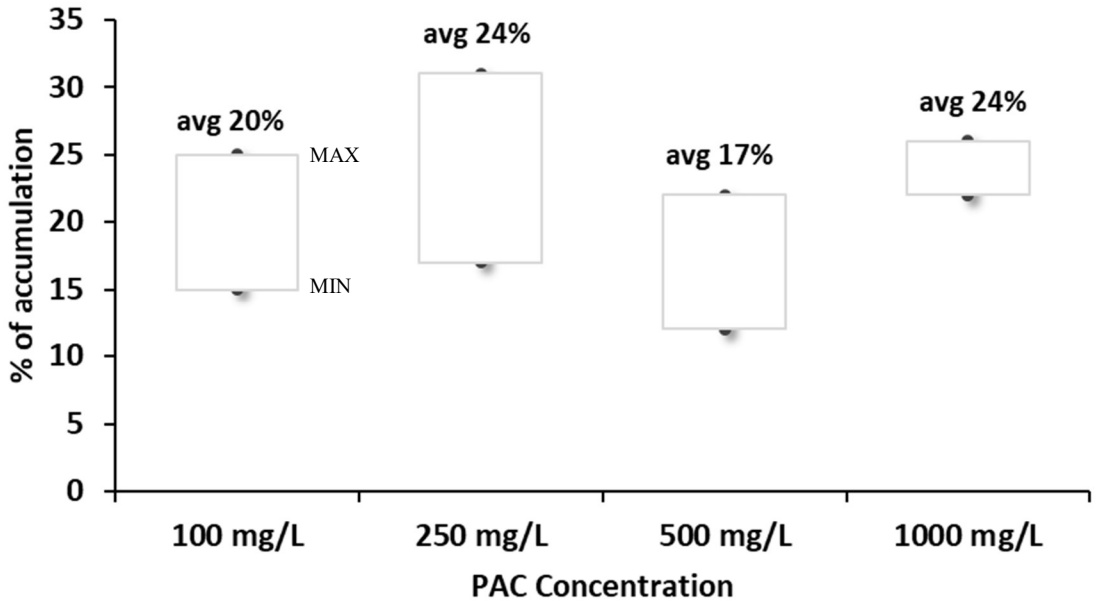

Figure 5-2 Effect of PAC concentration over the percentage of PAC accumulated on the reactor filter.

Hydraulic retention time (HRT)

Increasing the flow rate in a reactor decreases the HRT. As shown in Figure 5-3, the percentage of PAC accumulation decreased significantly from test #5 (HRT = 7.5 min) to test #6 (HRT= 15 min) and decreased slightly in test #7 (HRT = 30 min). However, the duration of test #7 is four times higher than test#6. But PAC accumulation in test #7 is 76 % less than in test #6. This result shows that the advection force is more important than sedimentation force in making PAC film on the surface of the membrane.

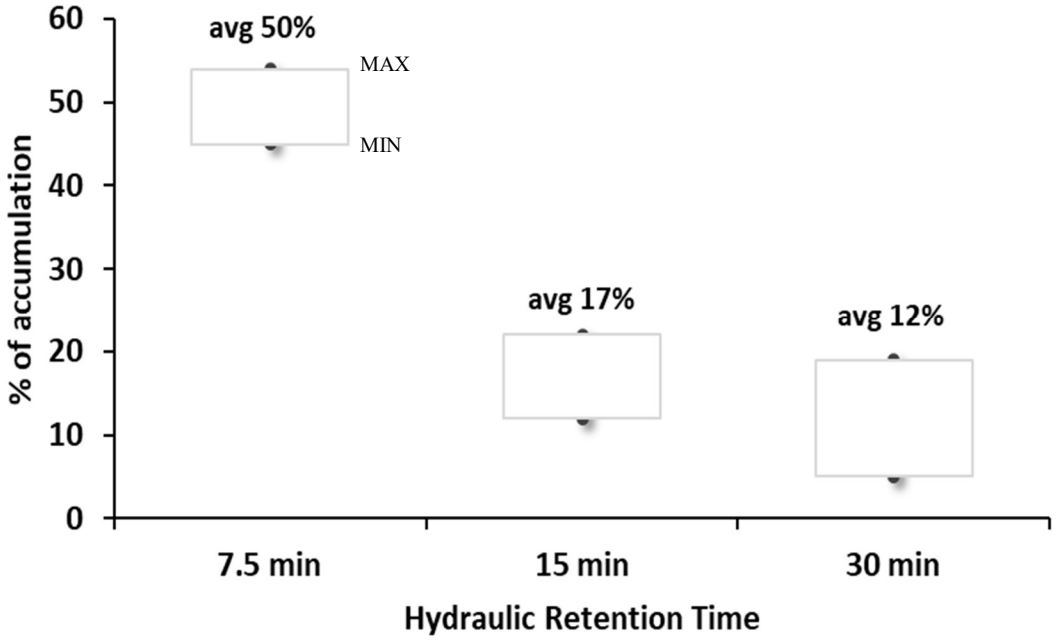

Figure 5-3 Effect of HRT over the percentage of PAC accumulated on the reactor filter.

Flow direction

At the end of test #16, it was observed that a significant accumulation of PAC was found on the surface of the membrane, and only an insignificant amount of sediment was found on the bottom of the reactor. Therefore, it was concluded that even when the flow direction is the same as the gravitational force, a significant fraction of the accumulation is due to advection and not under the influence of gravity and sedimentation.

Membrane diameter

Figure 5-4 shows that, at the end of test #17, only an insignificant amount of PAC was accumulated on the surface of the wax paper. Also, PAC was accumulated between the paper and the membrane (under the wax paper, in the areas where the water flow had separated the wax paper from the filter surface). The result of test#17 confirms the results of previous tests. Therefore, there is no doubt that advection is the main reason for PAC accumulation of the membrane surface.

Figure 5-4 PAC accumulation on the filter surface. The left picture belongs to test#17 and the right one is a sample of normal membrane operation

Impact of Stirrer's rotation speed

In experiments conducted previously in our laboratory by Dauphin (2017), the SRS was fixed at about 165 rpm, which was chosen due to the limitations of the Amicon cell reactor. By applying minor modifications to the Amicon cell reactor, we could reach 400 rpm. Figure *5-5* shows that in the absence of a stirrer, almost all PAC accumulates on the surface of the filter (the PAC accumulation rate for test #8 was measured at 30 L_{water}/ g_{PAC}). Stirring at a speed of 165 rpm resulted in the suspension of about 79% of PAC after treatment of 50 L_{water}/ g_{PAC} and increasing the SRS to 300 rpm slightly improved the suspended PAC percentage (83%). And finally, increasing the SRS to 400 rpm did not have a significant effect on PAC suspension (82%). In our laboratory condition, the agitator of the Amicon cell did not work stably at 400 rpm, and in some experiments, the agitator stopped suddenly. Therefore, the speed of 300 rpm was chosen as the standard SRS for the rest of the study. It seems unavoidable to have about 17% deposition at the end of the test.

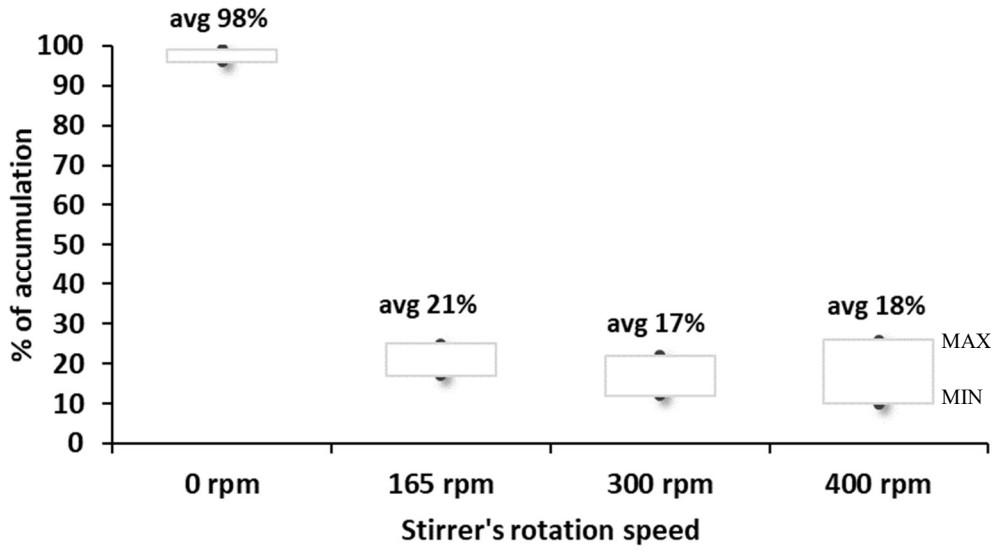

Figure 5-5 Effect of SRS over the percentage of PAC accumulated on the reactor filter.

Impact of Carbon usage rate (CUR)

Figure 5-6 shows that the CUR increases the percentage of PAC accumulation. When the CUR reached 100 L_{water}/ g_{PAC}, less than half of the PAC was suspended in the reactor. And by increasing the CUR to 125 L_{water}/ g_{PAC}, only a tiny fraction of PAC remained suspended. Figure 5-7 shows the Amicon cell reactor after CURs of 50, 100, and 125 L_{water}/ g_{PAC}, respectively.

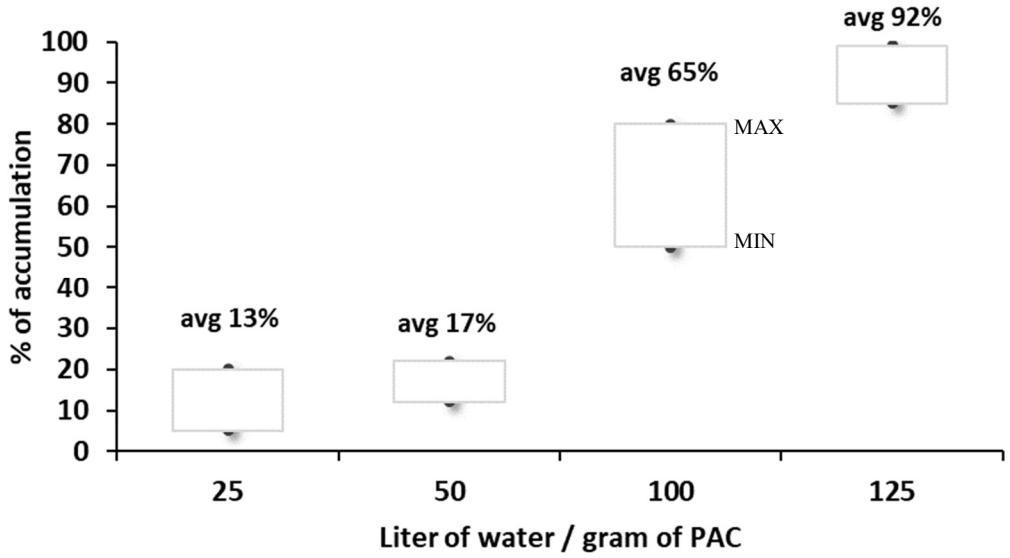

Figure 5-6 Effect of CUR of water over the percentage of PAC accumulated on the reactor filter.

Table 5-1 shows a summary of the result of the different tested parameters on deposition.

Table 5-1 Summary of the effects of different tested parameters on deposition

Test number	Parameter studied	Result and conclusion
1 to 4	PAC concentration	PAC concentration did effect on PAC accumulation rate
5 to 7	HRT	Higher flow leads to higher deposition, which indicates that PAC accumulation related to the advection
8 to 11	SRS	300 rpm was selected to running the Amicon cell
12 to 15	CUR	After treating 100 L/g of PAC the majority of PAC was deposited on the surface of membrane
16	Flow direction	It has observed PAC always accumulated on the surface of membrane, whether the membrane located at the button of reactor or on the top. Which shows the advection is main reason of deposition of PAC on the membrane surface.
17	Membrane diameter	A significant fraction of PAC accumulation on the surface of the membrane, where it was not covered by the wax paper. Which confirms the result of test 16

Figure 5-7 Amicon cell after treating 50, 100, and 125 L water/ g PAC respectively.

5.1.2 UV_{254}/DOC correlation and desorption in Amicon cell

As shown in Figure 5-8, it was observed that there is a high correlation between DOC and UV_{254} absorbance in the effluent until the C_{eff} gets close to the C_{inf}. The effluent DOC value reached influent before the effluent UV_{254} did. In other words, while DOC adsorption has finished, UV absorbance still decreases in the reactor.

As shown in Table 5-2 for samples 16 and 17, the effluent DOC is higher than the influent (marked with green in Table 5-2). It shows that at this stage, total desorption is more than total adsorption. However, at these points, UV absorbance is less in the effluent than the influent. It shows that the characteristics of NOM in the effluent and influent are different.

Table 5-2 UV254/DOC in the effluent of Amicon cell

Sample number	UVA_{254} (cm^{-1})	DOC (mg / L)	Sample number	UVA_{254} (cm^{-1})	DOC (mg / L)
1	0.0045	0.56	10	0.0402	2.45
2	0.0100	0.89	11	0.0415	2.53
3	0.0170	1.40	12	0.0438	2.68
4	0.0190	1.40	13	0.0442	2.67
5	0.0275	1.87	14	0.045	2.69
6	0.0310	2.12	15	0.0457	2.71
7	0.0355	2.24	16	0.0467	2.80
8	0.0365	2.38	17	0.047	2.77
9	0.0400	2.48	18	0.0477	2.72
Milli-Q	**0.0000**	**0.035**	**Raw water**	**0.0506**	**2.73**

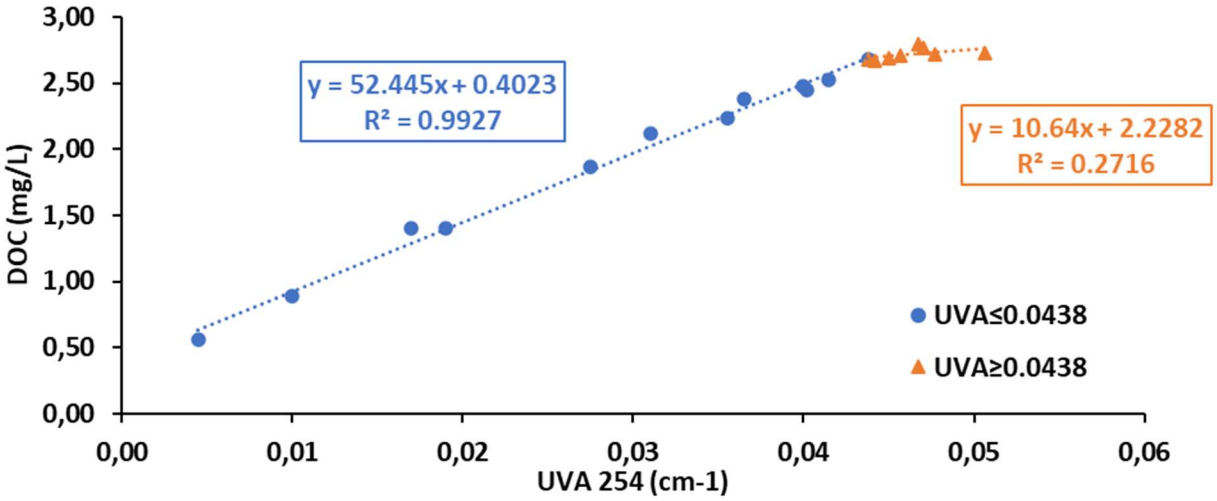

Figure 5-8 Correlation UV254/DOC in Amicon cell

5.1.3 The effect of PAC concentration, Membrane diameter, HRT and SRS on the breakthrough curve

PAC concentration

Figure 5-9 to Figure 5-11 show the Breakthrough curve of the Amicon cell for tests #18 to #24 on virgin PAC and the raw water from Saint Lawrence River (DOC = 2.7 mg/L for tests #21 and #22, and DOC =2.9 for the rest of the tests).

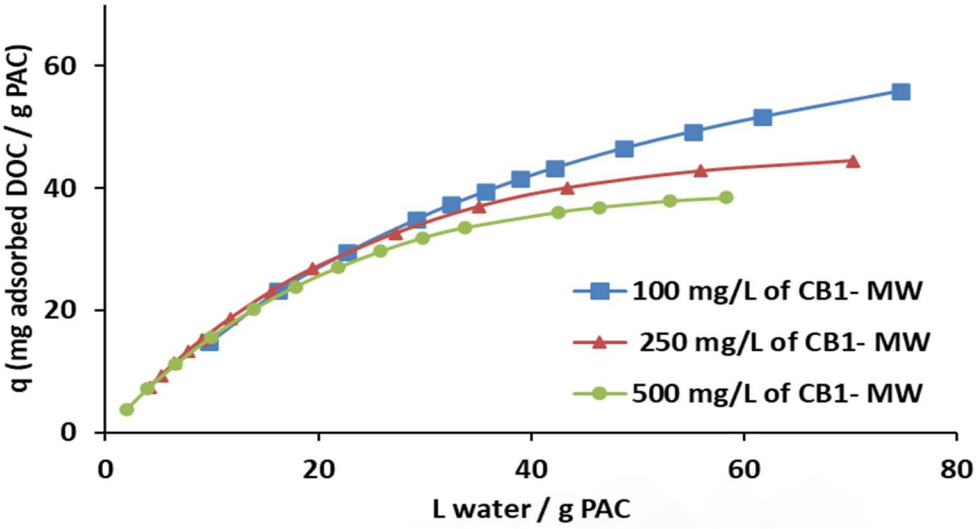

Figure 5-9 Breakthrough curve of Amicon cell with 100, 250, and 500 mg/L of PAC concentration, influent DOC= 2.9 mg/L, HRT=15 min (test #18 to test #20)

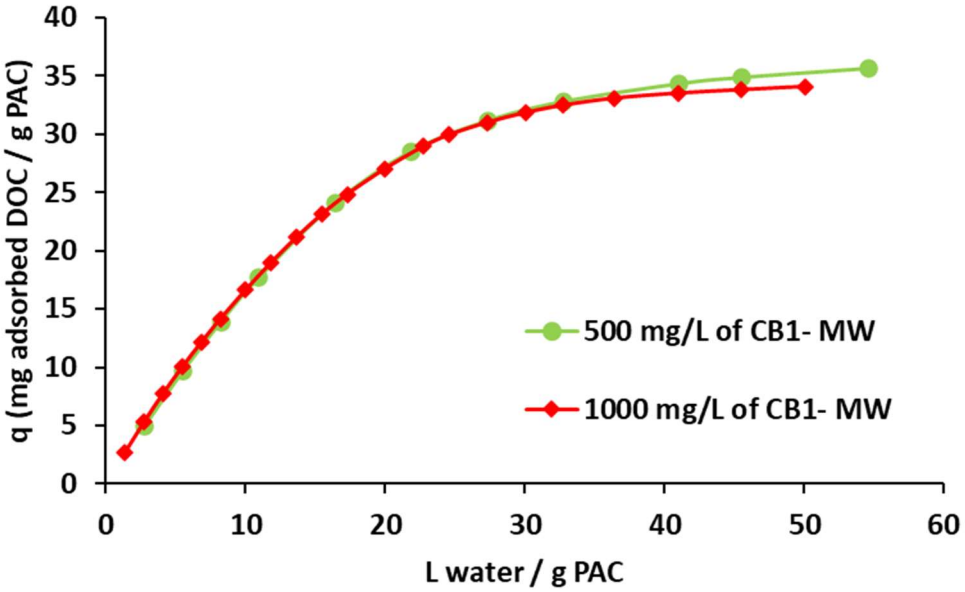

Figure 5-10 Breakthrough curve of Amicon cell with 500 and 1000 mg/L of PAC, influent DOC= 2.7 mg/L, HRT=11 min (test #23 and test #24)

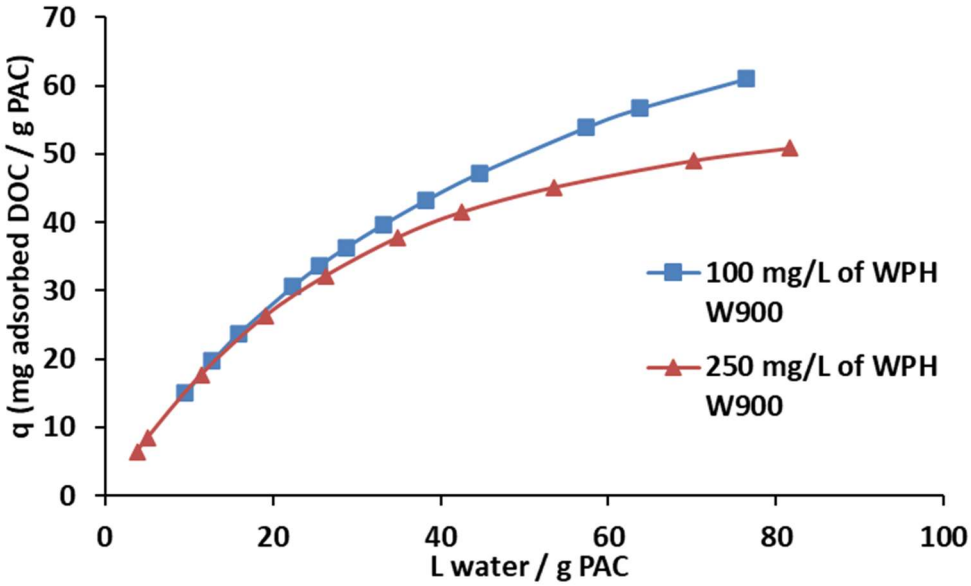

Figure 5-11 Breakthrough curve of Amicon cell with 100, and 250 mg/L of PAC, influent DOC= 2.9 mg/L, HRT=15 min (test #21 and test #22)

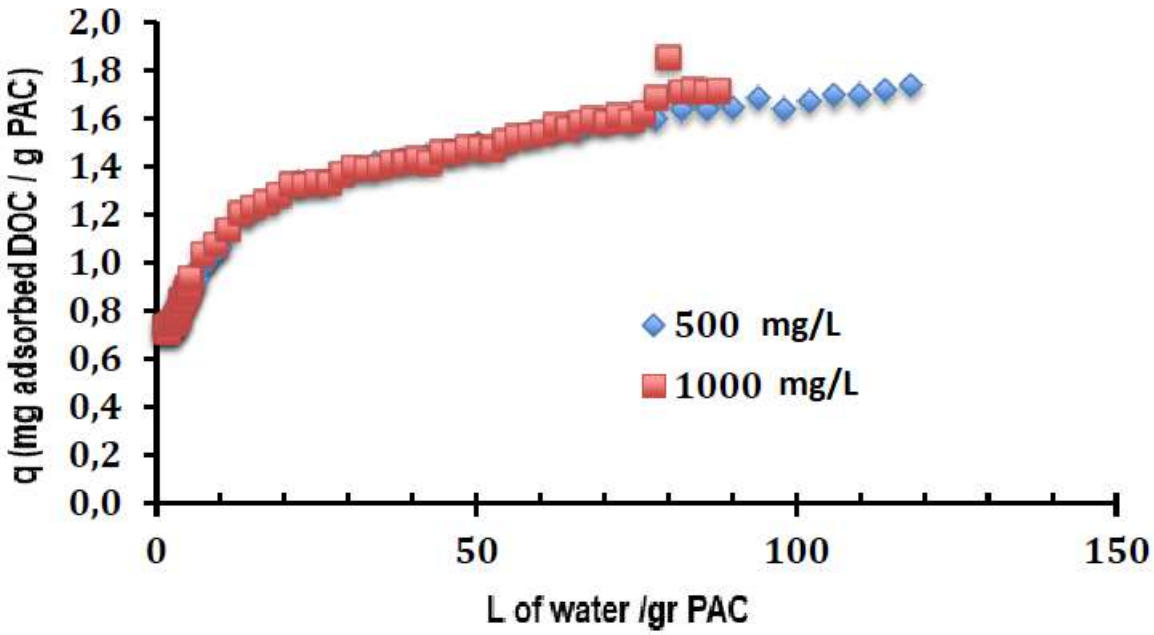

Figure 5-12 Breakthrough curve of Amicon cell with 500, and 1000 mg/L, PAC-S, influent DOC= 1.7 mg/L (Dauphin, 2017)

Figure 5-9 to Figure 5-12 show that the increase in PAC concentration leads to a decrease in PAC efficiency at the same CUR. This decrease in efficiency is more severe when the PAC concentration is increased from 100 to 500 mg/L, and with the increase of PAC concentration from 500 mg/L to 1000 mg/L, the reduction in efficiency is negligible. As mentioned in the previous chapter, the axes of the graphs are normalized by utilization PAC rate to compare different PAC concentrations. Indeed, PAC will be saturated more quickly when its concentration is lower, as shown in Figure 5-13. Figure 5-12 shows the result of a test done by Dauphin with tap water from the Montreal distribution network (DOC= 1.7 mg/L) and PAC-S (AquaSorb MP 23) from Jacobi ®. As shown in figure 5-12 there is no significant difference between the PAC efficiency when PAC concentration increased from 500 mg/L to 1000 mg/L. which is similar to our results.

Figure 5-13 and Figure 5-14 show PAC in the Amicon cell with lower PAC concentration will be saturated faster but at a higher CUR.

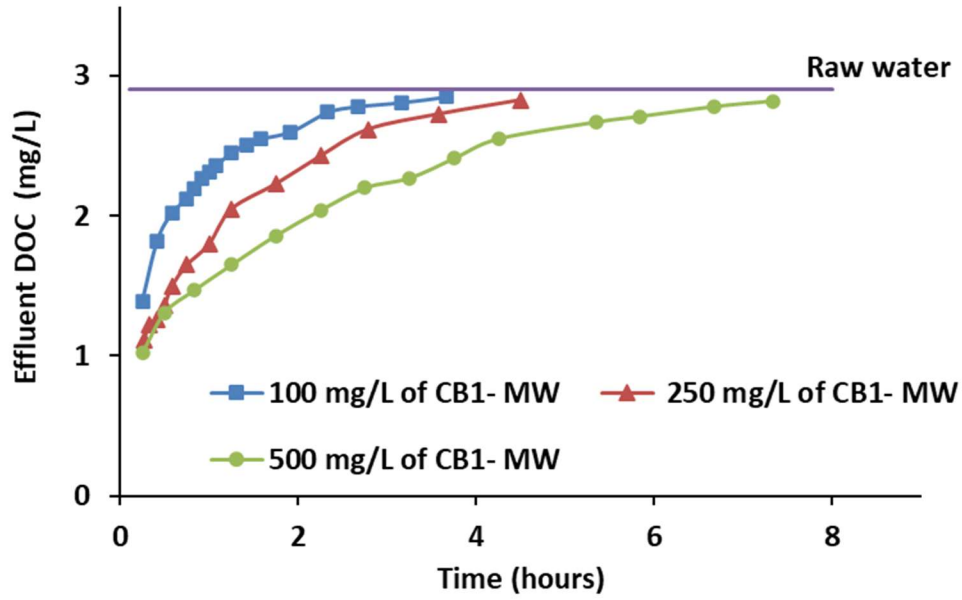

Figure 5-13 Effluent DOC versus time for the tests #18 to #20, with raw water from Saint Lawrence River for doses of 100, 250, and 500 mg/L of PAC, influent DOC= 2.9 mg/L

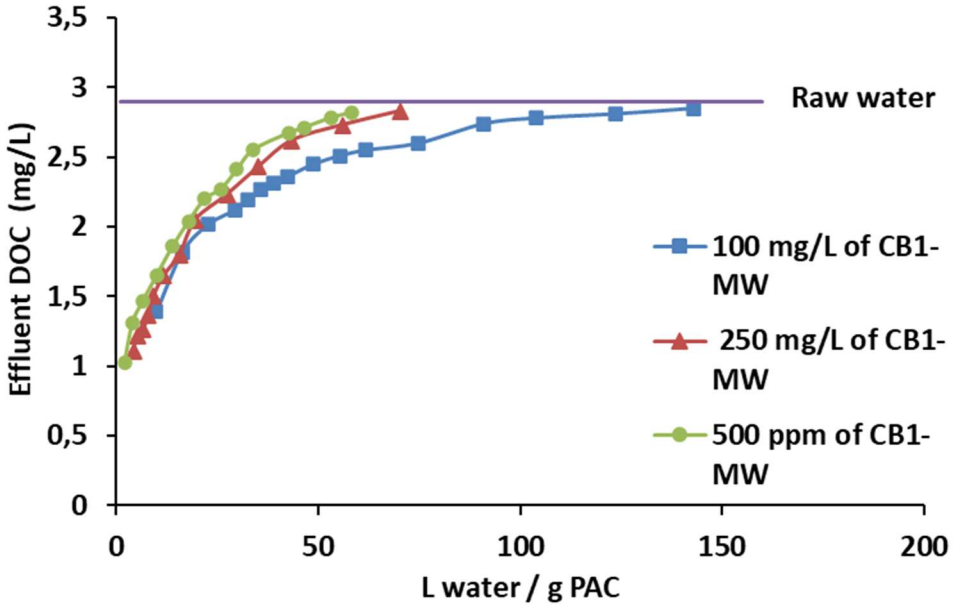

Figure 5-14 Effluent DOC versus CUR for the tests #18 to #20, with raw water from Saint Lawrence River for doses of 100, 250, and 500 mg/L of PAC, influent DOC= 2.9 mg/L

Contrary to the initial assumption, which was assumed that PAC concentration does not affect the breakthrough curve. The results of this study rejected this assumption. Also, as the above figures show, PAC maximum load depends on its concentration. However, it should be kept in mind that

the maximum loading of PAC in an Amicon cell reactor occurs when all PAC particles have accumulated on the membrane, which questions our assumption of a perfectly stirred-tank reactor.

Membrane diameter.

Figure 5-15 shows that decreasing membrane increases the amount of adsorption even at a low CUR. At the end of the experiment, it was observed that the thickness of the cake was greater in the smaller membrane. So, it would be calculated that, here, the adsorption in the PAC on the membrane is higher than in the suspended PAC.

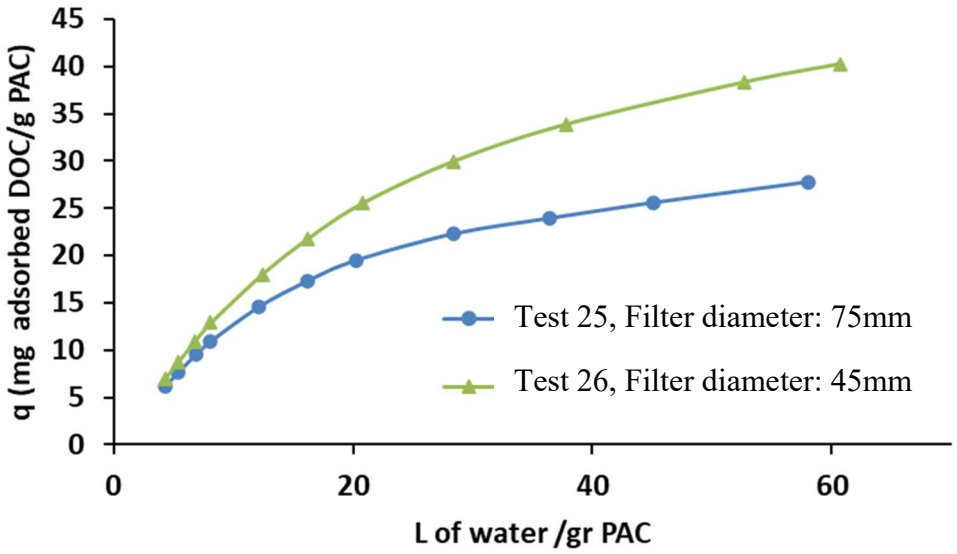

Figure 5-15 The influence of membrane diameter on breakthrough of Amicon cell, influent DOC= 2.67 mg/L

Figure 5-16 shows that the small Amicon cell (50 ml) performs better than the large Amicon cell (400 ml). Which could be because of the difference of PAC accumulation between these two reactors. However, it is not possible to confirm this hypothesis since PAC accumulation rate was not measured for the small membrane. Since the breakthrough curves of these two reactors are entirely different, the above models could not be used to predict a new reactor.

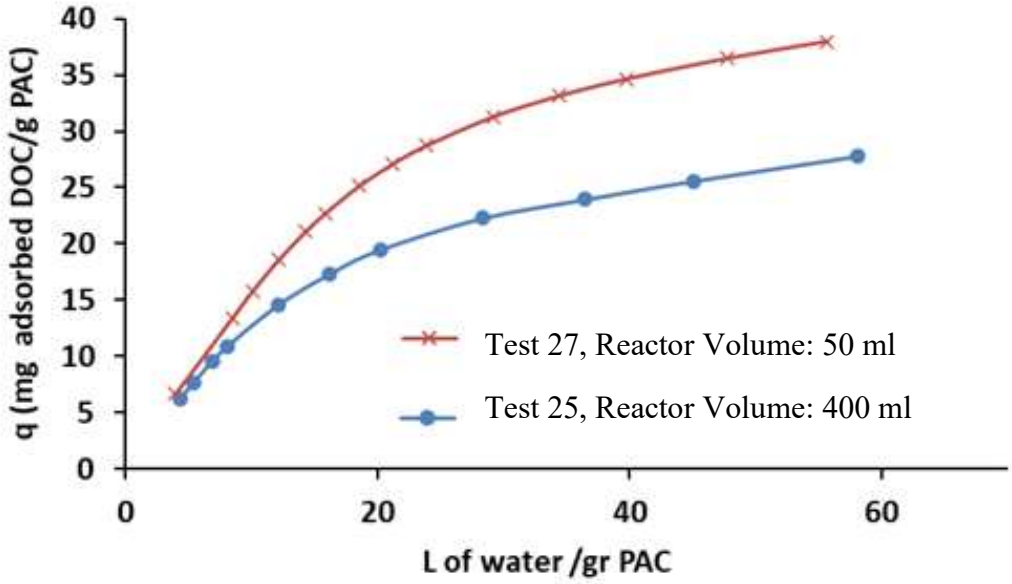

Figure 5-16 The influence of volume of reactor on breakthrough, influent DOC= 2.67 mg/L

HRT and SRS

Before conducting the experiments with the Amicon cell reactor, it was assumed that increasing the ratio of suspended PAC compared to accumulated PAC would improve the performance of the reactor and the adsorption process. In contrast, the breakthrough curves show that increasing in suspension rate in the Amicon cell sometimes leads to decreasing the amount of adsorption. Figure 5-5 showed the PAC accumulation rate in test #8 is higher than in tests #11 and #10. Also, Figure 5-17 shows increasing the PAC accumulation rate leads to better performance.

On the other hand, before conducting the experiments, it was thought that decreasing HRT (increasing flow rate) would reduce adsorption. But it was observed increasing HRT from 7.5 min to 15 min leads to a higher adsorption rate (Figure 5-3). By comparing the accumulation rate between tests #28 and #15, it would be calculated that, here, the adsorption in the PAC on the membrane is higher than in the suspended PAC. Interestingly, stopping the stirring led to the best performance (test #8 vs. tests #10 and #11).

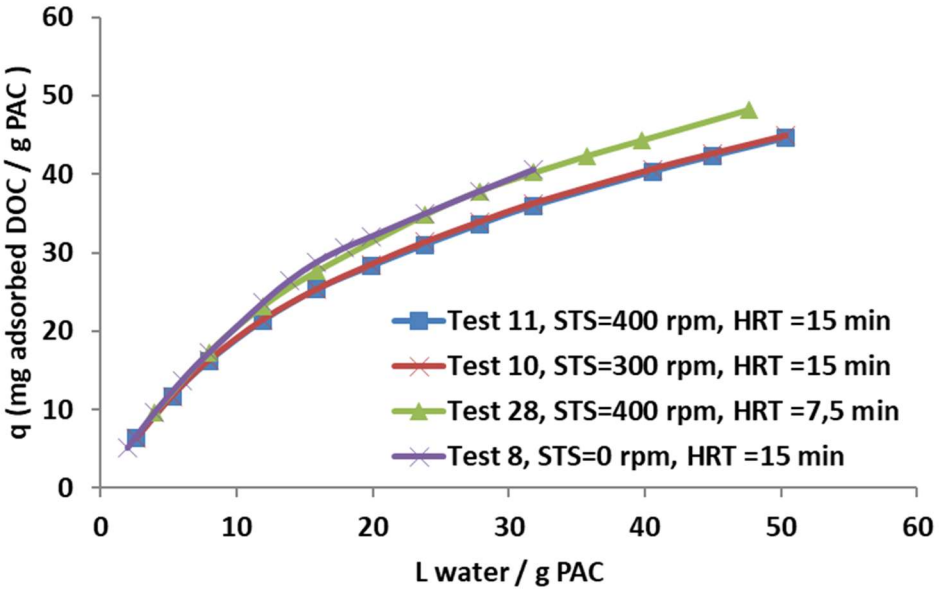

Figure 5-17 The influence accumulation rate on breakthrough, influent DOC= 2.66 mg/L

Dauphine (2017) has already shown (working with the same Amicon cell) that the adsorption rate does not change significantly when the HRT is increased from 15 to 30 minutes (Figure 5-18). Since the accumulation rate for HRT=15 min and HRT=30 is in the same range (17% and 12 %, respectively). It can be concluded that the results of these two test groups are consistent.

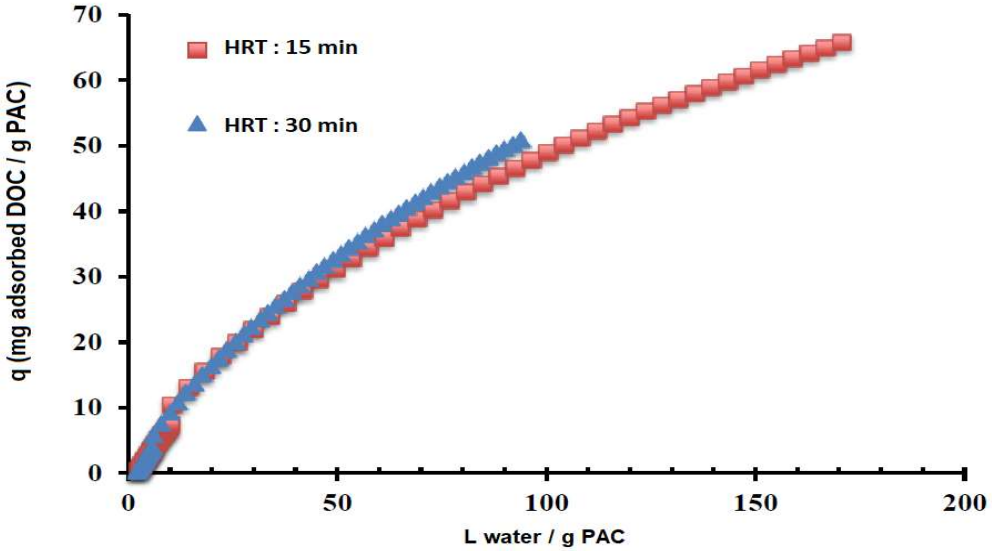

Figure 5-18 The influence of HRT on breakthrough, water from the City of Montreal distribution network, and 500 mg/L PAC (AquaSorb MP 23, PAC-S, d50 15-35 µm)(Dauphin, 2017).

5.1.4 Modeling The Amicon cell reactor

Each breakthrough curve from tests #18 to #24 was modeled according to the pseudo-first-order, pseudo-second-order, and Elovich empirical models. Figure 5-19 shows that the Elovich model is well-fitted to all tests since the coefficient of determination (R^2) is greater than 0.96.

Where the PAC concentration is higher, the rate of increase of q is slower. For instance, in test #20 (500 mg/L PAC), 4 hours are needed to reach q = 30 mg/g, while 35 min is required for test #18 (100 mg/L PAC) to get the same q.

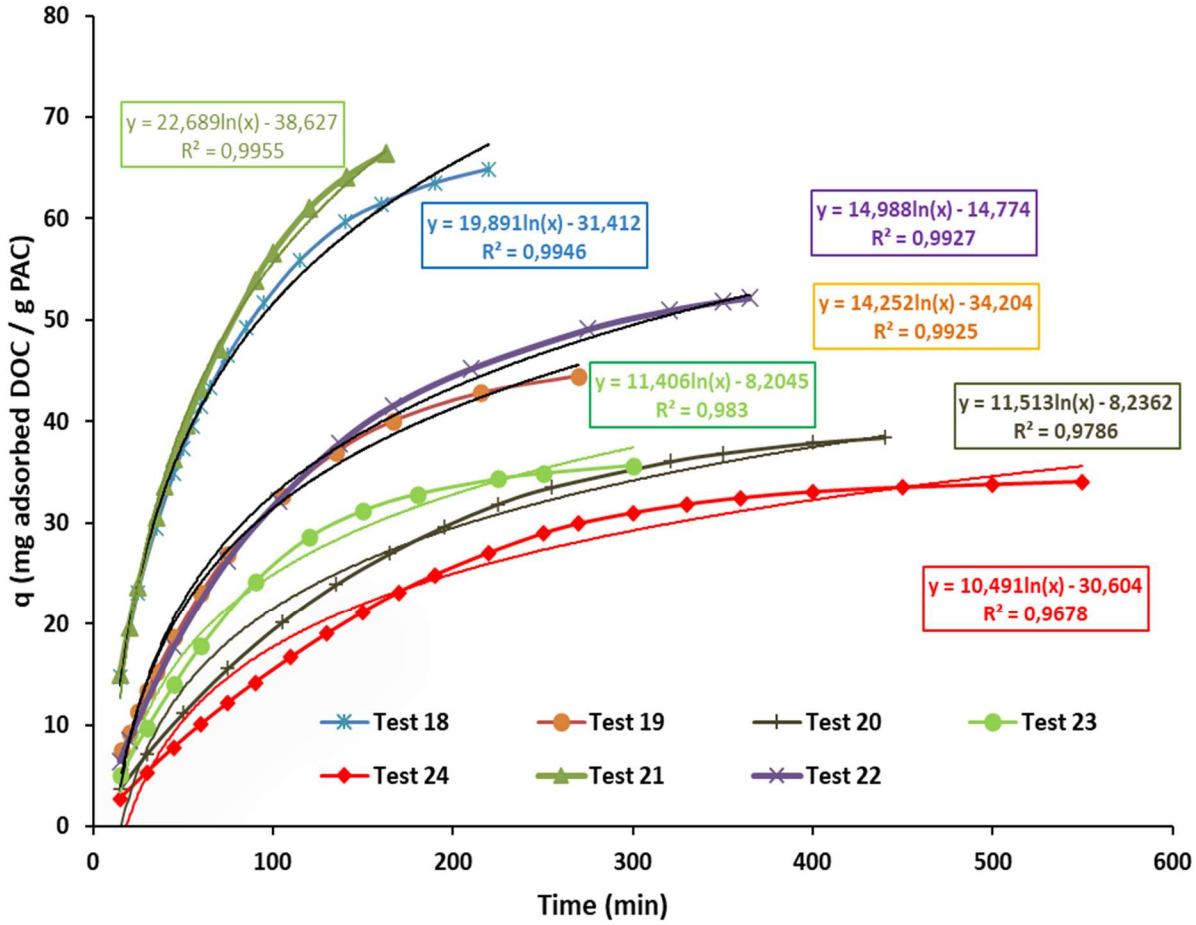

Figure 5-19 Fitting Elovich model on results of test #18 to test #24

Figure 5-20 shows that the pseudo-second-order model is well-fitted to all tests since the R^2 is greater than 0.97. In the pseudo-second-order model, the slope of the line is equal to the inverse of q_{eq}. Therefore, the lower the slope of the graph line, the higher the q_{eq}. as shown in the increasing

PAC concentration, the slope of the graph also increases. Therefore, increasing PAC concentration decreases the q_{eq}.

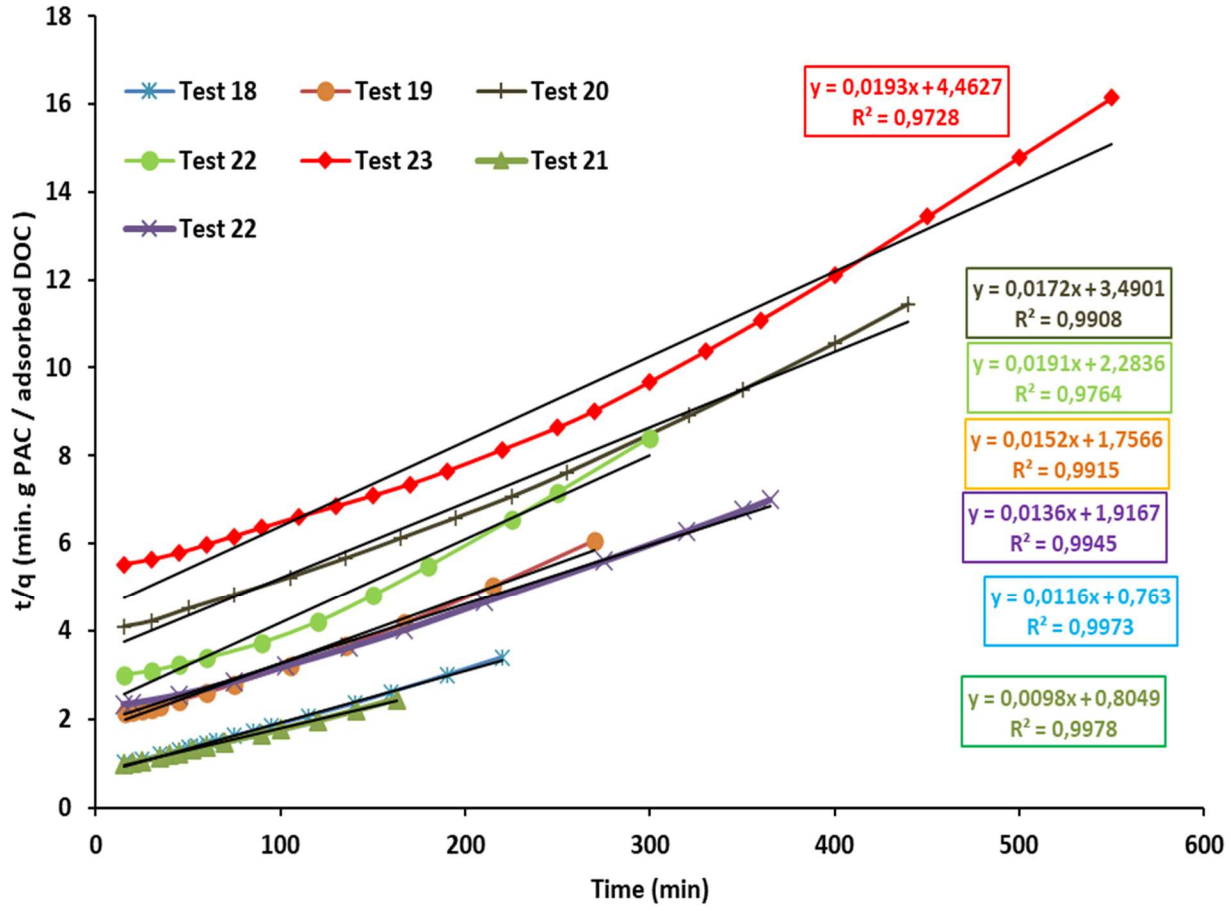

Figure 5-20 Fitting Pseudo-Second-order model on results of test #18 to test #24

Table 5-3 shows that the value of qeq is dependent on PAC concentration. PAC concentration increasing leads to a decrease in the value of q_{eq}.

Table 5-3 The parameter of qe for test #18 to test #24

Test #	18	19	20	21	22	23	24
$1/q_{eq}$	0.0116	0.0152	0.0172	0.0191	0.0193	0.0098	0.0136
q_{eq} (mg adsorbed DOC/ g PAC)	86.2	65.2	58.1	52.4	51.8	102.0	73.5

Figure *5-21* The pseudo-first-order model is fitted to all tests. This model is less accurate than the pseudo-second-order model and the Elovich model. Also, the error of this model increases with time.

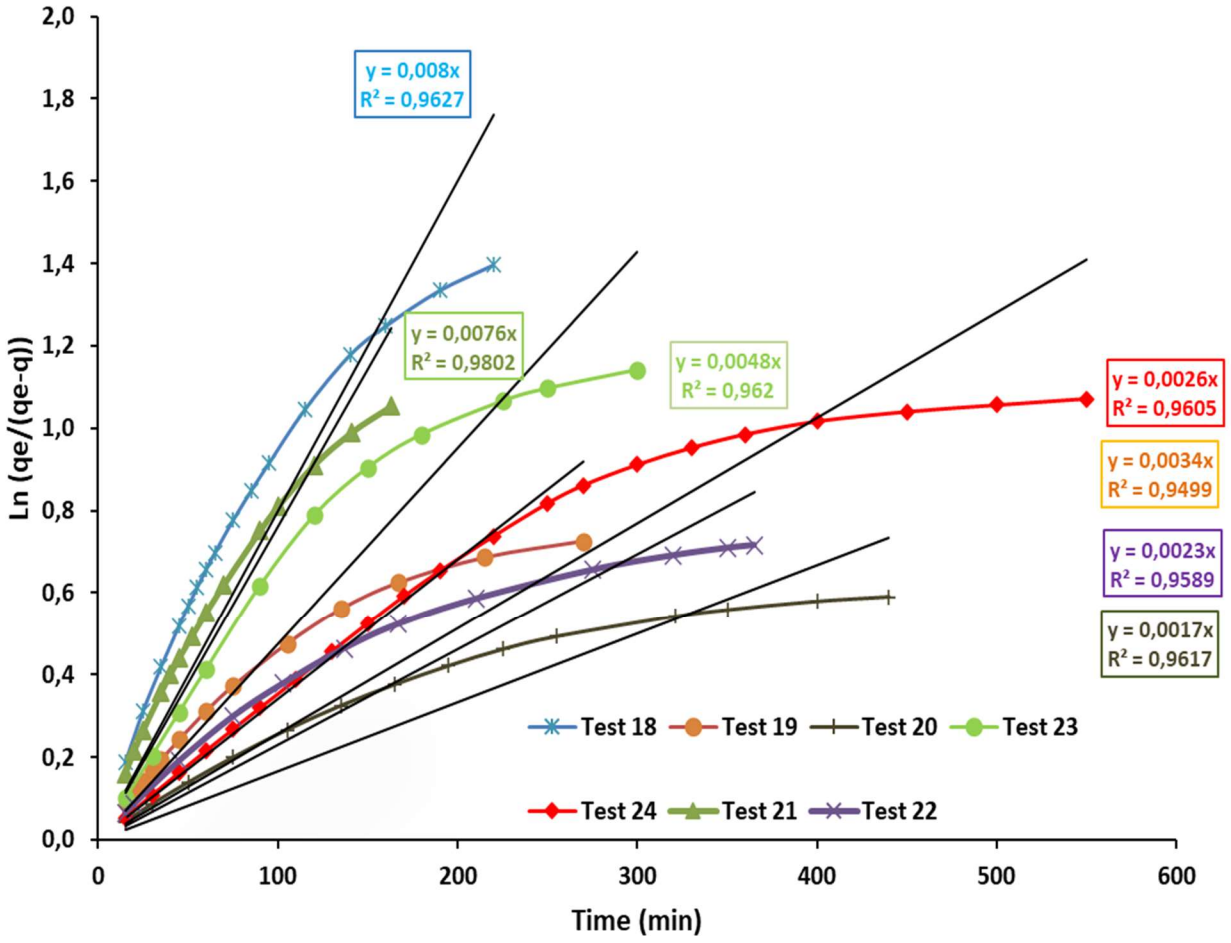

Figure 5-21 Fitting Pseudo-first-order model on result of test #18 to test #24

Table 5-4 shows a summary of coefficients and parameters for kinetic models. The Pseudo-second-order model is the most accurate and has fewer errors than the other models, while the Pseudo-first-order model is the least accurate model.

Table 5-4 Summaries of the coefficients and parameters for kinetic models

Test #	α Elovich parameter	β Elovich parameter	R^2 Elovich parameter	K_{p1} (1/min)	R^2 Pseudo-first-order	K_{p2} (1/min)	R^2 Pseudo-second-order
18	0.010	19.891	0.99	0.008	0.96	1.76E-04	0.997
19	0.006	14.252	0.99	0.0034	0.95	1.32E-04	0.99
20	0.042	11.513	0.98	0.0017	0.96	8.48E-05	0.99
21	0.043	11.406	0.98	0.0048	0.96	1.60E-04	0.98
22	0.005	10.491	0.97	0.0026	0.96	8.35E-05	0.97
23	0.008	22.689	0.99	0.0076	0.98	1.19E-04	0.998
24	0.025	14.988	0.99	0.0023	0.96	9.65E-05	0.99

5.1.5 Verifying the Amicon cell's Models

Figure 5-22 shows the results of the Freundlich equilibrium. And

Table 5-5 shows Freundlich equilibrium's parameter and the virgin PAC adsorption capacity. As mentioned earlier the virgin PAC adsorption capacity is found by Freundlich isotherm.

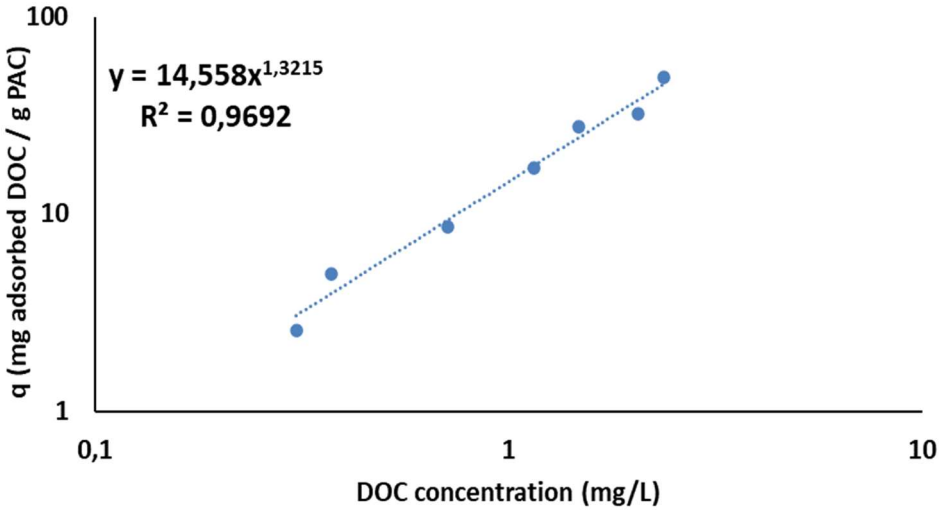

Figure 5-22 Freundlich isotherm curve with raw water from the St. Lawrence River (DOC= 2.9 mg/L) and PAC AquaSorb MP23-F

Table 5-5 Sorption parameters from Freundlich equilibrium

Sorption parameter	Value
1/n	1.3215
K_F (mg adsorbed DOC/g PAC) /(mg DOC/L) $^{(1/n)}$	14.58
Virgin PAC adsorption capacity (mg/g)	58.64

Test #29 has performed for 76 Lwater/ g PAC. But to reduce the advection effect it was modeled for a CUR of 51 Lwater/ g PAC. Figure 5-23 show the Elovich, and pseudo-second-order, for test #29. The q_{eq} obtained from pseudo-second-order for this Amicon cell is 49.75 mg/g, which equals 85% of Virgin PAC adsorption capacity.

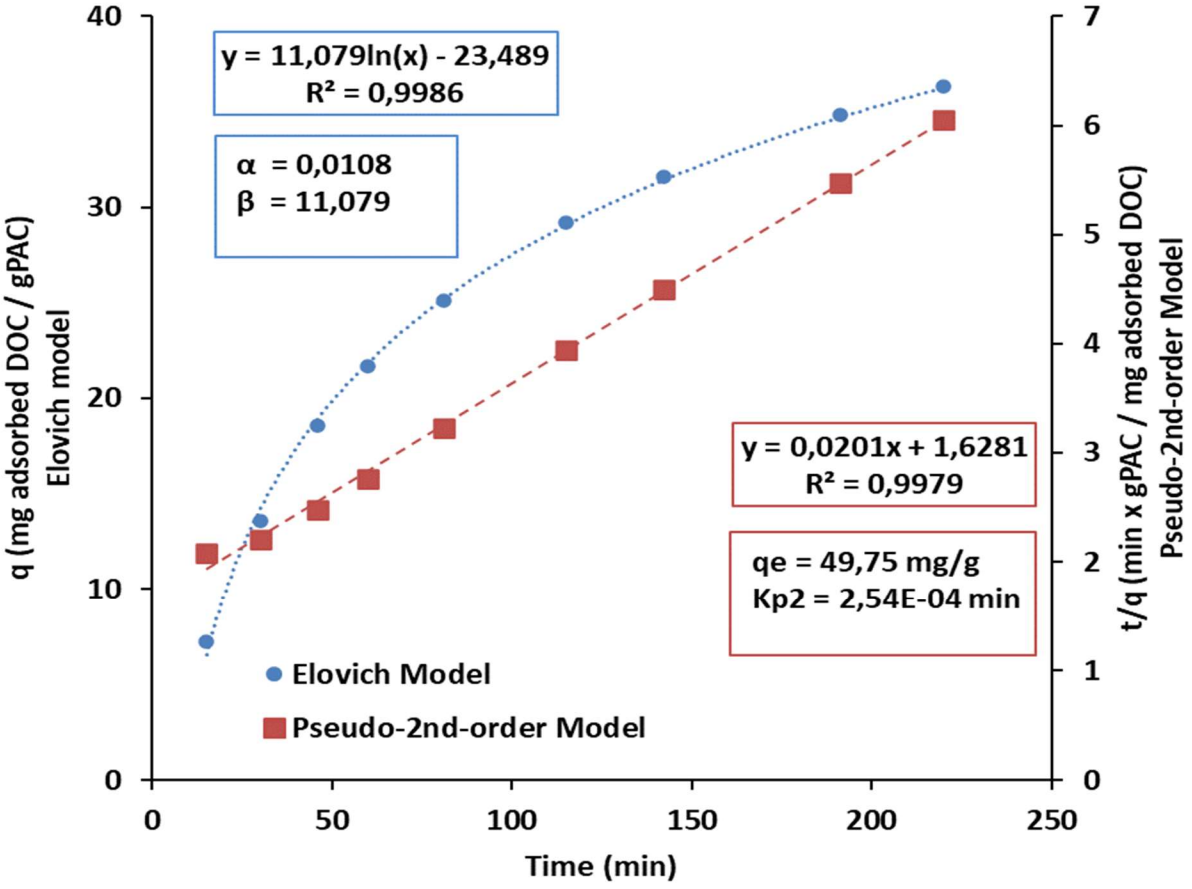

Figure 5-23 Elovich model and Pseudo-second-order model for test #29 with raw water from Saint Lawrence River with 250 mg/L of PAC, influent DOC= 2.87 mg/L

- **Verifying the models with the Amicon cell filled by aged PAC.**

Table 5-6 shows the parameters of q_0 and t_0 for tests #30 to #32.

Table 5-6 Parameters of q_0 and t_0 for tests #30 to #31

Test #	q_0 (mg/g)	PAC age (%)	t_0 (min) for Elovich	t_0 (min) for Pseudo-second-order	t_0 (min) for Pseudo-first-order
30	9.2	15.7	18.9	18.1	30.1
31	13.11	22.4	27.2	29.0	45.7
32	15.25	26.0	33.0	35.8	54.6

Figure 5-24 shows that although the pseudo-first-order model is less accurate in the modeling of test #29, for test #30, the pseudo-first-order model predicts the adsorption rate better than the other models prediction

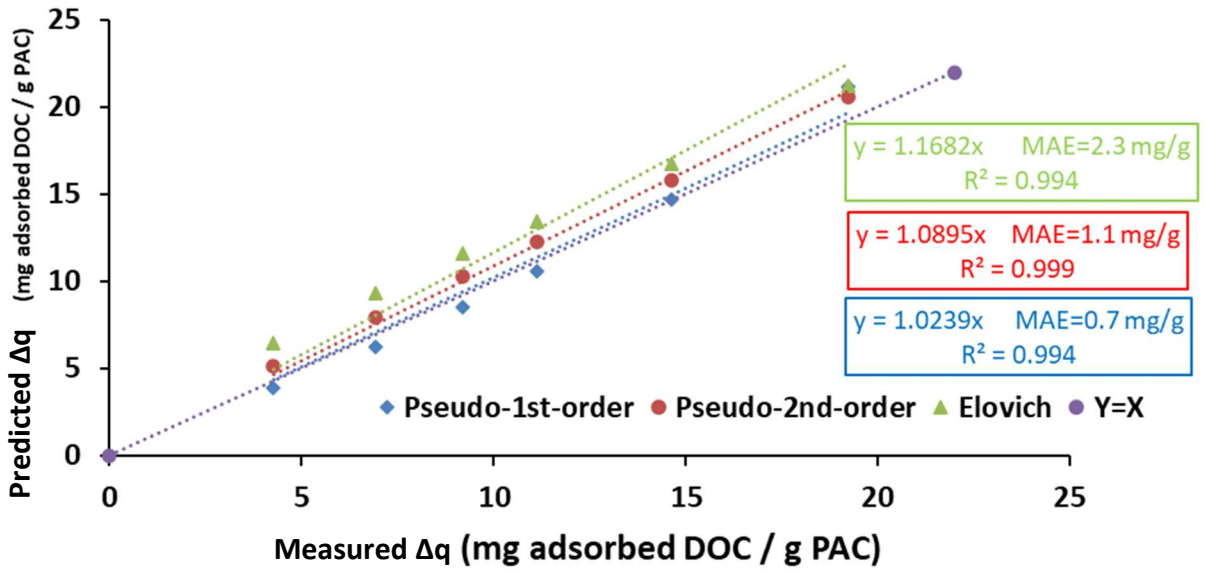

Figure 5-24 Predicted Δq obtained by Elovich, Pseudo-first-order, and Pseudo-second-order models versus Δq measured in test #30 at the laboratory.

Table 5-7 shows that the pseudo-first-order model predicts better at test #26. And the result of the prediction of the Elovich model has the highest error. As mentioned earlier in chapter 4, to have an

accurate prediction, in the "predicted versus actual (measured) plot", the m coefficient in the equation Y=mX must be close to one.

Table 5-7 Accuracy of Δq prediction for Elovich, Pseudo-first-order, and Pseudo-second-order models for test #30

Model	m coefficient	MAE (mg/g)
Elovich	1.16	2.25
Pseudo-first model	1.02	0.72
Pseudo-second model	1.09	1.11

Figure 5-25 shows that for test #31, all three models are less accurate than test #30.

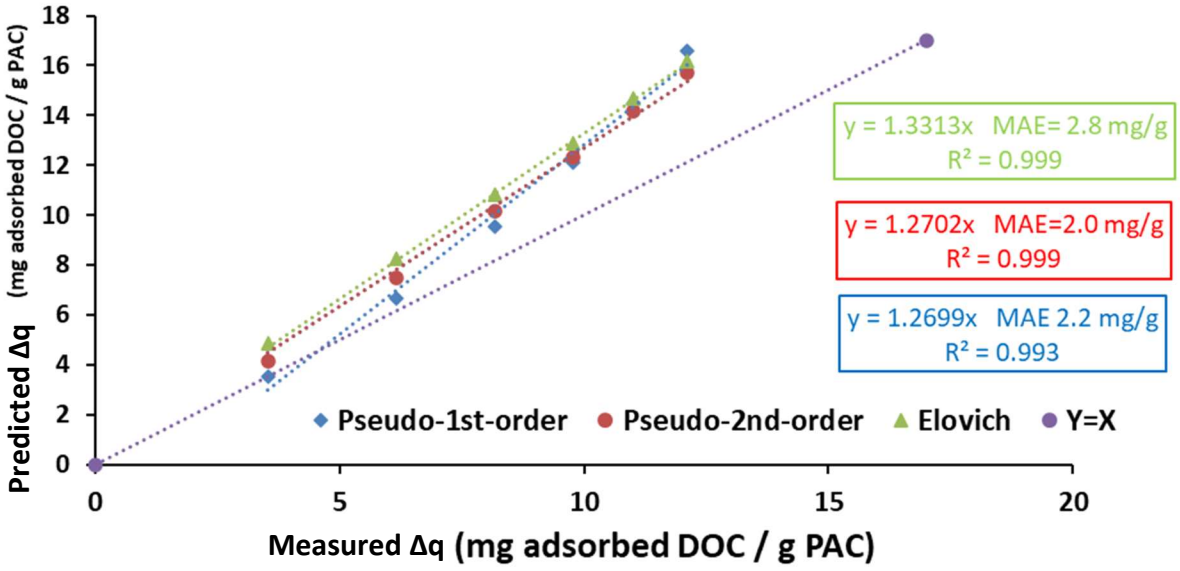

Figure 5-25 Predicted Δq obtained by Elovich, Pseudo-first-order, and Pseudo-second-order models versus Δq measured in test #31 at the laboratory

Table 5-8 shows that MAE for all three models is more than 2 mg/g, which is quite a high error. Also, the m value for all models is around 1.3, meaning that the prediction results are approximately 30% more than the measured data.

Table 5-8 Accuracy of Δq prediction for Elovich, Pseudo-first-order, and Pseudo-second-order models for test #31

Model	m value	MAE (mg/g)
Elovich	1.33	2.8
Pseudo-first model	1.27	2.2
Pseudo-second model	1.27	2.0

Figure *5-26* shows that for test #32, all three models are less accurate than test #30.

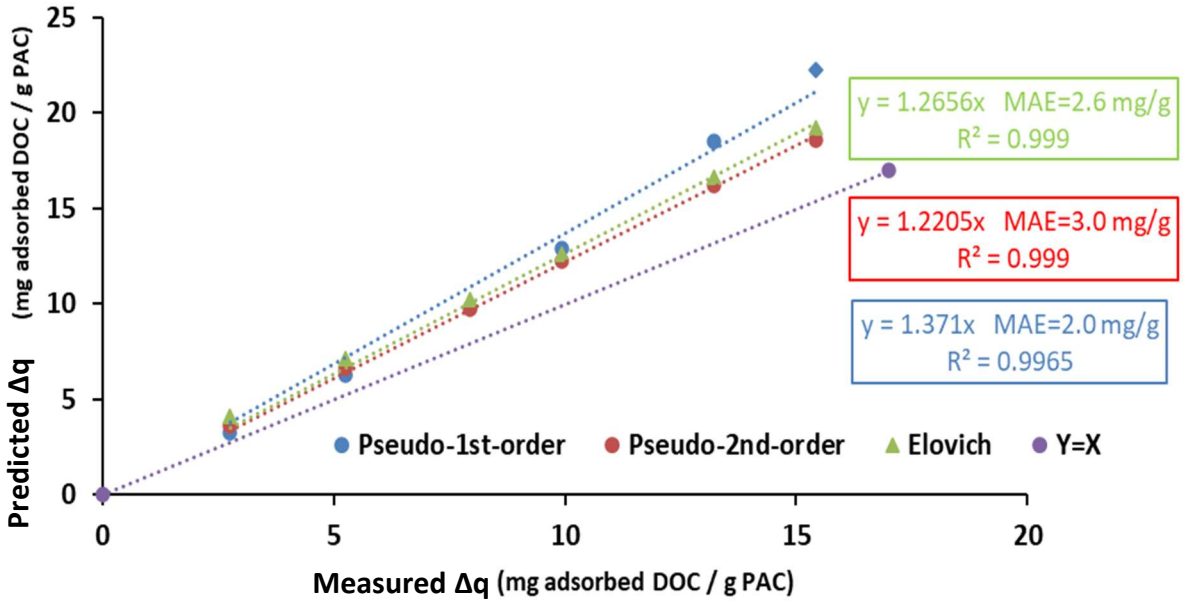

Figure 5-26 Predicted Δq obtained by Elovich, Pseudo-first-order, and Pseudo-second-order models versus Δq measured in test #32 at the laboratory.

Table 5-9 shows that MAE for all three models is more than 2 mg/g, which is quite a high error. Also, the m value for all models is between 1.2 to 1.4, which means that the prediction results are around 20-40 % more than the measured data.

Table 5-9 Accuracy of Δq prediction for Elovich, Pseudo-first-order, and Pseudo-second-order models for test #32

Model	m value	MAE (mg/g)
Elovich	1.27	2.6
Pseudo-first model	1.22	2.0
Pseudo-second model	1.37	3.0

The results of tests #18 to #32 show that modeling an Amicon cell reactor is an unacceptable way to predict another Amicon cell reactor. Therefore, using a bench-scale hybrid membrane reactor is not a suitable approach to predict the Actiflo® Carb process.

5.2 Investigation of the effect of PAC aging and mixing different aged PACs on sorption parameters

5.2.1 Parameters adjusting of isotherm models for single-aged PAC suspensions

Figure 5-27 and Figure 5-28 show that at the equilibrium point (24hr), the final balance of q_{eq} and DOC concentration are independent of q_0 and could be modeled by Freundlich isotherm. In other words, the equilibrium curve is independent of the initial conditions, and it is only influenced by the concentration of the adsorbent in the solvent and adsorbent (responsible forces for mass transfer). This observation indicates that the behavior of the loaded PAC can be described by the isotherm of fresh PAC, which implies that pore plugging by NOM is not important on the loaded PAC.

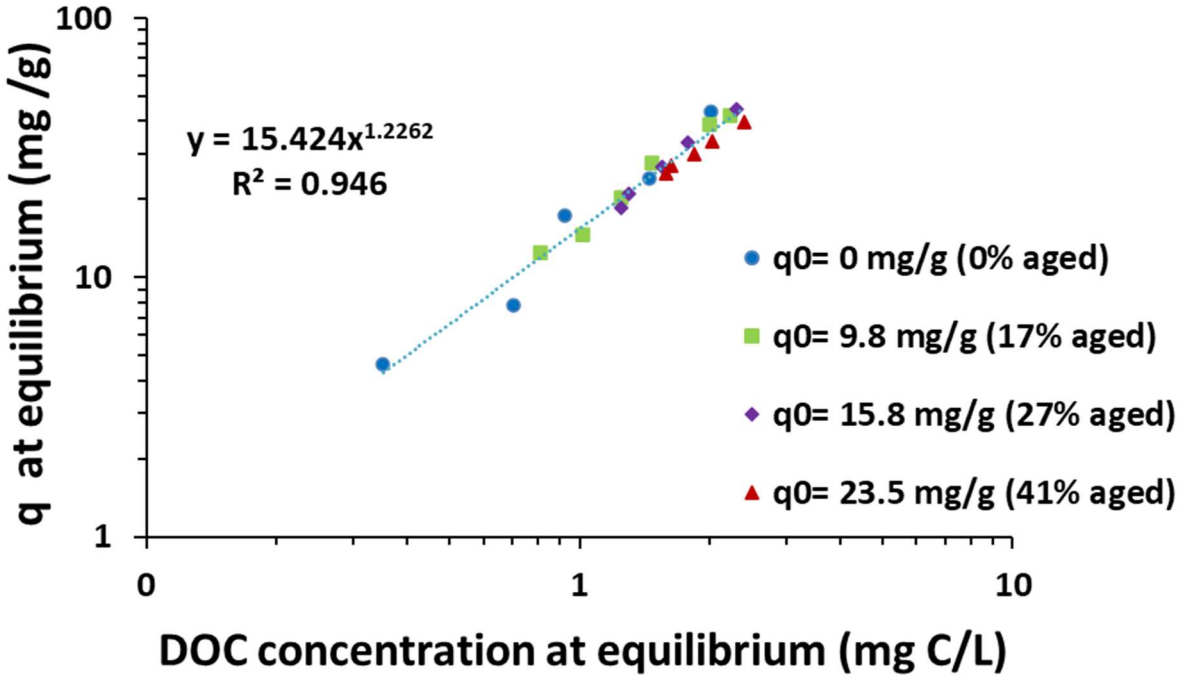

Figure 5-27 parameters adjusting for all PACs for Freundlich isotherm (logarithmic scale)

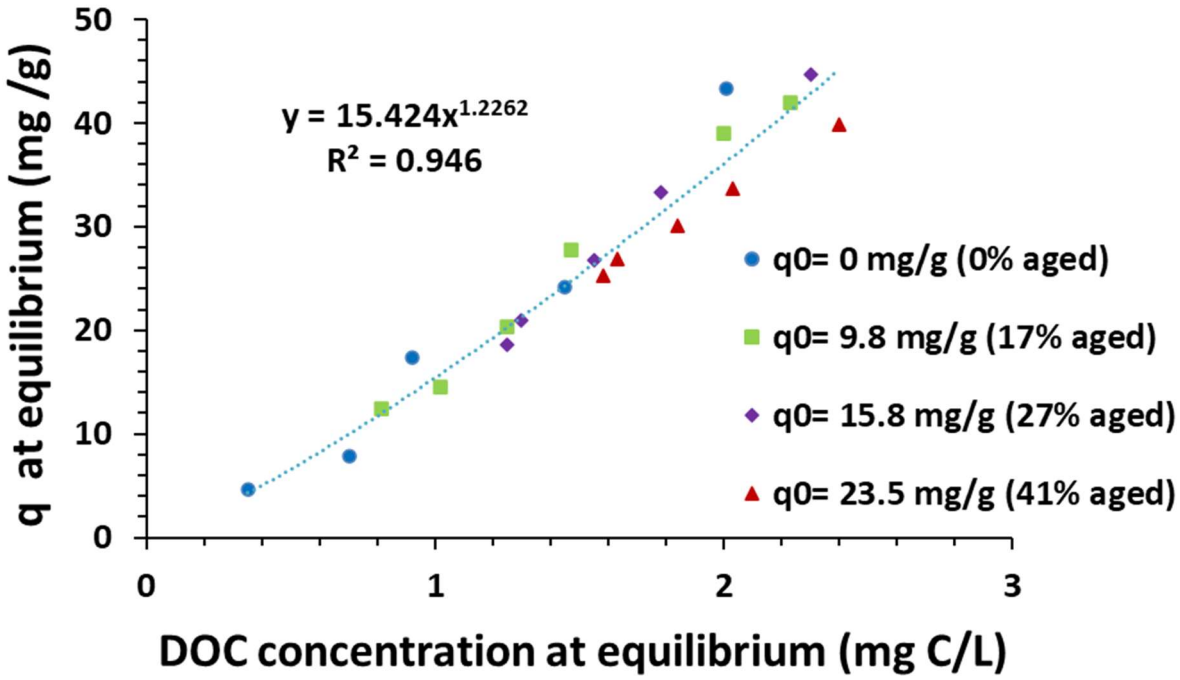

Figure 5-28 parameters adjusting for all PACs for Freundlich isotherm (linear scale)

Table 5-10 shows the result of the parameter adjusting for each test individually versus when parameters were adjusted for all tests (all q_0) for Freundlich isotherm. Changes in Freundlich parameters with PAC aging are insignificant and negligible. As shown in Table 5-10, when 1/n and K_F are fixed as 1.23 and 15.42, respectively, for all preloaded PACs, the MAE (mean absolute error between measured Ceff and predicted Ceff by Freundlich isotherm equation) is less than 0.073 mg/L. This shows the hypothesis that using one Freundlich equilibrium for all preloaded PACs is quite accurate.

Table 5-10 Parameters of the Freundlich isotherm for each PAC specifically versus the parameters using all PACs together

PAC preload (mg/g)	**0**	**9.8**	**15.8**	**23.5**	**All PACs**
1/n	1.30	1.29	1.41	1.07	1.23
K_F (mg adsorbed DOC/g PAC) /(mg DOC/L) $^{(1/n)}$	16.21	15.50	13.21	15.75	15.42
MAE (mg C/L) (When 1/n = 1.23, and K_F is 15.42)	0.060	0.073	0.066	0.051	0.063

Figure 5-29 shows the result of the parameter adjusting for all PACs together with the Langmuir isotherm. Like Freundlich isotherm, the result of parameter adjusting with Langmuir isotherm shows that at the equilibrium point, q_∞ is independent of q_0. Therefore, the equilibrium point for a suspension with q_0 could be found with the equilibrium curve of virgin PAC.

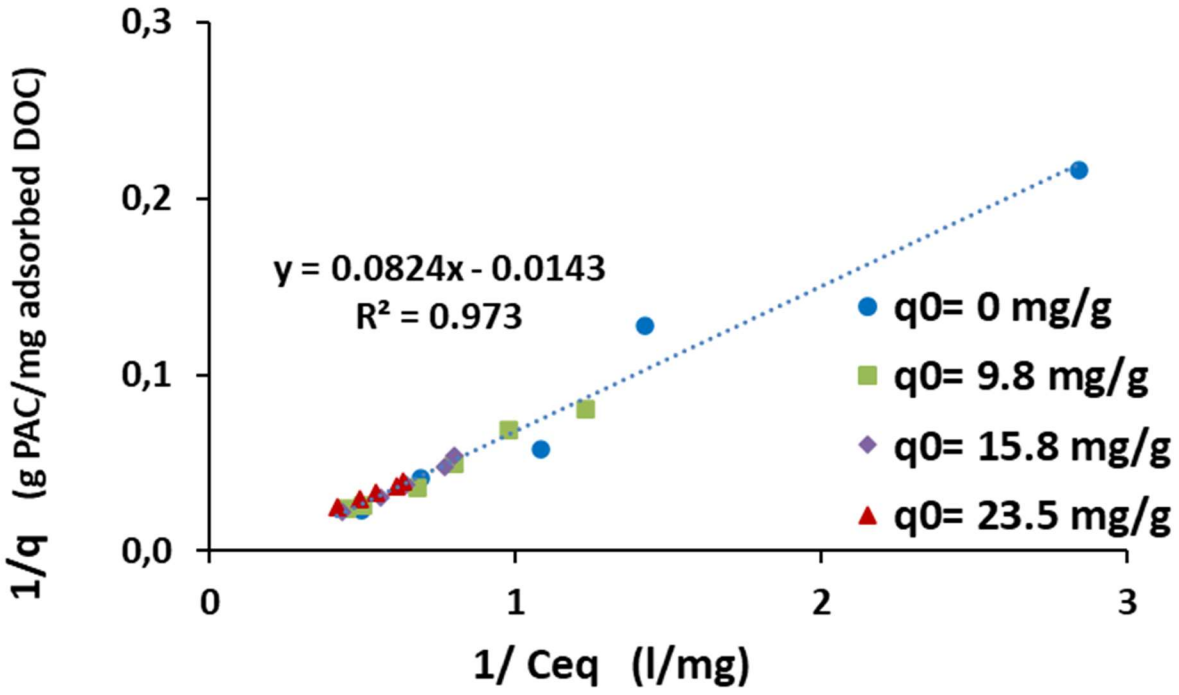

Figure 5-29 parameters adjusting for all PACs for Langmuir isotherm

5.2.2 Parameter adjusting of the HSDM of single aged PAC suspensions, and investigating of PAC aging influence of Ds

By using Equation 4-15 and the Freundlich parameters obtained in Section 5.2.1, the diffusivity coefficient Ds was adjusted individually for each aged PAC and then simultaneously for all aged PACs. The second column from the left in Table 5-11 shows adjusted Ds for each loaded PAC (q_0). As shown in Figure 5-30 shows the influence of Ds on MAE, when Ds changes from 2.5E-12 to 5.2E-12 cm^2/s is not significant. Therefore, changes in Ds for the different loaded PACs would be considered negligible, in other words, **Ds is independent of q_0** and could be considered a constant amount. This suggests that the PAC pores are not plugged during the NOM adsorption process (in the matrix of filtered raw water and PAC). Here the surface diffusion coefficient Ds = 3.3E-12 (cm^2/s) once minimized for all aged PACs were considered simultaneously (four loads and a total of 147 data points). The MAE for each PAC is less than 0.1 mg/L which is a value similar to the experimental DOC analytical error (the first column from the right in Table 5-11)

Table 5-11 Adjusted Ds for each PAC individually versus adjusted Ds for all PACs

Aged PAC	Adjusted Ds (cm^2/s)	MAE (µg/L) (for adjusted Ds for each aged PAC)	MAE (µg/L) (When Ds is 3.3E-12)
Virgin PAC	4.1E-12	75	81
1St aged PAC (q_0 =9.8 mg/g)	5.2E-12	74	81
2nd aged PAC (q_0 =15.8 mg/g)	2.4E-12	64	71
3rd aged PAC (q_0 =23.5 mg/g)	2.4E-12	92	98
All PACs	3.3E-12	83	83

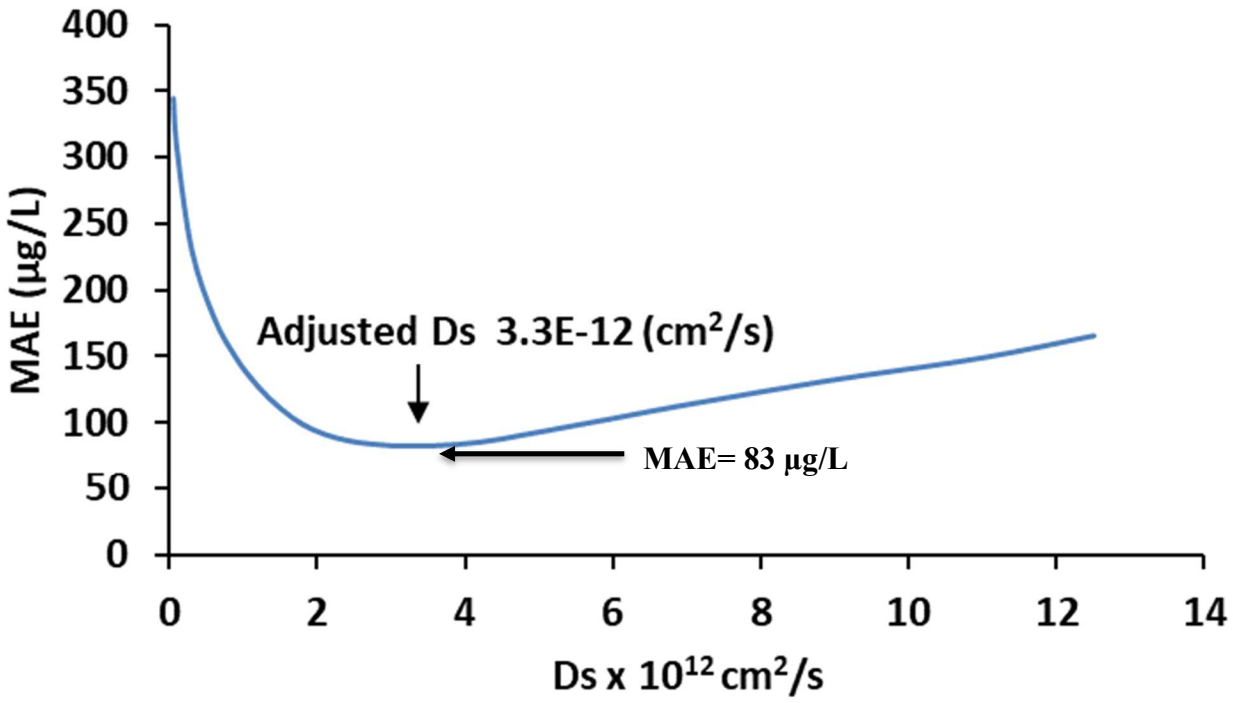

Figure 5-30 Adjusting D_s for all PACs

Figure 5-31 shows the impact of Ds changing on MAE for each aged PACs and when all PACs considered simultaneously

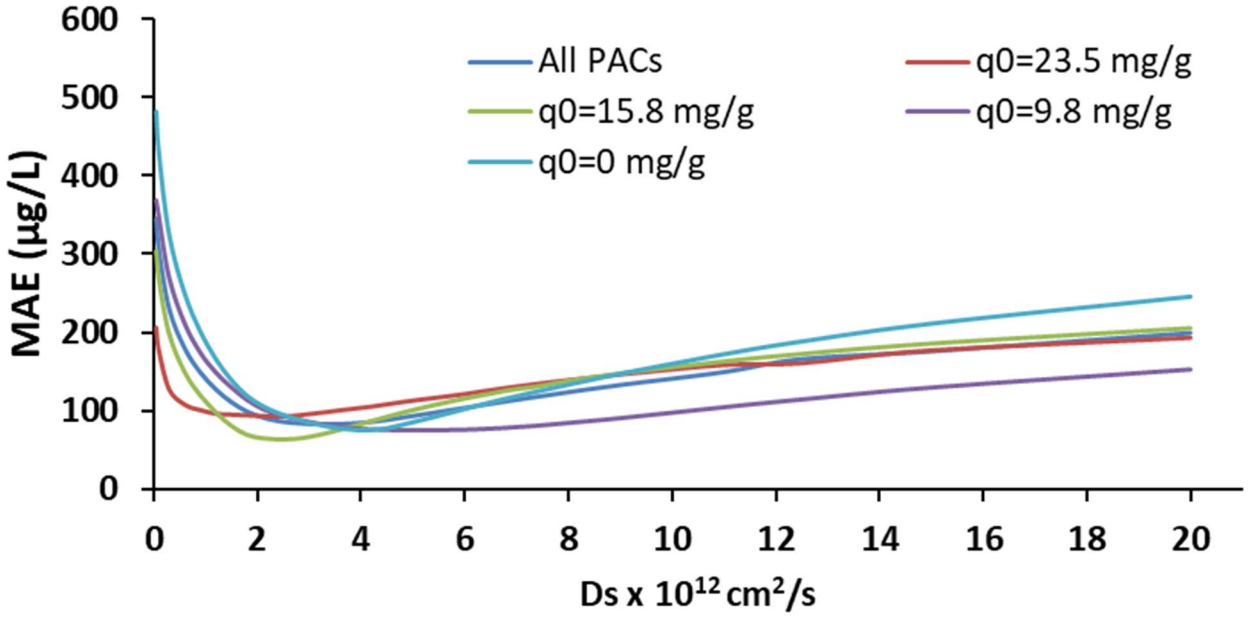

Figure 5-31 Impact of Ds on MAE for different PACs pre-loads.

Figure 5-32 shows the C_{eff} obtained by the HSDM (when the overall average value of Ds is used, 3.3E-12 cm^2/s and K_F is 15.42 (mg adsorbed DOC/g PAC) /((mg DOC/L) $^{(1.23)}$ and, 1/n is 1.23) versus the measured effluent concentration, C_{eff}. As shown in Figure 5-32, the HSDM is well suited for both virgin PAC and aged PAC. It also indicates that sorption parameters (K_F, 1/n, and Ds) are independent of the PAC age and could be considered constant. Therefore, the isotherm/kinetic test is a reliable choice for calculating the load of an aged PAC by adjusting the sorption parameter for the virgin PAC.

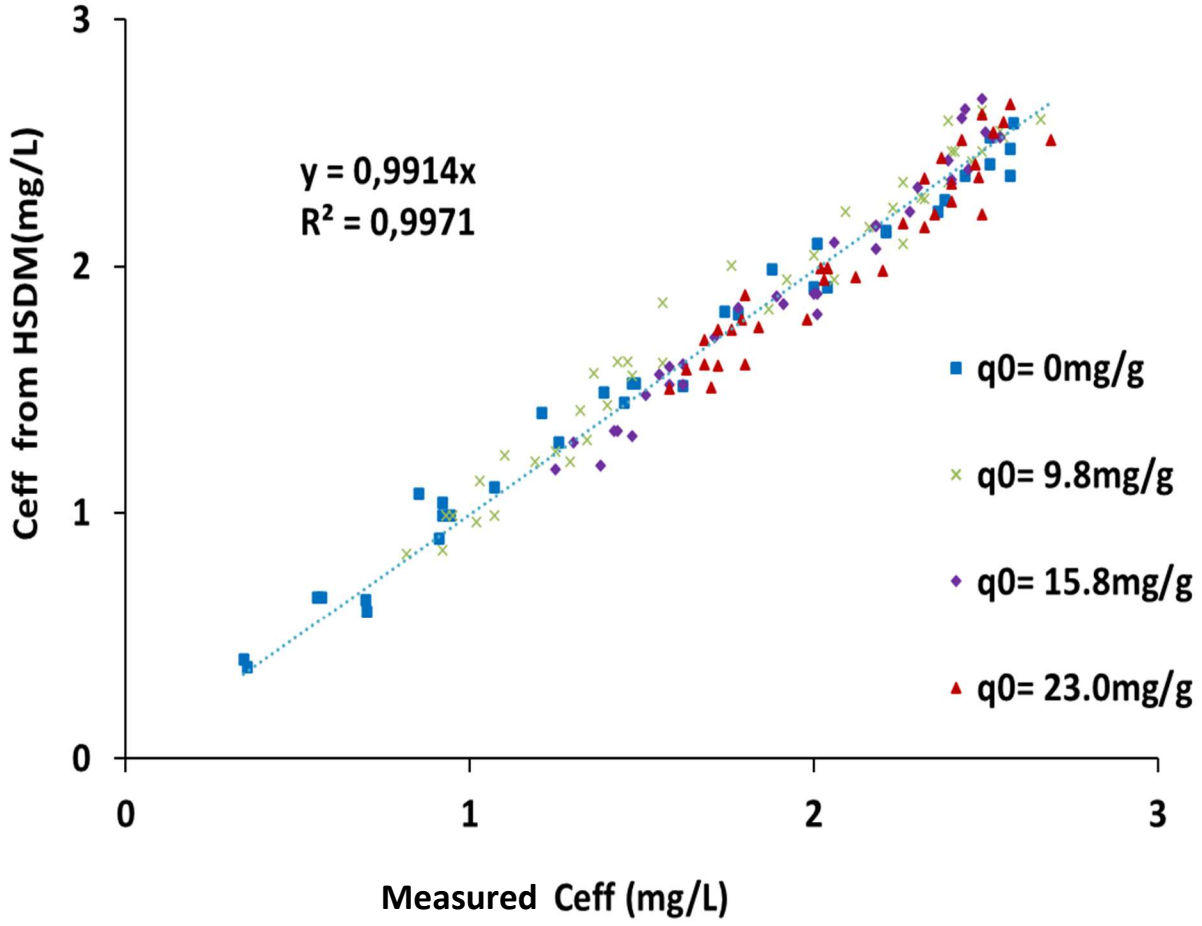

Figure 5-32 C_{eff} of DOC calculated by the HSDM versus measured C_{eff} when Ds is 3.3E-12 cm^2/s for PACs with increasing loadings

5.2.3 Parameters adjusting of isotherm models and the HSDM in a suspension containing mix-aged PACs

Table 5-12 shows MAE for each PACs separately and for all four mix-loaded PACs together (98 data points). The average MAE for all mix-loaded PACs is only 170 ppb.

Table 5-12 MAE of the HSDM for Mix-loaded PACs

Mix-loaded PAC	**MAE** (µg/L)
1St Mix-loaded PAC ($\overline{q_0}$ =12.8)	128
2nd Mix-loaded PAC ($\overline{q_0}$ =16.6)	237
3rd Mix-loaded PAC ($\overline{q_0}$ =7.9)	111
4th Mix-loaded PAC ($\overline{q_0}$ =25.7)	161
All Mixed-aged PAC	**170**

The 1st mixed-aged PAC ($\overline{q_0}$ =12.8 mg/L)

This suspension is an approximately fifty-fifty blend of virgin PAC and an aged PAC (q_0=24.5 mg/g). The assumption of using a mass-weighted average of q_0 is more accurate when the PAC concentration is between 15 mg/L and 103 mg/L. when the PAC concentration is 257 mg/L, the measured C_{eff} is less than the predicted C_{eff}. It means the suspension behaves like a suspension with a fresher PAC. This is probably because the loading is low.

The 2nd mixed-aged PAC ($\overline{q_0}$ =12.8 mg/L)

This suspension is an approximately fifty-fifty blend of virgin PAC and an aged PAC (q_0=35 mg/g). In high PAC concentrations, the effect of virgin PAC is more than the effect of aged PAC. Therefore, the suspension behaves like one with a fresher PAC, while in low PAC concentration. The effect of aged PAC is more than for virgin PAC. The highest error happened when the Ceff is less than 1 mg C/L

The 3rd Mix-aged PAC ($\overline{q_0}$ =7.9 mg/L)

This suspension contains 15% virgin PAC, 60 % of aged PAC I (q_0= 5 mg/g), and 25% of aged PAC II (q_0= 19.7 mg/g). Figure 5-33 and Figure 5-34 show that the model is accurate for both examined concentrations.

The 4th mix-aged PAC ($\overline{q_0}$ =25.7 mg/L)

This suspension contains 5% of virgin PAC, 5% of aged PAC III (q0 =6.3 mg/g), 9 % of aged PAC IV (11.2 mg/g), 10 % of aged PAC V (17.5 mg/g), 10 % of aged PAC VI (25 mg/g), and 63 % of aged PAC VII (31.8 mg/g).

Figure 5-33 and Figure 5-34 show that the assumption that a mixture of different PAC ages has the same performance as a suspension with a mass-weighted average age of all PACs is relatively accurate, especially for a target operating effluent concentration, Ceff, of 1.5 - 2.0 mg C/L. The MAE for four suspensions (N=98) is +/- 170 µg C/L. The highest error is related to the mixed PAC 2, where an aged PAC with the highest load (q_0=35) is mixed with the virgin PAC in almost equal proportion. In practice, this condition of operation is unrealistic, given the very high PAC dosage which would be needed to achieve it. The observation that the error is higher when the effluent concentration is very low (< 1.0 mg C/L) can be explained by the fact that achieving such high performance imposes maintaining a higher sorption gradient in the reactor (qe-q). Under such an operating condition, the mass-weighted hypothesis of loading is disputable given the nonlinearity of sorption kinetic (as was shown by the fit to the pseudo-second order model).

Operating range means the target DOC level at water treatment plants which is between 1.5 and 2 mg C/L. As shown in Figure 5-33 and Figure 5-34 , this assumption is relatively accurate.

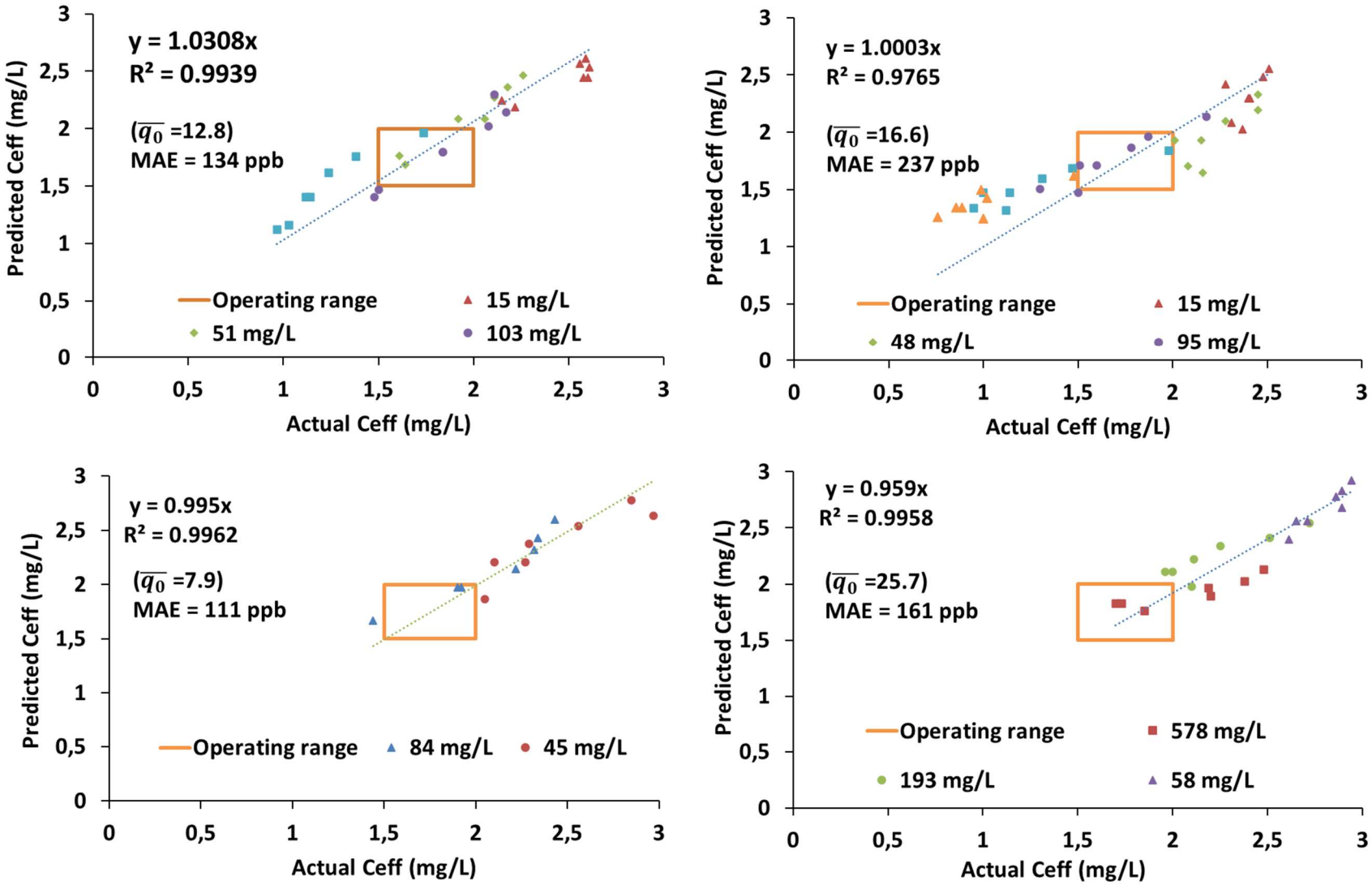

Figure 5-33 Predicted C_{eff} by the HSDM versus measured C_{eff} for all mix-aged PACs (separately)

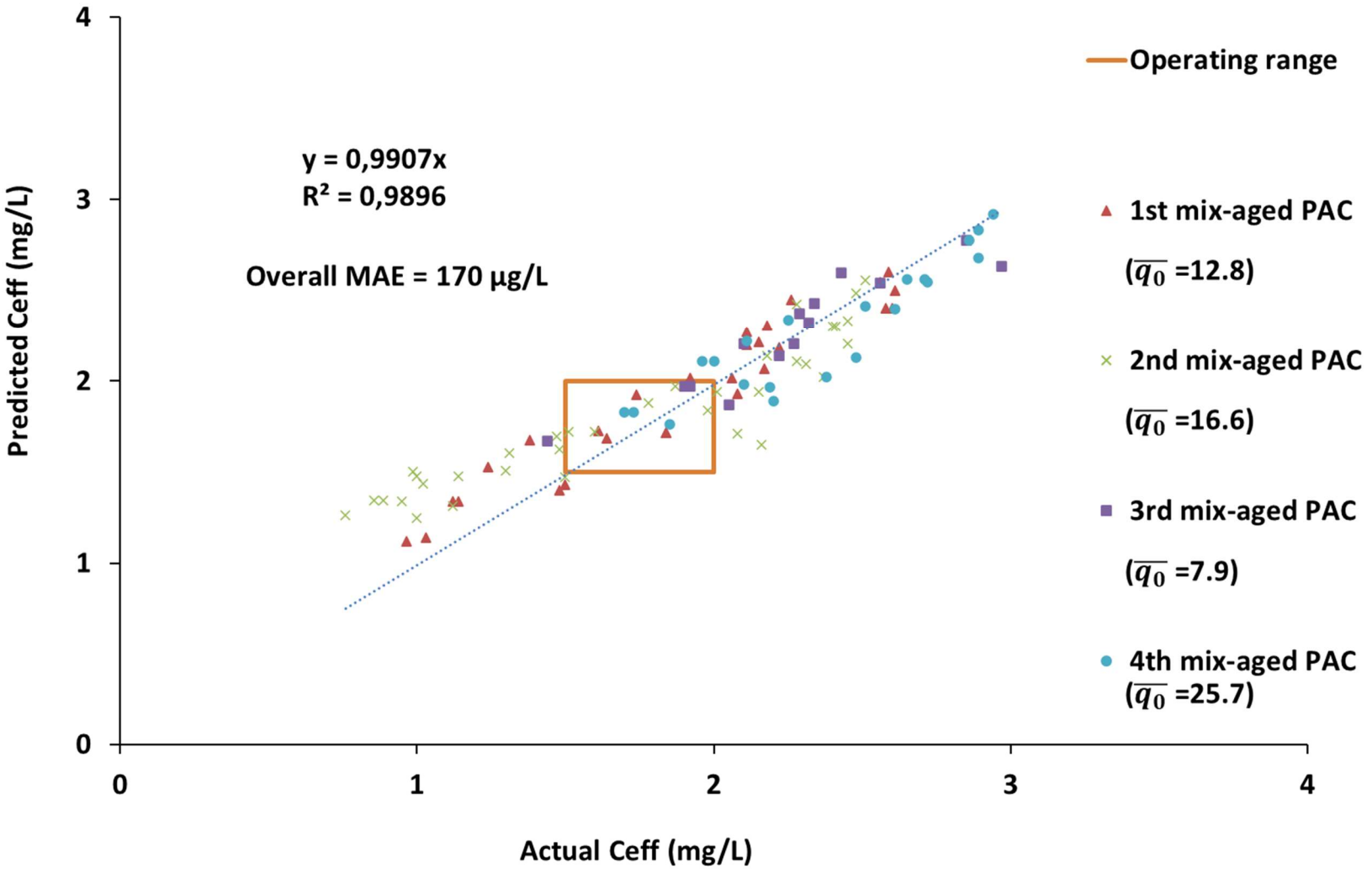

Figure 5-34 Predicted C_{eff} by the HSDM versus measured C_{eff} for all mix-aged PACs (all together), N= 98

5.2.4 UV_{254}/DOC Correlation in kinetic/isotherm tests

During the experiments, it was observed that when there is no significant desorption, there is an accurate correlation between DOC and UVA_{254} adsorption. Figure 5-35 is an example of the correlation between UVA_{254} and DOC where there is no significant desorption.

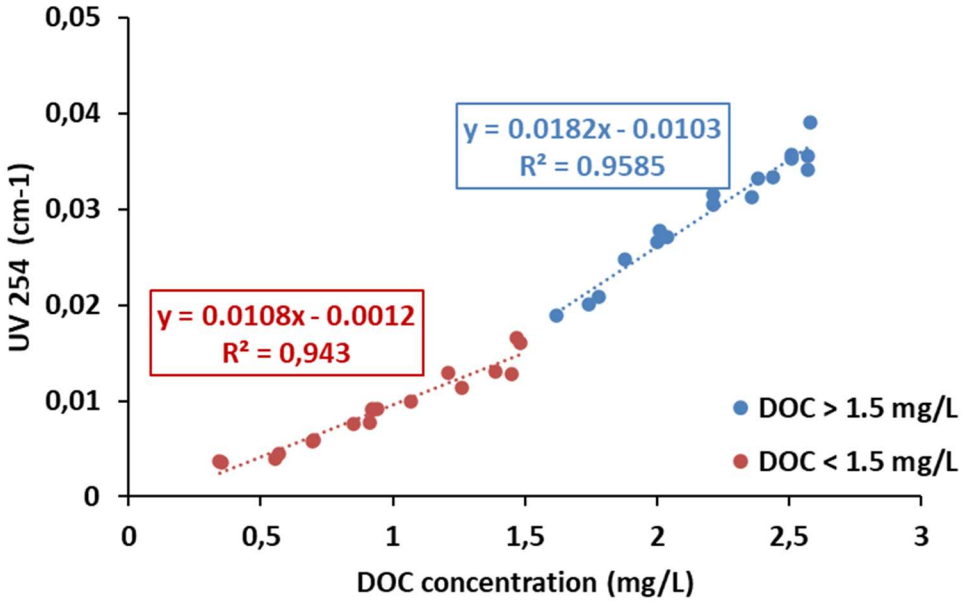

Figure 5-35 UV_{254}/DOC correlation in the effluent of kinetic/isotherm test on virgin PAC

5.3 Prediction of adsorption in the Actiflo® Carb process

Adsorption prediction in a full-scale Actiflo® Carb process (CA, USA)

Table 5-13 shows the sorption parameters obtained from kinetic/isotherm test raw water and virgin PAC received from the industrial plant. The surface diffusion coefficient was found to be 13 times higher than in the Montreal raw waters while the Freundlich capacity (KF) was 1.6 times higher.

Table 5-13 Sorption parameters for raw water- virgin PAC matrix

	Parameters	Industrial Actiflo® Carb	St. Lawrence
Freundlich Parameters	1/n	1.03	1.23
	Kf (mg adsorbed DOC/g PAC) /(mg DOC/L) $^{(1/n)}$	23.7	15.4
Surface Diffusion Coefficient	Ds (cm^2/s)	2.50E-11	3.30E-12

The PAC tank was modeled using sorption parameters from Table 5-13 and Equations 4-20 to 4-23. Table 5-14 shows the result of the modeling of the PAC tank in the Actiflo® Carb reactor. According to this modeling, the DOC concentration at the PAC tank is expected to be 2.26 mg/L which means that 37% of the influent DOC is removed in the PAC tank. Recirculating PAC in this reactor reduces by 29% the virgin PAC dosage, compared to a slurry reactor without a PAC recirculation system for the same DOC removal target. As mentioned in chapter 4, DOC concentration at the Actiflo® Carb reactor effluent was modeled by the result of a jar test.

Table 5-14 The Actiflo® Carb reactor modeling

DOC concentration at the PAC tank effluent (mg/L)	**DOC concentration at the Actiflo® Carb reactor effluent (mg/L)**	**Recirculated PAC load (mg/g)**	**q_τ (mg adsorbed DOC/ PAC)**	**DOC removal (%)**	**PAC usage reduction (%)**
2.26	1.27	52.0	5.3	37	29

Table 5-15 compares the performance of the treatment unit versus the modeling results of the Actiflo® Carb reactor. As shown in this table, DOC removal in the plant is 6% less than the prediction (58% compared to 64%). The treatment facility uses 32 mg/L of ferric chloride coagulant, which could affect total performance by blocking the pores of the recirculated PACs. While in the modeling assumption, this effect was not considered. On the hand, a recent study shows that when PAC and ferric coagulant are used simultaneously, DOC concentration increases during the settling tank (Sang et al., 2022). While in this modeling, the effect of coagulation and adsorption are considered separately. For these two reasons, it makes sense that DOC removal in the actual process is less than predicted.

Table 5-15 Performance of the treatment unit versus the modeling of Actiflo® Carb reactor

Actual DOC at Actiflo CARB effluent	**1.50 (mg C/L)**
DOC predicted at Actiflo CARB effluent	**1.27 (mg C/L)**
Actual Actiflo CARB DOC removal	**58 %**
Predicted Actiflo CARB DOC removal	**64 %**

Kinetic/ Isotherm test on the sludge

By PAC tank modeling, $q_{(recirculated\ PAC)}$ is calculated at 52 mg C/g. On the hand, by performing the Kinetic/ Isotherm test on the sludge, $q_{(recirculated\ PAC)}$ was estimated at 57 mg C/g. As shown in Table 5-16, the result of the isotherm/kinetic test on the recirculated PAC sample, the $q_{(recirculated\ PAC)}$, is 10% higher than the results obtained from the modeling. This shows that recirculated PAC in the sludge sample has less adsorption capacity than the modeling expectation. This could be the result of PAC pores plugging by coagulation/ flocculation.

Table 5-16 Recirculated PAC load,

Calculated by PAC tank modeling	52 mg/g
Estimated by kinetic/isotherm test on sludge sample	57 mg/g

Figure 5-36 shows the C_{eff} obtained from the HSDM versus Measured C_{eff} for the isotherm/kinetic test, when Ds is 2.50E-11cm^2/s and $q_{(recirculated\ PAC)}$ is 57 mg/g.

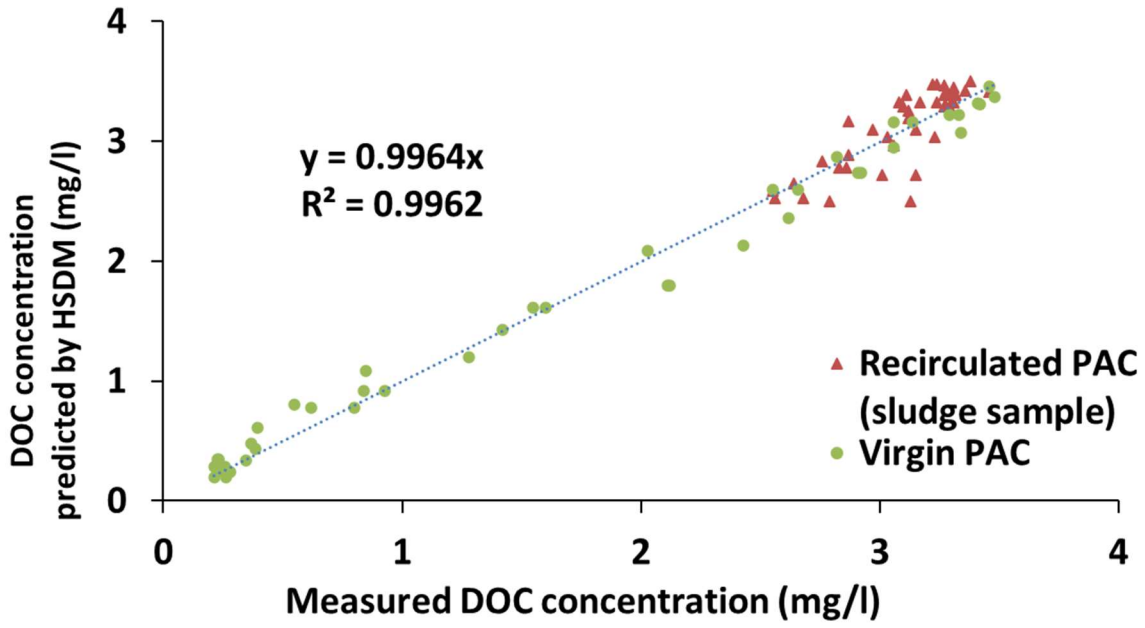

Figure 5-36 Predicted C_{eff} by the HSDM versus measured C_{eff} for virgin PAC and recirculated PAC

5.3.1 Effect of PAC characteristics and the reactor on the performance of the Actiflo® Carb process

In Table 5-17, a simulation is provided to predict performance under variable conditions of the Actiflo® Carb process.

Simulation results showed that a 6-fold increase in the treatment water flow leads to only a 3% reduction in DOC removal (from 37 % to 34 %). At the same time, "PAC usage reduction" increases rapidly from 29% to 58%. This shows that installing the Actiflo® Carb system at higher treatment flow rates (lower HRT) has a higher economic value.

Doubling the total PAC concentration (while maintaining the virgin PAC dosage as 25 mg/L) in the reactor does not significantly impact the reactor performance, but it could increase system operating costs by increasing the flow rate of recirculating sludge PAC.

Increasing the virgin PAC dosage increases the percentage of DOC removal. Therefore, In case of a sudden increase in DOC concentration in raw water, increasing the virgin PAC dosage would be the best option to keep DOC concentration at the effluent at the desirable level.

Using a PAC with a larger particle size leads to a slight decrease in DOC removal and a significant increase in PAC usage reduction. This shows that installing the Actiflo® Carb system has a higher economic value when the system uses a PAC with larger particle size.

The last two rows of Table 5-17 show the DOC removal for a system without recirculating PAC (100% Virgin PAC) to determine the effectiveness of using aged PAC. For instance, using 220 mg/L of recirculated PAC beside 25 mg/L of virgin PAC (245 mg/L of total PAC) instead of using only 25 mg/L of virgin PAC increases DOC removal from 18 % to 34 % (when the HRT is 5 min)

Table 5-17 Simulation Actiflo® Carb with changing characteristics of PAC and the reactor

	Virgin PAC Concentration (mg/L)	Total PAC Concentration (mg/L)	HRT (min)	DOC concentration after the PAC tank (mg/L)	DOC removal (%)	PAC usage reduction (%)
Actual treatment plant	25	245	30	2.26	37	29
Reducing HRT (vs 30 min)	25	245	20	2.27	36	36
	25	245	10	2.31	35	47
	25	245	5	2.35	34	58
Using PAC-S (versus PAC-F)	25	245	30	2.31	35	48
	25	245	5	2.47	31	70
Increasing Virgin PAC dosage	50	245	30	1.70	52	25
	75	245	30	1.39	61	23
Decreasing Virgin PAC dosage	15	245	30	2.63	26	31
	10	245	30	2.89	19	29
Increasing total PAC concentration	25	500	30	2.24	37	31
Decreasing total PAC concentration	25	100	30	2.31	35	24
No recirculation	25	25	30	2.52	29	-
	25	25	5	2.92	18	-

CONCLUSION AND RECOMMENDATIONS

In this project, the performance of aged PAC in adsorbing and removing NOM from raw water was investigated with the main objective of developing a simple and quick tool to predict the performance of preloaded PAC along with virgin PAC in the Actiflo® Carb process. Experiments and modeling carried out in the framework of this research project made it possible to achieve sub-objectives and validate the proposed hypothesis.

Sub-objective 1: To assess the suitability of the bench-scale flow-through HMP reactor (Amicon cell) for modeling the Actiflo® Carb process

PAC accumulation on the membrane surface

we noted that PAC accumulation on the membrane surface in the reactor is unavoidable. The accumulation was dependent on the membrane diameter, the HRT, the stirring, and the reactor size. And it was noticed that the advection force is the main reason for the formation of a PAC cake on the membrane.

The effect of physical conditions of the reactor on the PAC performance

The experiments carried out in the laboratory show, contrary to the initial hypothesis, the physical conditions of the reactor influence the PAC performance significantly.

For instance, the PAC concentration inside the reactor affects the breakthrough curve of the Amicon cell even when the performance of the reactor is normalized by the CUR. Lower PAC concentration in the Amicon cell leads to an increase in final adsorption capacity and adsorption rate. Increasing the PAC concentration from 100 to 200 and then 500 mg/L leads to a sharp decrease in the amount of absorption per unit of PAC. However, the breakthrough curve was similar once the PAC concentration reached more than 500 mg/L. This can depend on the thickness of the cake layer formed on the filter. However, this hypothesis needs more tests on the adsorption rate in the cake.

Empirical Models

Although several empirical models can accurately fit on a given breakthrough curve, None of these models are able to predict the Amicon cell filled by aged PAC.

So, the hypothesis of using a bench-scale HPM reactor (Amicon cell) to predict the Actiflo® Carb process is refuted. According to unavoidable PAC accumulation on the membrane surface.

Sub-objective 2: Investigation of the effect of PAC aging and mixing different aged PACs on sorption parameters

The maximum capacity of an aged PAC

Isotherm experiments on single-aged PAC showed that the maximum capacity of an aged PAC could be modeled with the Freundlich equation. It was noticed that, at the equilibrium point, q_e and C_{eff} are independent of q_0 and could be modeled by Freundlich isotherm equations. Therefore, the equilibrium condition is only influenced by the NOM concentration in water and PAC surface.

The aged PAC kinetics in a batch reactor

Kinetic tests showed that PAC aging does not affect Ds, which means the NOM adsorption process did not plug the PAC pores in the water tested (St Lawrence River). The aged PAC kinetics in a batch reactor is well described by the **HSDM**.

The performance of a mixture of different aged PACs

The performance of a perfectly mixed reactor including several of the exhausted PACs can also be described by the HSDM model using the mass-weighted average of the DOC loading on the suspended PACs, as long as the targeted effluent concentration was not too low (< 1.5 mg C/L).

Therefore, performing the isotherm/kinetic test in batch reactors is a reliable choice to predict more complicated systems such as the Actiflo® Carb reactor.

Sub-objective 3: Prediction of adsorption in the Actiflo® Carb process

The first prediction made on an Actiflo® Carb process seems to work well (based on combining the jar test with the PAC tank simulation).

It was predicted that the Actiflo® Carb process removes 64% of DOC concentration, while the performance of the treatment facility plant only 6% is less than the prediction.

All in all, the results of this research show that performing kinetic/isotherm tests on virgin PAC is a reliable rapid approach to predict the Actiflo® Carb process.

RECOMMENDATIONS

The results showed that it is possible to simulate the performance of the PAC tank process in the Actiflo® Carb reactor by conducting laboratory tests and using the HSDM model and adsorption parameters. However, a more thorough validation should be performed based on DOC concentration measurements in the effluent of the PAC tank. It would also be desirable to select an Actiflo Carb process where the coagulant dosage is minimal.

In addition, as previously mentioned, this simulation does not include the pre-disinfection, coagulation/ flocculation, and pH adjustment processes in the Actiflo® Carb reactor. Therefore, to simulate the entire Actiflo® Carb reactor, these processes and their effect on the adsorption performance should be investigated. The impact of the coagulant on aged PAC sorption performance should also be investigated.

Only NOM removal was considered in this research project. However, PAC can also remove micropollutants. Therefore, it would be interesting to conduct kinetic/isotherm tests considering other pollutants, then integrate prediction models into the calculation tool to predict performance. The calculation tool should also allow for the integration of competition for NOM and micro-pollutant sorption sites. The development of such equations would make it possible to model the complete operation of the Actiflo® Carb reactor.

BIBLIOGRAPHY

Afghan, B., & Chau, A. S. (1989). Analysis of trace organics in the aquatic environment. CRC press.

Albrektienė, R., Rimeika, M., Zalieckienė, E., Šaulys, V., & Zagorskis, A. (2012). Determination of organic matter by UV absorption in the ground water. Journal of Environmental Engineering and Landscape Management, 20(2), 163-167.

Ali, I., & Gupta, V. (2006). Advances in water treatment by adsorption technology. Nature protocols, 1(6), 2661-2667.

Aliverti, N., Callegari, A., Capodaglio, A. G., & Sauvignet, P. (2011). NOM removal from freshwater supplies by advanced separation technology. In Advanced Water Supply and Wastewater Treatment: A Road to Safer Society and Environment (pp. 49-61). Springer.

Aljamali, N. M., Aldujaili, R. A. B., & Alfatlawi, I. O. (2021). Physical and Chemical Adsorption and its Applications. International Journal of Thermodynamics and Chemical Kinetics, 7(2), 1-9.

Alresheedi, M. T., Barbeau, B., & Basu, O. D. (2019). Comparisons of NOM fouling and cleaning of ceramic and polymeric membranes during water treatment. Separation and Purification Technology, 209, 452-460.

Amiri, Z., Moussavi, G., Mohammadi, S., & Giannakis, S. (2021). Development of a VUV-UVC/peroxymonosulfate, continuous-flow Advanced Oxidation Process for surface water disinfection and Natural Organic Matter elimination: Application and mechanistic aspects. Journal of Hazardous Materials, 408, 124634.

Aschermann, G., Neubert, L., Zietzschmann, F., & Jekel, M. (2019). Impact of different DOM size fractions on the desorption of organic micropollutants from activated carbon. Water research, 161, 161-170.

Aschermann, G., Schröder, C., Zietzschmann, F., & Jekel, M. (2019). Organic micropollutant desorption in various water matrices-Activated carbon pore characteristics determine the reversibility of adsorption. Chemosphere, 237, 124415.

Aschermann, G., Zietzschmann, F., & Jekel, M. (2018). Influence of dissolved organic matter and activated carbon pore characteristics on organic micropollutant desorption. Water research, 133, 123-131.

Bhatnagar, A., Hogland, W., Marques, M., & Sillanpää, M. (2013). An overview of the modification methods of activated carbon for its water treatment applications. Chemical Engineering Journal, 219, 499-511.

Bolto, B., Dixon, D., & Eldridge, R. (2004). Ion exchange for the removal of natural organic matter. Reactive and Functional Polymers, 60, 171-182.

Bonilla-Petriciolet, A., Mendoza-Castillo, D. I., & Reynel-Ávila, H. E. (2017). Adsorption processes for water treatment and purification (Vol. 256). Springer.

Botes, M., de Kwaadsteniet, M., & Cloete, T. E. (2013). Application of quantitative PCR for the detection of microorganisms in water. Analytical and bioanalytical chemistry, 405(1), 91-108.

Bradshaw, A., & Hoffmann, F. (1978). The chemisorption of carbon monoxide on palladium single crystal surfaces: IR spectroscopic evidence for localised site adsorption. Surface Science, 72(3), 513-535.

Butler, J., & Ockrent, C. (1930). Studies in electrocapillarity. III.The Surface Tensions of Solutions Containing Two Surface-Active Solutes. The Journal of Physical Chemistry, 34(12), 2841-2845.

Calvet, R. (1989). Adsorption of organic chemicals in soils. Environmental health perspectives, 83, 145-177.

Campos, C., Marinas, B. J., Snoeyink, V. L., Baudin, I., & Lainé, J. M. (2000). PAC-membrane filtration process. I: Model development. Journal of environmental engineering, 126(2), 97-103.

Çeçen, F., & Aktas, Ö. (2011). Activated carbon for water and wastewater treatment: integration of adsorption and biological treatment. John Wiley & Sons.

Cool, G., Delpla, I., Gagnon, P., Lebel, A., Sadiq, R., & Rodriguez, M. J. (2019). Climate change and drinking water quality: Predicting high trihalomethane occurrence in water utilities supplied by surface water. Environmental Modelling & Software, 120, 104479.

Crittenden, J. C., Trussell, R. R., Hand, D. W., Howe, K. J., & Tchobanoglous, G. (2012). MWH's water treatment: principles and design. John Wiley & Sons.

Crozes, G., Anselme, C., & Mallevialle, J. (1993). Effect of adsorption of organic matter on fouling of ultrafiltration membranes. Journal of Membrane Science, 84(1-2), 61-77.

Dauphin, L. (2017). Développement d'un test rapide pour prédire la performance d'un réacteur à haute concentration de charbon actif recirculé. Ecole Polytechnique, Montreal (Canada).

del Hombre Bueno, B.-R., de los Ángeles, M., Boluda-Botella, N., & Prats Rico, D. (2019). Removal of emerging pollutants in water treatment plants: adsorption of methyl and propylparaben onto powdered activated carbon. Adsorption, 25(5), 983-999.

Delgado, L. F., Charles, P., Glucina, K., & Morlay, C. (2012). The removal of endocrine disrupting compounds, pharmaceutically activated compounds and cyanobacterial toxins during drinking water preparation using activated carbon—a review. Science of the total environment, 435, 509-525.

Desjardins, R. (1997). Le traitement des eaux. Presses inter Polytechnique.

Duan, X., Liao, X., Chen, J., Xie, S., Qi, H., Li, F., & Yuan, B. (2020). THMs, HAAs and NAs production from culturable microorganisms in pipeline network by ozonation, chlorination, chloramination and joint disinfection strategies. Science of The Total Environment, 744, 140833.

Eikebrokk, B., Vogt, R., & Liltved, H. (2004). NOM increase in Northern European source waters: discussion of possible causes and impacts on coagulation/contact filtration processes. Water Science and Technology: Water Supply, 4(4), 47-54.

El-Shafey, E., Al-Mashaikhi, S., Al-Busafi, S., & Suliman, F. (2022). Effect of alkylamine immobilization level on the performance of hydrophobic activated carbon. Materials Chemistry and Physics, 286, 126154.

Fernández-Reyes, B., Ortiz-Martínez, K., Lasalde-Ramírez, J. A., & Hernández-Maldonado, A. J. (2020). Engineered adsorbents for the removal of contaminants of emerging concern from water. In Contaminants of Emerging Concern in Water and Wastewater (pp. 3-45). Elsevier.

Gupta, V., Carrott, P., Singh, R., Chaudhary, M., & Kushwaha, S. (2016). Cellulose: a review as natural, modified and activated carbon adsorbent. Bioresource technology, 216, 1066-1076.

[Record #62 is using a reference type undefined in this output style.]

Hempel, S. (2007). The strange case of the Broad Street pump: John Snow and the mystery of cholera. Univ of California Press.

Ho, Y.-S., & McKay, G. (1998). Sorption of dye from aqueous solution by peat. Chemical engineering journal, 70(2), 115-124.

Hu, J., Martin, A., Shang, R., Siegers, W., Cornelissen, E., Heijman, B., & Rietveld, L. (2014). Anionic exchange for NOM removal and the effects on micropollutant adsorption competition on activated carbon. Separation and Purification Technology, 129, 25-31.

Jain, J. S., & Snoeyink, V. L. (1973). Adsorption from bisolute systems on active carbon. Journal (Water Pollution Control Federation), 2463-2479.

Jiang, J., Zhang, X., Zhu, X., & Li, Y. (2017). Removal of intermediate aromatic halogenated DBPs by activated carbon adsorption: a new approach to controlling halogenated DBPs in chlorinated drinking water. Environmental science & technology, 51(6), 3435-3444.

Jiuhui, Q. (2008). Research progress of novel adsorption processes in water purification: a review. Journal of environmental sciences, 20(1), 1-13.

Kalev, S., & Toor, G. S. (2020). Concentrations and loads of dissolved and particulate organic carbon in urban stormwater runoff. Water, 12(4), 1031.

Karanfil, T., & Kilduff, J. E. (1999). Role of granular activated carbon surface chemistry on the adsorption of organic compounds. 1. Priority pollutants. Environmental science & technology, 33(18), 3217-3224.

Kim, J., & Kang, B. (2008). DBPs removal in GAC filter-adsorber. Water research, 42(1-2), 145-152.
Kocsis, L., Herman, P., & Eke, A. (2006). The modified Beer–Lambert law revisited. Physics in Medicine & Biology, 51(5), N91.
Komulainen, H. (2004). Experimental cancer studies of chlorinated by-products. Toxicology, 198(1-3), 239-248.
Kornegay, B. H., Kornegay, K. J., & Torres, E. (2000). Natural organic matter in drinking water: recommendations to water utilities. American Water Works Association.
Krasner, S. W., Croué, J. P., Buffle, J., & Perdue, E. M. (1996). Three approaches for characterizing NOM. Journal-American Water Works Association, 88(6), 66-79.
Krasner, S. W., Weinberg, H. S., Richardson, S. D., Pastor, S. J., Chinn, R., Sclimenti, M. J., . . . Thruston, A. D. (2006). Occurrence of a new generation of disinfection byproducts. Environmental science & technology, 40(23), 7175-7185.
Largitte, L., & Pasquier, R. (2016). A review of the kinetics adsorption models and their application to the adsorption of lead by an activated carbon. Chemical engineering research and design, 109, 495-504.
Le Clercq, M., Van der Plicht, J., & Meijer, H. A. (1998). A supercritical oxidation system for the determination of carbon isotope ratios in marine dissolved organic carbon. Analytica chimica acta, 370(1), 19-27.
Leenheer, J. A., & Croué, J.-P. (2003). Peer reviewed: characterizing aquatic dissolved organic matter. Environmental science & technology, 37(1), 18A-26A.
Li, K., Wen, G., Li, S., Chang, H., Shao, S., Huang, T., . . . Liang, H. (2019). Effect of pre-oxidation on low pressure membrane (LPM) for water and wastewater treatment: A review. Chemosphere, 231, 287-300.
Lima, J. P., Alvarenga, G., Goszczynski, A. C., Rosa, G. R., & Lopes, T. J. (2020). Batch adsorption of methylene blue dye using Enterolobium contortisiliquum as bioadsorbent: experimental, mathematical modeling and simulation. Journal of Industrial and Engineering Chemistry, 91, 362-371.
Lipczynska-Kochany, E. (2018). Effect of climate change on humic substances and associated impacts on the quality of surface water and groundwater: A review. Science of the total environment, 640, 1548-1565.
Liu, Z., Haddad, M., Sauvé, S., & Barbeau, B. (2021). Alleviating the burden of ion exchange brine in water treatment: From operational strategies to brine management. Water Research, 205, 117728.
Loganathan, P., Kandasamy, J., Jamil, S., Ratnaweera, H., & Vigneswaran, S. (2022). Ozonation/adsorption hybrid treatment system for improved removal of natural organic matter and organic micropollutants from water–A mini review and future perspectives. Chemosphere, 133961.
Lompe, K. M. (2018). Magnetic Powdered Activated Carbon for Drinking Water Treatment, Ecole Polytechnique, Montreal (Canada)].
Lompe, K. M., Menard, D., & Barbeau, B. (2017). The influence of iron oxide nanoparticles upon the adsorption of organic matter on magnetic powdered activated carbon. Water research, 123, 30-39.
Löwenberg, J., Zenker, A., Baggenstos, M., Koch, G., Kazner, C., & Wintgens, T. (2014). Comparison of two PAC/UF processes for the removal of micropollutants from wastewater treatment plant effluent: Process performance and removal efficiency. Water Research, 56, 26-36.
Luengas, A., Barona, A., Hort, C., Gallastegui, G., Platel, V., & Elias, A. (2015). A review of indoor air treatment technologies. Reviews in Environmental Science and Bio/Technology, 14(3), 499-522.
Manocha, S. M. (2003). Porous carbons. Sadhana, 28(1), 335-348.
Marczewski, A. W., Seczkowska, M., Deryło-Marczewska, A., & Blachnio, M. (2016). Adsorption equilibrium and kinetics of selected phenoxyacid pesticides on activated carbon: effect of temperature. Adsorption, 22(4), 777-790.

Matilainen, A., Gjessing, E. T., Lahtinen, T., Hed, L., Bhatnagar, A., & Sillanpää, M. (2011). An overview of the methods used in the characterisation of natural organic matter (NOM) in relation to drinking water treatment. Chemosphere, 83(11), 1431-1442.

Matsui, Y., Yoshida, T., Nakao, S., Knappe, D. R., & Matsushita, T. (2012). Characteristics of competitive adsorption between 2-methylisoborneol and natural organic matter on superfine and conventionally sized powdered activated carbons. Water research, 46(15), 4741-4749.

Mirnasab, M., Hashemi, H., Samaei, M., & Azhdarpoor, A. (2021). Advanced removal of water NOM by Pre-ozonation, Enhanced coagulation and Bio-augmented Granular Activated Carbon. International Journal of Environmental Science and Technology, 18(10), 3143-3152.

Montreuil, K. R. (2011). Natural organic matter characterization in drinking water.

Myers, A. L., & Prausnitz, J. M. (1965). Thermodynamics of mixed-gas adsorption. AIChE journal, 11(1), 121-127.

Najm, I. N. (1996). Mathematical modeling of PAC adsorption processes. Journal-American Water Works Association, 88(10), 79-89.

Noroozi, B., & Sorial, G. A. (2013). Applicable models for multi-component adsorption of dyes: A review. Journal of Environmental Sciences, 25(3), 419-429.

O'Driscoll, C., Ledesma, J. L., Coll, J., Murnane, J. G., Nolan, P., Mockler, E. M., . . . Xiao, L. W. (2018). Minimal climate change impacts on natural organic matter forecasted for a potable water supply in Ireland. Science of the total environment, 630, 869-877.

Okoro, B. U., Sharifi, S., Jesson, M. A., & Bridgeman, J. (2021). Natural organic matter (NOM) and turbidity removal by plant-based coagulants: A review. Journal of Environmental Chemical Engineering, 9(6), 106588.

Pan, L., Nakayama, A., Matsui, Y., Matsushita, T., & Shirasaki, N. (2022). Desorption of micropollutant from superfine and normal powdered activated carbon in submerged-membrane system due to influent concentration change in the presence of natural organic matter: Experiments and two-component branched-pore kinetic model. Water Research, 208, 117872.

Pan, L., Nishimura, Y., Takaesu, H., Matsui, Y., Matsushita, T., & Shirasaki, N. (2017). Effects of decreasing activated carbon particle diameter from 30 μm to 140 nm on equilibrium adsorption capacity. Water research, 124, 425-434.

Pendashteh, A. R., A. & Fathi, H. (2015). Introduction to water treatment processes.

Pivokonsky, M., Kopecka, I., Cermakova, L., Fialova, K., Novotna, K., Cajthaml, T., . . . Pivokonska, L. (2021). Current knowledge in the field of algal organic matter adsorption onto activated carbon in drinking water treatment. Science of the Total Environment, 799, 149455.

Qiu, H., Lv, L., Pan, B.-c., Zhang, Q.-j., Zhang, W.-m., & Zhang, Q.-x. (2009). Critical review in adsorption kinetic models. Journal of Zhejiang University-Science A, 10(5), 716-724.

Queiroz, V., de Almeida, D. S., de Oliveira Miglioranza, G. H., Steffani, E., Barbosa-Coutinho, E., & Schwaab, M. (2022). Analysis of commonly used batch adsorption kinetic models derived from mass transfer-based modelling. Environmental Science and Pollution Research, 1-15.

Rakovic, J., Huser, B. J., & Futter, M. N. (2018). Increasing DOC concentrations in surface waters of boreal lakes and possible consequences for hypolimnetic element cycling. EGU General Assembly Conference Abstracts (pp. 18098).

Sang, D., Cimetiere, N., Giraudet, S., Tan, R., Wolbert, D., & Le Cloirec, P. (2022). Adsorption-desorption of organic micropollutants by powdered activated carbon and coagulant in drinking water treatment. Journal of Water Process Engineering, 49, 103190.

Sethia, G., & Sayari, A. (2016). Activated carbon with optimum pore size distribution for hydrogen storage. Carbon, 99, 289-294.

Shi, Z., Chow, C. W., Fabris, R., Liu, J., & Jin, B. (2022). Applications of online UV-Vis spectrophotometer for drinking water quality monitoring and process control: a review. Sensors, 22(8), 2987.

Sillanpää, M., Matilainen, A., & Lahtinen, T. (2015). Characterization of NOM. Natural Organic Matter in Water, 2, 17-53.

Sillanpää, M., Ncibi, M. C., & Matilainen, A. (2018). Advanced oxidation processes for the removal of natural organic matter from drinking water sources: A comprehensive review. Journal of environmental management, 208, 56-76.

Singh, N., Nagpal, G., & Agrawal, S. (2018). Water purification by using adsorbents: a review. Environmental technology & innovation, 11, 187-240.

Siyal, A. A., Shamsuddin, M. R., Low, A., & Rabat, N. E. (2020). A review on recent developments in the adsorption of surfactants from wastewater. Journal of environmental management, 254, 109797.

Sleighter, R. L., & Hatcher, P. G. (2007). The application of electrospray ionization coupled to ultrahigh resolution mass spectrometry for the molecular characterization of natural organic matter. Journal of Mass Spectrometry, 42(5), 559-574.

St-Jean, G. (2003). Automated quantitative and isotopic (13C) analysis of dissolved inorganic carbon and dissolved organic carbon in continuous-flow using a total organic carbon analyser. Rapid communications in mass spectrometry, 17(5), 419-428.

Stoquart, C., Servais, P., Bérubé, P. R., & Barbeau, B. (2012). Hybrid Membrane Processes using activated carbon treatment for drinking water: A review. Journal of membrane science, 411, 1-12.

Suwanayuen, S., & Danner, R. P. (1980a). A gas adsorption isotherm equation based on vacancy solution theory. AIChE Journal, 26(1), 68-76.

Suwanayuen, S., & Danner, R. P. (1980b). Vacancy solution theory of adsorption from gas mixtures. AIChE Journal, 26(1), 76-83.

Tan, K. B., Vakili, M., Horri, B. A., Poh, P. E., Abdullah, A. Z., & Salamatinia, B. (2015). Adsorption of dyes by nanomaterials: recent developments and adsorption mechanisms. Separation and Purification Technology, 150, 229-242.

Thurman, E. M. (2012). Organic geochemistry of natural waters (Vol. 2). Springer Science & Business Media.

Veolia. (2022). Veolia Eau Solutions & Technologies l technologies actiflo-carb https://www.veoliawatertechnologies.com/en/technologies/actiflo-carb.

Villabona-Ortíz, A., Tejada-Tovar, C., & Ortega-Toro, R. (2020). Modelling of the adsorption kinetics of Chromium (VI) using waste biomaterials. Revista Mexicana de Ingeniería Química, 19(1), 401-408.

Westerhoff, P., Chao, P., & Mash, H. (2004). Reactivity of natural organic matter with aqueous chlorine and bromine. Water Research, 38(6), 1502-1513.

Worch, E. (2012). Adsorption technology in water treatment: Fundamentals. Processes, and Modeling, 1-332.

Xia, M., Chen, Z., Li, Y., Li, C., Ahmad, N. M., Cheema, W. A., & Zhu, S. (2019). Removal of Hg (II) in aqueous solutions through physical and chemical adsorption principles. RSC advances, 9(36), 20941-20953.

York, R., & Bell, N. G. (2020). Molecular tagging for the molecular characterization of natural organic matter. Environmental science & technology, 54(6), 3051-3063.

Zeldowitsch, J. (1934). Über den mechanismus der katalytischen oxydation von CO an MnO2. Acta physicochim. URSS, 1, 364-449.

Appendix A Increasing PAC particles size with aging

For solving HSDM (Equations 2.14 to 2.21, 4.12, and 4.14), it was assumed that the PAC particle size is constant during adsorption. While the particle size investigation, in batch reactors, showed that the size of PAC particles can increase during the adsorption process. On the other hand, the shape of the size distribution also changes during the absorption process. In such a way that the distribution pattern leaves the state of the bell curve (Gaussian distribution), it becomes a bimodal distribution with two maximum points. To measure the size of aged PAC particles, five suspensions were made using Virgin PAC and filtered raw water (from 50 to 2000 mg/L), and after 72 hours, the particle size was measured by Malvern Mastersizer 3000 device.

Table A. 1 Comparing particle size for virgin and aged PAC

PAC concentration (mg/L)	q (mg/g)	d 50 (µm)
100 (in Milli-Q water)	0	12
2000	2	20
200	14	21
100	32	23
50	42	18
5800 (Actiflo carb sludge)	57	16

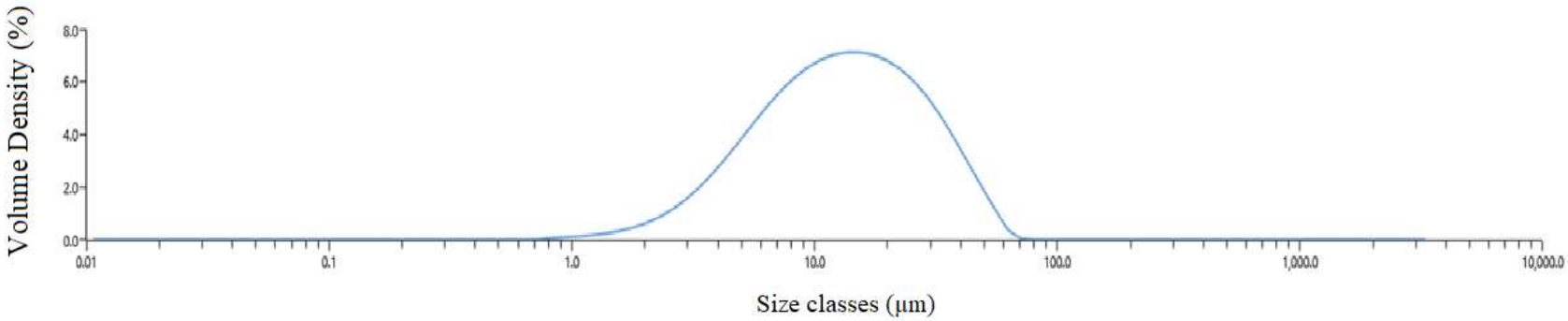

Figure A. 1 Particle size distribution of virgin PAC, d50 = 12 µm

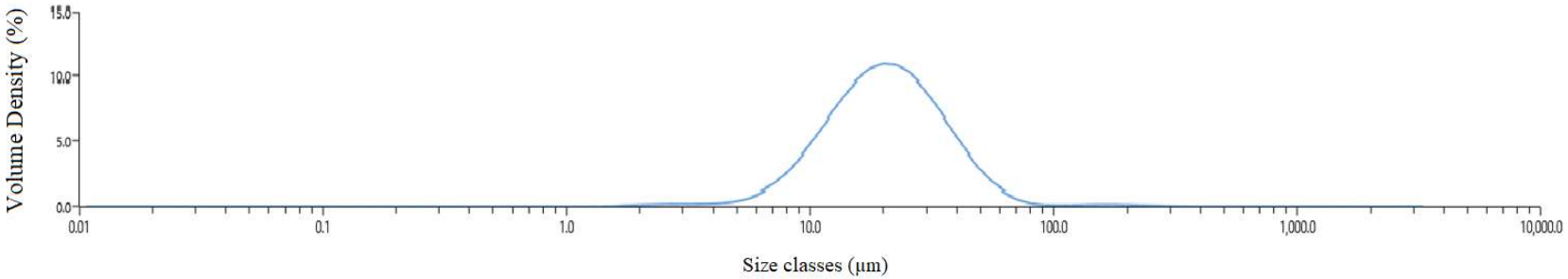

Figure A. 2 Particle size distribution of an aged PAC 2000 mg/L, d50 = 20 µm

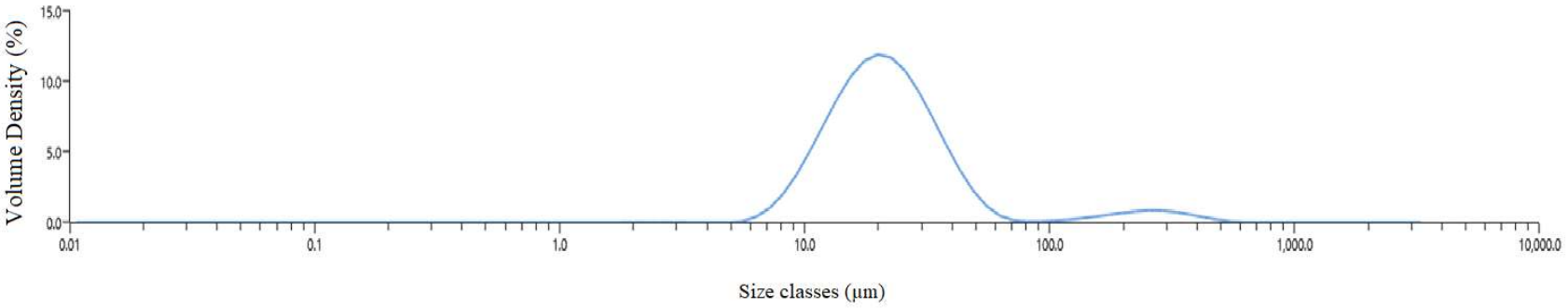

Figure A. 3 Particle size distribution of an aged PAC 200 mg/L d50= 21 µm

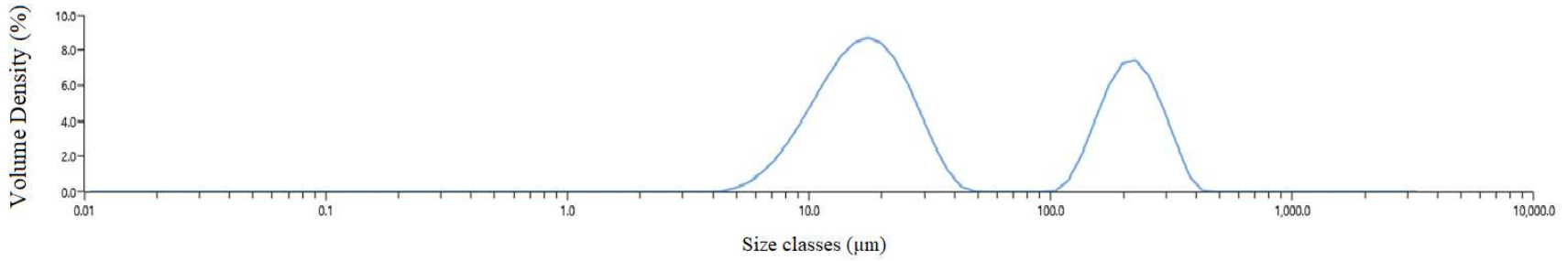

Figure A. 4 Particle size distribution of an aged PAC 100 mg/L, d50= 23 µm

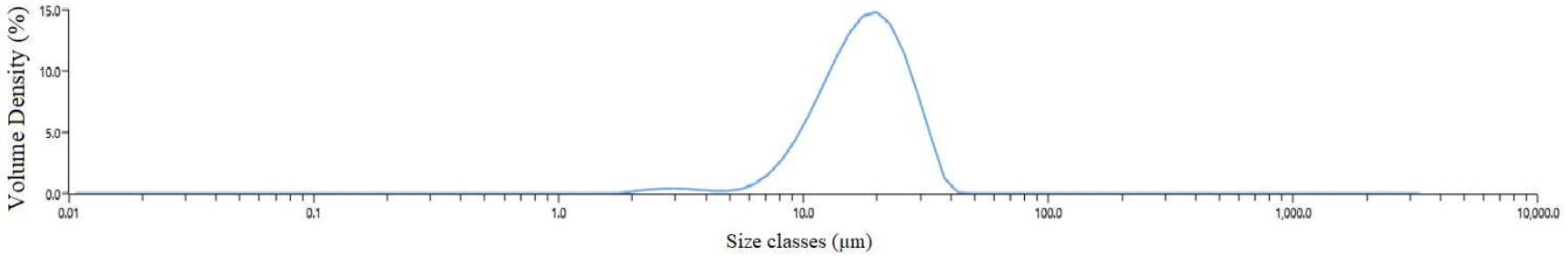

Figure A. 5 Particle size distribution of an aged PAC 50 mg/L d50= 18 µm

The Actiflo carb sludge contains recirculated PAC, coagulant, polymer etc.

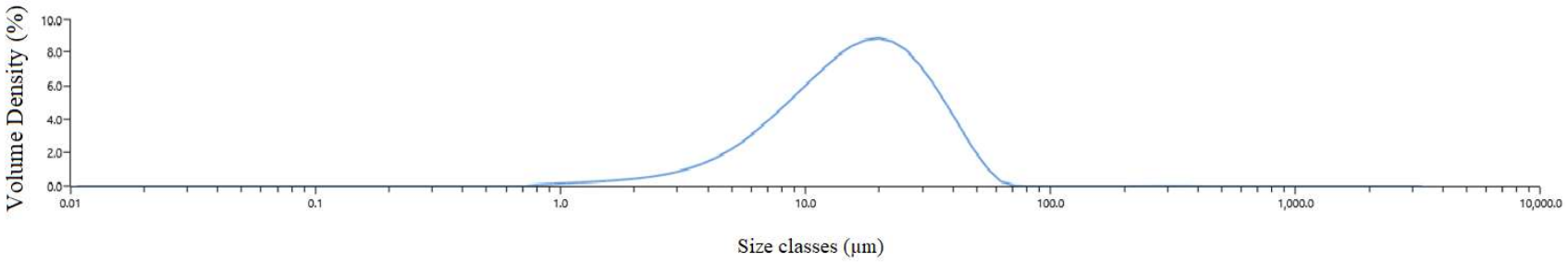

Figure A. 6 Particle size distribution of recirculating PAC from Actiflo carb process d50=16 µm

Appendix B Desorption of NOM from aged PAC

NOM desorption was observed during some kinetic/ isotherms tests.

For example: for producing the 3rd preloaded PAC (q_0 =23.5 mg/g) in the Amicon cell, the DOC concentration at the effluent of the Amicon cell, was 2.5 mg/L when treatment was stopped (when load of PAC inside the Amicon reached to the target load). Then as described in Chapter 4, the suspension was concentrated until the PAC concentration reached to 11 335 mg/L. After letting the suspension reach equilibrium, the DOC reached 4.6 mg C/L which was even higher than C_{inf} (2.7 mg/L). Which shows that during concentrating and reaching equilibrium condition, desorption happened in this suspension.

Another condition that we observed desorption from an aged PAC was during pre-tests of kinetic/isotherm tests on aged PAC.

In the first attempt to perform a kinetic/isotherm test on preloaded PAC, the aged PAC produced in the Amicon cell was concentrated to about 1000-2000 mg/L (instead of more than 7000 mg/L) and used immediately after production in kinetic/isotherm tests (so the suspension did not reach equilibrium). In this way, when the preloaded PAC was added to raw water, the DOC concentration increased immediately

Figure A.7 presents a kinetic/isotherm test on a preloaded PAC with 24.5 mg/g loading, where the concentration of preloaded PAC in suspension was 1000 mg/L and the suspension of preloaded PAC did not reach equilibrium condition. As shown in Figure A.8, when the PAC concentration is low, at first, the rate of desorption is much higher than adsorption. And then, adsorption overcomes desorption gradually. By increasing the PAC concentration, the influence of desorption will decrease. Also, the desorption phenomenon occurred with less intensity in the experiments conducted on the preloaded PACs with a lower load. For the suspension with 12 mg/L of preloaded PAC (q0= 24.5) it was observed that at time= 1 min, desorption was 28.8 mg/g while q_0 was 24.5 mg/g, which was quite strange. This result led to performing a kinetic isotherm test on virgin PAC/Milli-Q water, to investigate that is there a preloaded DOC on virgin PAC or not.

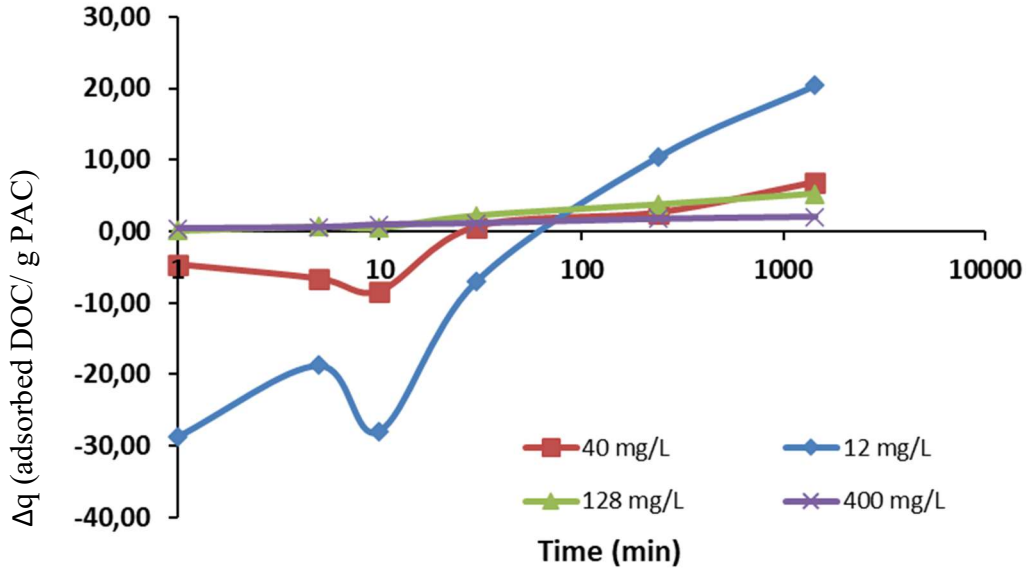

Figure A. 7 Desorption during aged PAC kinetic/ isotherm test, q_0 = 24.5 mg/g, DOC of raw water= 2.5 mg/L (Δq over time)

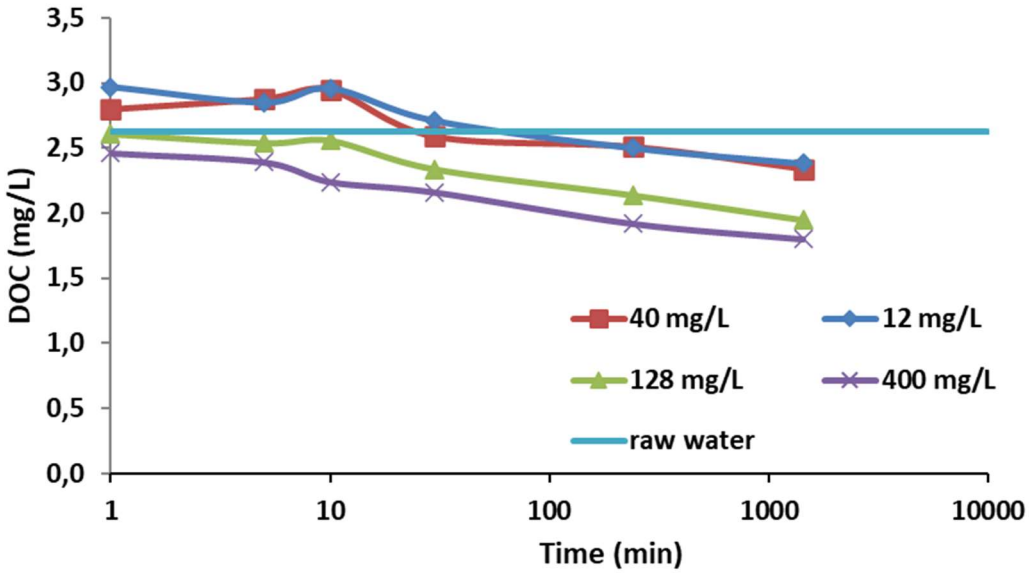

Figure A. 8 Desorption during aged PAC kinetic/ isotherm test, q_0 = 24.5 mg/g, DOC of raw water= 2.5 mg/L (DOC over time)

DOC desorption from PAC matrix

As described in section 4, prior to using virgin PAC, a very high concentration suspension of PAC was made in Milli-Q water with dehumidified PAC. Then, after 24 hours of mixing, the desired amount of PAC was removed from it to perform the various tests. We have noted that adding virgin PAC in ultrapure water leads to small increase in DOC. For example, Figure A.9 shows that resuspending 25 mg/L of PAC in Milli-Q water increased the DOC concentration to 0.55 mg/L in 5 min; the DOC concentration then decreased gradually to 0.087 mg/L in one day. The UVA_{254} remained at zero at all which suggests that the DOC release is composed of aliphatic organics. time.

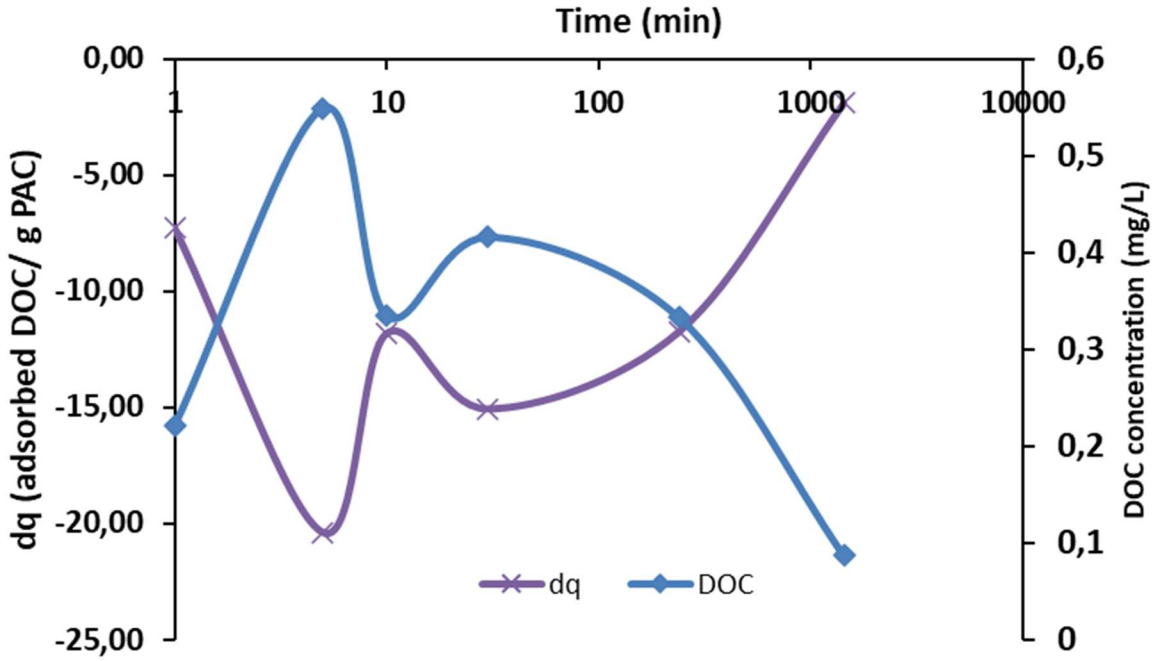

Figure A. 9 Desorption during Virgin PAC/ Milli-Q water test, C_{PAC} = 25 mg/L, DOC of Milli-Q water= 0.039 mg/L

Desorption between 4hr and 24hr in the kinetic test on mixed- aged PACs

During kinetic tests on mixed aged PACs, it was observed that the DOC concentration after one day of contact time was usually higher than the one after 4 hours. Considering that, in mixture of different preloaded PACs, load of each PAC is different from others. Fresh adsorbents can rapidly adsorb high amounts of NOM from the solvent. Therefore, aged PACs (with high q_0) would be

supersaturated compared to C_{eff}. Which increases the probability of NOM desorption from the PAC surface.

Table A. 1 shows the higher the concentration of the virgin adsorbent and the more significant the PAC initial load difference, the more likely the conditions for desorption from the aged PAC will be. The kinetic/isotherm test using the 2nd mix-preloaded PAC is an example of when desorption is substantial. At PAC concentration of 238 mg/L, DOC concentration increased from 0.95 to 1.12 mg/L between 4 hr. and 24 hr., but at the same time, UVA_{254} decreased from 0.013 to 0.093 cm^{-1}. This observation suggests that the desorption is caused by non-aromatic compounds such as low molecular weight neutrals.

Table A. 1 DOC desorption from mix-aged PAC between 4hr and 24 hr.

	PAC concentration (mg/L)	**DOC at 4hr (mg/L)**	**DOC at one day (mg/L)**	**UV_{254} at 4hr (cm^{-1})**	**UV_{254} at one day (cm^{-1})**
1st Mix-preloaded PAC	15	2.15	2.22	0.0283	0.0275
	51	1.61	1.64	0.0165	0.0155
	103	1.5	1.48	0.0151	0.0145
	257	1.03	0.966	0.0080	0.0068
2nd Mix-preloaded PAC	14	2.31	2.37	0.0387	0.0374
	48	2.08	2.16	0.0316	0.0312
	95	1.3	1.5	0.0170	0.0102
	238	0.950	1.12	0.0134	0.093

* For 3rd and 4th mixed-aged PACs, DOC concentration did not measure at 4hr.

Appendix C DOC Desorption from an aged PAC in Milli-Q water

In an isotherm experiment, the desorption process from an aged PAC in Milli-Q water was investigated. For this experiment, the aged PAC (q= 37 mg/g) was produced in an Amicon cell reactor and then concentrated to 12500 mg/L. The concentrated suspension was given one day to equilibrate before consuming in the isotherm test. The DOC at equilibrium point for high concentrated aged PAC was 4.4 mg/L while the DOC at raw water was 3.2. That shows concentring aged PAC leads to desorption (less than 0.1 mg/g). To calculate the amount of desorption, C_{inf} considered as mass-weighted average of DOC in Milli-Q water (0.06 mg/L) and concentrated aged PAC suspension (4.4 mg/L). Figure A.10 and Table A. 2 show that the final q for four diluted suspensions is around 30 mg/g, which means around 20 % of adsorbed DOC could dissolve in Milli-Q water

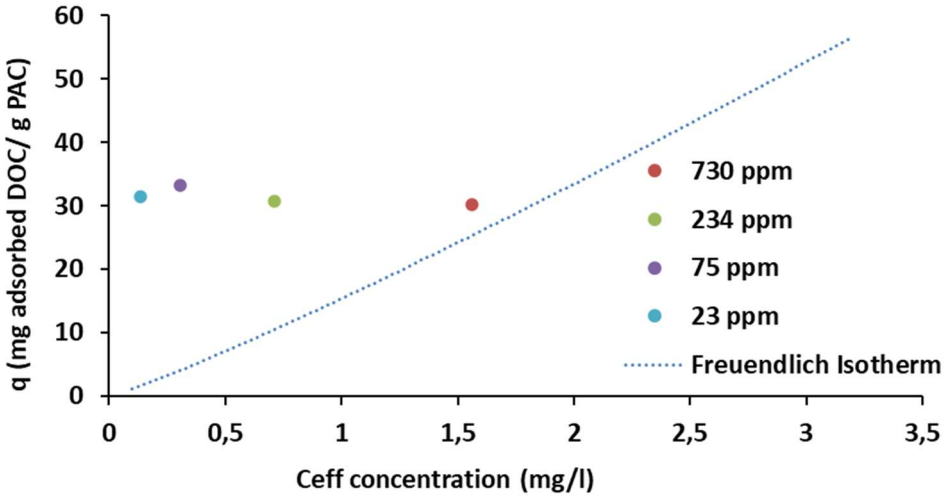

Figure A.10 Particle size distribution of an aged PAC 50 mg/L d50= 18 µm

Table A. 2 Comparing particle size for virgin and aged PAC

PAC concentration (mg/L)	q (mg/g)	C_{inf} (mg/L)	C_{eff} (mg/L)
23	32	0.06	0.135
75	33	0.06	0.305
234	31	0.14	0.711
730	30	0.31	1.56